KATHOLIEKE UNIVERSITEIT LEUVEN
FACULTEIT PSYCHOLOGIE EN PEDAGOGISCHE WETENSCHAPPEN

Laboratorium voor Neuro- en Psychofysiologie

EXPERIENCE-RELATED EFFECTS ON THE RESPONSE SELECTIVITY OF MACAQUE INFERIOR TEMPORAL NEURONS

Proefschrift aangeboden tot het verkrijgen van de graad van
Doctor in de Psychologie

door *Wouter De Baene*

Promotor: Prof. Dr. Rufin Vogels

2008

KATHOLIEKE UNIVERSITEIT LEUVEN
FACULTEIT PSYCHOLOGIE EN PEDAGOGISCHE WETENSCHAPPEN

Laboratorium voor Neuro- en Psychofysiologie

EXPERIENCE-RELATED EFFECTS ON THE RESPONSE SELECTIVITY OF MACAQUE INFERIOR TEMPORAL NEURONS

Proefschrift aangeboden tot het verkrijgen van de graad van
Doctor in de Psychologie

door *Wouter De Baene*

Promotor: Prof. Dr. Rufin Vogels

2008

Wouter De Baene

Ervaringsgerelateerde effecten op de antwoordselectiviteit van inferio-temporale neuronen bij rhesusapen

Promotor: Prof. Dr. Rufin Vogels Laboratorium voor Neuro- en Psychofysiologie

Proefschrift ingediend tot het behalen van de graad van Doctor in de Psychologie

---

De laatste decennia hebben verschillende studies de tradionele visie op corticale veranderingen in de volwassen cortex ten gevolge van visuele ervaringen, die erg gelimiteerd zijn na de 'kritische periode', ondergraven. In verschillende corticale gebieden werden namelijk ervaringsgerelateerde veranderingen in de functionele organisatie en in de eigenschappen van neuronale responsen gevonden. In dit proefschrift onderzochten we veranderingen in stimulusselectiviteit van neuronen in the inferio-temporale (IT) cortex bij rhesusapen ten gevolge van veranderingen in de stimulus statistieken, categorizatie-leren en adaptatie.

Om na te gaan hoe de stimulusselectiviteit van IT neuronen, die gevoelig zijn voor objecteigenschappen als vorm, kleur of textuur, zich aanpast aan veranderingen in de stimulusdistributie statistieken, werd het stimulusbereik op een bepaalde dimensie gemoduleerd, resulterend in twee vormsets die in twee opeenvolgende blokken werden gepresenteerd. De stimuli werden gepresenteerd in een Rapid Serial Visual Presentation (RSVP) paradigma waarvan de validiteit in het bestuderen van vorm-selectiviteit van IT neuronen binnen parametrische vormsets eerst werd aangetoond. De neuronale vormdiscriminatie verbeterde wanneer een vormset met een smaller stimulusbereik (wat onlosmakelijk verbonden was met minder variantie, grotere densiteit en meer inter-stimulus similariteit op pixel-niveau) werd aangeboden. Dit suggereert dat de selectiviteit van IT neuronen zich aanpast aan de stimulusdistributie statistieken bij het snel aanbieden van een beperkte set van stimuli.

In een tweede deel onderzochten we de effecten van categorizatie-leren op de neuronale representatie van complexe vormen in IT cortex. Door registraties voor en na het categorizatie-leren en contrabalancering van de relevante dimensie over apen konden we de categorie-gerelateerde effecten onderscheiden van de stimulus-gerelateerde selectiviteitseffecten. We vonden een expansie van de relevante dimensie en een iets gelijkaardiger neuronaal antwoordpatroon voor exemplaren van dezelfde categorie in vergelijking met een verschillende categorie als gevolg van de categorizatie-training. Deze resultaten suggereren dat vorm categorizatie-leren enkel kleine categorie-gerelateerde veranderingen kan induceren in de vormselectiviteit van IT neuronen in volwassen apen.

In het laatste deel onderzochten we, zowel met extracellulair gemeten aktiepotentialen van enkelvoudige neuronen als met lokale veld potentialen (LFPs), de effecten van adaptatie op de stimulusselectiviteit van IT neuronen. Voor zowel de aktiepotentialen als de LFP gamma power (61-100Hz) verlaagden de neuronale responses met stimulusrepetitie, zonder dat de tuningbreedte veranderde. De mate van adaptatie was niet enkel afhankelijk van de antwoordsterkte maar werd ook beïnvloed door de relatie tussen adapter en test stimulus, zowel voor veranderingen in vormeigenschappen als positieveranderingen: er was meer adaptatie wanneer de adapter en test stimulus identieke vormeigenschappen hadden en beiden op dezelfde positie gepresenteerd werden in vergelijking met wanneer deze stimuli verschilden in vorm of positie. We vonden ook een dalend adaptatieniveau met dalende adapter-test stimulus similariteit. Deze resultaten suggereren dat adaptatie plaatsvindt voor of op het niveau van de synapse.

Wouter De Baene

Experience-related effects on the response selectivity of macaque inferior temporal neurons

Promotor: Prof. Dr. Rufin Vogels Laboratorium voor Neuro- en Psychofysiologie

Dissertation submitted to obtain the degree of Doctor in the Psychology

---

In the last few decennia, experience-related changes in the functional organization and in the neuronal response properties were observed over a wide range of time scales in different cortical areas in adults, undermining the traditional view that cortical changes dependent on visual experience were limited after the *critical period*. In this dissertation, we studied changes in stimulus selectivity of neurons in the macaque inferior temporal (IT) cortex as an effect of changes in the stimulus statistics, categorization learning and adaptation.

To examine how the stimulus selectivity of IT neurons, which are strongly selective for object attributes as shape, color or texture, adapts to changes in the stimulus distribution statistics, we constructed two shape sets which were presented in two subsequent blocks by modulating the stimulus range on a particular dimension. The shapes were presented in a Rapid Serial Visual Presentation (RSVP) paradigm, of which the validity to study the shape selectivity of IT neurons within parametric shape sets was ascertained first. When a shape set with a narrower stimulus range (which was inextricably bound up with less variance, less (pixel-based) dissimilarity and higher density) was presented, the neural shape discrimination improved, suggesting that the tuning of IT neurons adapts to the stimulus distribution statistics when a restricted set of shapes is presented at a high rate.

In a second part, we examined the effects of categorization learning on the neuronal representation of complex shapes in IT cortex. By comparing the IT responses in two monkeys before and after categorization learning, while counterbalancing the relevant categorization dimension across animals, we could disentangle the learned category-related effects from the pre-learned stimulus selectivity effects. We found that categorization learning resulted in an expansion of the representation of the trained dimension and that the responses of the neurons were somewhat more similar for exemplars that belong to the same, compared to different, categories. These results suggest that learning to categorize shapes can only induce minor category-related changes in the shape selectivity of IT neurons in adult monkeys.

In the last part, we examined the effects of adaptation on the stimulus selectivity of IT neurons, both with single-cell spiking activity and local field potentials (LFPs). Both for the spiking activity and the LFP gamma (61-100Hz) power, stimulus repetition scaled down the neuronal responses without changing the tuning width. The degree of adaptation was not only response strength dependent but was affected by the relationship between adapter and test stimulus for both shape feature and position changes: more adaptation was found when adapter and test stimulus had identical shape features and were presented at the same position than when these stimuli differed in shape or position. We also found that the degree of adaptation decreased with decreasing similarity between adapter and test stimulus. Our results suggest that adaptation occurs at or before the level of the synapses onto the neuron.

CONTENTS

ACKNOWLEDGEMENTS

A word of gratitude is more than appropriate in the beginning of this dissertation, since it wouldn't have made it to the press without the generous help of a great number of people.

First and foremost I would like to thank my supervisor, Prof. Rufin Vogels for introducing me in the world of monkeys and single cells and for the years of extensive guidance. His incredible drive and expertise in this domain set an example difficult to match.

Second, I would like to thank my parents for their true and unconditional support over the years and for offering me the ideal circumstances to realize my ambitions. I'm grateful to my sisters for worrying about their little brother, my sisters-, brothers- and parents-in-law for their encouragement and enthusiasm.

Many thanks go to the members and former members of the Laboratorium voor Neuro-en Psychofysiologie for their helping hand whenever necessary and for creating an excellent working atmosphere.

Thanks goes also to my friends, for allowing me to work of steam whenever necessary by playing soccer together, playing music, discussing scientific, political, ethical, sociological, economical, practical, … issues.

Finally, I would like to thank my wife Laurence Anne, for being the wonderful person she is, for supporting me every single day, for listening to my work-related nagging, for taking up all household duties when I was again arriving home late, for giving me the best gifts ever. This dissertation is dedicated to 'the boyz', for being the main source of pleasure and joy.

Wouter De Baene, De Pinte, Juli 1, 2008

CHAPTER 1
EXPERIENCE-RELATED CHANGES IN NEURONAL TUNING OF IT NEURONS: AN OVERVIEW

Traditionally, it was thought that cortical changes dependent on visual experience could only occur in narrow time epochs in early animal life. The discovery of this *'critical period'* suggested a limited potential for the adult cortex to change its properties (Wiesel and Hubel 1963, 1965; Van der Loos and Woolsey 1973; Dawson and Killackey 1987). Although some properties (e.g. ocular dominance) are indeed fixed in adulthood (Hubel and Wiesel 1977), recent evidence pointed out that experience-related changes in the functional organization and in the neuronal response properties can arise in all cortical areas over a wide range of time scales (from seconds up to months).

From a theoretical point of view, investigations of experience-related changes are important to learn how neuronal responses depend on the stimulation history, which can increase our understanding of the information processing of neurons in a natural environment. The importance of this research, however, goes beyond potential theoretical contributions (e.g. to models of adaptation). Knowledge of how experience affects the brain is critical as the functional changes that occur with experience possibly also underlie the recovery following brain damage. This knowledge might thus help in our understanding of the mechanisms of repair and recovery in damaged or malfunctioning brains. Understanding the neural correlates of categorization and categorization learning, for instance, can assist the diagnosis and revalidation of some brain dysfunctions that affect categorization or categorization learning, such as Parkinson disease (e.g. Brown and Marsden 1988; Ashby et al. 2003) or Alzheimer disease (e.g. Keri et al. 1999).

In this introductory chapter, I will give an overview of the major findings on experience-related changes in neuronal tuning in the macaque brain. Because this review, like the dissertation itself, is mostly confined to neuronal changes in the inferior temporal cortex, I will introduce this brain region first. This chapter ends with the presentation of the research issues addressed in this present dissertation.

INFERIOR TEMPORAL CORTEX

The macaque Inferior Temporal (IT) cortex is located in the anterior ventral part of the temporal lobe and is the endpoint of the ventral visual stream[1], also known as the *'What Pathway'*, which extends from primary visual cortex (V1) over V2 and V4 to culminate in the IT cortex and mediates object recognition and long-term memory. IT cortex is also interconnected with various brain areas, including perirhinal cortex, prefrontal cortex, parietal cortex, amygdala and striatum (Ungerleider and Mishkin 1982; Ungerleider et al. 1989; Webster et al. 1994; Murray et al. 2000). IT cortex can be divided into different subregions (e.g. posterior and anterior IT) based on, for instance, functional properties (Tanaka et al. 1991). Posterior and anterior IT roughly correspond to the cytoarchitectural areas TEO and TE, respectively (von Bonin and Bailey 1947; Iwai and Mishkin, 1969; see Figure 1). As TE seems to be the essential part for the flexible properties of visual object recognition (Tanaka 1996), the focus in this dissertation is on the anterior part of IT cortex.

[1] As opposed to the dorsal visual stream or *"Where Pathway"*, extending from V1 over V2 and MT to the parietal cortex, which is associated with motion, representation of object locations and spatial perception in general. The view on the function of this dorsal stream has evolved throughout the years towards processing of visual information to control actions (Goodale and Milner 1992)

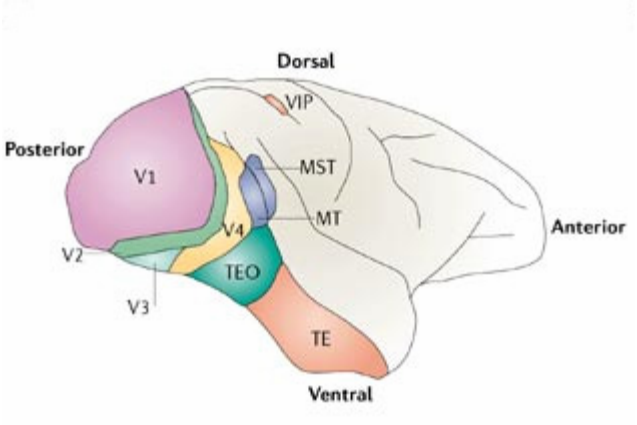

Figure 1. Lateral view on the macaque cerebral cortex with the approximate positioning of several visual areas (Figure from Komatsu 2006)

Neurons in the IT cortex are strongly selective for object attributes as shape, color or texture and are involved in visual object identification and categorization (Gross et al. 1969; Dean 1976; Tanaka 1996; Logothetis and Sheinberg 1996; Afraz et al. 2006). The shape selectivity of IT neurons shows considerable invariance despite drastic stimulus transformations: the preference for a particular shape over other shapes is largely unaffected by changes in the position or size of the object, by the defining cue or by partial occlusion (for a review, see Vogels and Orban 1996; Logothetis and Sheinberg 1996; Tanaka 1996; Riesenhuber and Poggio 2002).

Although some IT neurons have small receptive fields (Op de Beeck and Vogels 2000; Di Carlo and Maunsell 2003), in general, IT neurons tend to have larger receptive fields compared to more posterior areas of the ventral visual stream in awake monkeys. Additionally, IT neurons show a general preference for the foveal position with a bias towards the contralateral visual field (Schwartz et al. 1983, Komatsu and Ideura 1993; Tovee et al. 1994; Logothetis et al. 1995; Missal et al. 1999; Op de Beeck and Vogels 2000).

LEARNING EFFECTS IN IT CORTEX

Several studies have suggested that the representations of familiar, trained stimuli in IT cortex are enhanced. Kobatake et al. (1998) trained their monkeys to discriminate complex shapes and examined the IT stimulus selectivity. They found that the proportion of IT cells which were responsive to some of the trained stimuli was greater in the trained monkeys compared to that in untrained control monkeys. Kobatake et al. (1998) also found that a proportion of the IT cells responded more strongly to some of the learned objects compared to the control stimuli. A similar increase in neuronal responses to learned forms compared to altered versions of these forms in IT cortex was reported by Sakai and Miyashita (1994).

Also Freedman et al. (2006) showed a sharpening of neuronal tuning in IT for familiar compared to novel stimuli in monkeys who were passively fixating. They trained their monkeys in a visual categorization task and compared the stimulus selectivity for the trained stimuli and for the image-plain rotated versions of these same stimuli. The selectivity for the stimuli presented in the trained orientation was stronger than for these stimuli presented at the untrained, rotated orientation. Baker et al. (2002) trained their monkeys in discriminating between two-part stimuli. The two parts of these so-called 'baton'-stimuli were manipulated independently. They found a sharpened selectivity of IT cells for combinations of parts that were experienced together during training compared to unlearned batons. Also the selectivity for the individual parts of the learned batons was enhanced. In contrast with Kobatake et al. (1998), the increase in stimulus selectivity with training in the studies of Freedman et al. (2006) and Baker et al. (2002) was not accompanied by an increased response strength to the learned objects, but by a reduced firing strength to the trained, but ineffective shapes. A similar combination of increased selectivity and reduced response strength with

extensive exposure in IT cortex was observed by Mruczek and Sheinberg (2007) and Anderson et al. (2008). Op de Beeck et al. (2007) also found some evidence for increased selectivity in IT for the relevant (backward-masked) objects, but only in one of their two monkeys. Additionally, this increased selectivity for the relevant objects was combined with a reduction of the neuronal responses to the interfering irrelevant masking patterns. Some studies only reported decreases in firing strength to objects to which the monkeys had been extensively exposed (e.g. Fahy et al. 1993; Li et al. 1993), without reporting changes in stimulus selectivity.

Instead of focusing on the effects of familiarity or of extensive object discrimination training on the selectivity and responsiveness of IT cells, few studies focused on the effect of categorization learning on the neuronal tuning in IT neurons. The results of these few studies were diverse. In one study (Vogels 1999), monkeys were trained to categorize trees versus non-trees and fish versus non-fish. Some of the recorded IT neurons responded well to many of the stimuli from the trained category, while their response to untrained distractors was weak. In addition to this between-category selectivity, IT cells also displayed within-category selectivity: the responses were not sufficiently invariant to accommodate all variability present within a given category. These results suggested that object categories are not represented at the single cell level in IT cortex. Freedman et al. (2003), however, reported category effects for IT cells after training their monkeys to categorize their stimuli into a ‘cat’ and ‘dog’ category using a category-matching task. These effects, however, were very weak: responses to shapes from within one learned category were slightly more similar than responses to shapes from different learned categories. Since no pre-training measurements of selectivity were obtained in this study, this small effect could result from physical differences amongst the stimuli instead of differences in category membership. Sigala and Logothetis (2002) compared the IT representation for

features that were diagnostic for distinguishing between two learned stimulus categories with the representation of non-diagnostic features. They found an enhanced representation of the shape features that were relevant to categorize the stimuli. Sigala and Logothetis (2002), however, obtained no pre-training selectivity measurements either. As a consequence, the reported effect of categorization relevant feature selectivity could be due to mere stimulus selectivity, unrelated to categorization learning, all the more since the diagnostic feature was identical in both trained monkeys. Op de Beeck et al. (2001) studied the effect of applying different categorization rules based on integral dimensions on the selectivity of IT cells. Contrary to Sigala and Logothetis (2002), they found no expansion of the relevant dimension or any other metric changes.

ADAPTATION EFFECTS IN IT CORTEX

One of the most robust experience-related changes in neuronal responses is apparent when stimuli are repeated: in many cortical areas, the neuronal activity decreases with stimulus repetition. This phenomenon has been referred to as, among other things, adaptation (e.g. Ringo 1996; Krekelberg et al. 2006), repetition suppression (e.g. Desimone 1996; Grill-Spector et al. 2006), attenuation (Yi et al. 2006) or neural priming (Maccotta and Buckner 2004). Adaptation effects can occur at multiple time scales, from milliseconds (e.g. Sobotka and Ringo 1996), over minutes (e.g. Henson et al. 2000), up to days (van Turennout et al. 2000) and are believed to underlie several behavioral phenomena like perceptual aftereffects and priming (Schacter and Buckner 1998; Clifford and Rhodes 2005; but see McMahon and Olson 2007).

Adaptation was also observed in IT cortex: various single-cell studies have shown that stimulus repetition commonly reduces the firing rate of IT neurons (Gross et al. 1967, 1969; Baylis and Rolls 1987; Miller et al. 1991a; Riches et al. 1991; Sobotka and Ringo 1993; Vogels et al. 1995), even despite many intervening presentations of other stimuli (e.g. Brown et al. 1987; Miller et al. 1991b; Li et al. 1993; Miller and Desimone 1994; Xiang and Brown 1998; Sawamura et al. 2006). This adaptation effect was found in both awake behaving animals performing various visual tasks as well as in anesthetized animals.

Aside its fundamental scientific importance (e.g. to understand the underlying principles of perceptual aftereffects), studying the adaptation of neuronal responses is also important from a more practical, methodological point of view, since adaptation paradigms are being used to infer the stimulus selectivity of neuronal populations in humans employing functional imaging techniques (fMRI; MEG). Because of the invasive nature of the commonly used single unit recordings to study stimulus selectivity of neurons in macaques, an alternative method had to be found to study the neuronal stimulus selectivity in humans. The classical fMRI technique could not serve as an alternative, as studies using this technique could only show differences in brain region activation when presenting different stimuli (e.g. moving versus static stimuli) but did not provide any insight in the selectivity for stimulus parameters in the activated regions (e.g. direction selectivity). With the development of the fMRI-adaptation technique (fMR-A; Grill-Spector and Malach 2001; Nacache and Dehaene 2001), this problem has been

overcome and the non-invasive fMRI technique could serve as an alternative to study the stimulus selectivity of neuronal populations in humans[2].

At present, several different fMR-A paradigms have been developed but, contrary to the single unit recording studies in macaques in which stimulus selectivity can be assessed in a direct way, all the fMR-A paradigms need to infer the neuronal stimulus selectivity from cross-adaptation. The principle of cross-adaptation can be explained as follows: Consider 3 stimuli (A, B and C) and that the same neurons respond to stimulus A and B, but not to stimulus C. As mentioned before, adaptation will occur when stimulus A is repeated (A-A sequence). Because the same neurons are responsive for stimulus A and B, one expects also that activation is decreased when B is followed by A (cross-adaptation; B-A sequence). However, since different neurons respond to stimulus A and C, one does not expect cross-adaptation for the C-A sequence. The degree of cross-adaptation can thus be used to infer the stimulus selectivity of a neuronal population.

Because the cross-adaptation principle is fundamental to all fMR-A paradigms[3], it is important to examine the match between the stimulus selectivity of the neuronal responses and the stimulus selectivity of the adaptation effect. Sawamura et al. (2006) tested this match by performing a single-cell study on cross-adaptation in IT cortex. They selected for each IT neuron three stimuli: two to which the neuron responded (stimulus A and B), and one to which the neuron responded much less or not (stimulus C). They found little or no cross-adaptation for the C-A sequences, whereas the degree

[2] Note that fMR-A is not the only method used to measure selectivity of fMRI. Recently, multi-voxel pattern analysis methods have been employed on fMRI data, with some promising results (for a review, see Norman et al. 2006).

[3] Note that the validity of the fMR-A technique for inferring neuronal stimulus selectivity is also dependent on the link between neuronal signals and the hemodynamic BOLD response measured with fMRI. This fundamental link is currently also subject of intense research (e.g. Logothetis et al. 2001; Kim et al. 2004; Logothetis and Wandell 2004; Mukamel et al. 2005; Niessing et al. 2005).

of cross-adaptation for the B-A sequence was less than expected from the similarity of the responses to B and A. This implies a greater stimulus selectivity of the adaptation effect compared to the stimulus selectivity of the responses in IT. This mismatch between the stimulus selectivity and the adaptation effect of IT neurons implies that the fMR-A method may overestimate the selectivity of the neurons.

EFFECTS OF STIMULUS STATISTICS

The effect of stimulus presentation history on neuronal response characteristics is not only evident in learning or in adaptation effects. Recent work has demonstrated that early visual and auditory neurons adapt to recent stimulus statistics so that information transmission is enhanced (e.g. Smirnakis et al. 1997; Brenner et al. 2000; Fairhall et al. 2001; Sharpee et al. 2006; Dean et al. 2005, 2008). Brenner et al. (2000) and Dean et al. (2005), for instance, demonstrated an adaptive rescaling of neuronal responses in, respectively, the fly visual system and the guinea pig inferior colliculus when the variance of the stimulus distribution was altered. No similar effects of stimulus distribution statistics on the tuning of IT neurons have been reported. However, similar adaptive mechanisms might operate in IT cortex or effects of such adaptive mechanisms at earlier visual levels might be inherited in IT.

SINGLE CELL AND LOCAL FIELD POTENTIALS

By filtering the extracellular voltage in two different ways, the recorded signal can be split into spiking activity (by high-pass filtering, typically above ~300 Hz) and Local Field Potentials or LFPs (by low-pass filtering, e.g. below 300 Hz). The contribution from spikes to the LFPs is thought to be relatively small, except in the 100 to 300 Hz frequency range. This frequency band likely contains power resulting from nearby action potentials.

Spiking activity reflects local neural processing and the neuronal output of a single cell or multiple neurons near the tip of the electrode to other brain regions. LFPs, in contrast, arise largely from dendritic activity over large brain regions (Mitzdorf 1985, 1987; Juergens et al. 1999; Cruikshank et al. 2002; Kaur et al. 2004; Logothetis and Wandell 2004; Kreiman et al. 2006; Nielsen et al. 2006; Chen et al. 2007) and thus provide a measure of the synaptic input from other brain regions to and local processing, mediated by interneurons, within an area within 0.5-3 mm of the electrode tip (Mitzdorf 1985, 1987; Juergens et al. 1999). For IT cells, the synaptic input is largely composed of (a) feedforward signals from earlier areas (e.g. V4); (b) feedback signals (e.g. from prefrontal cortex); and (c) local connectivity (Kreimann et al. 2006).

Simultaneous recordings of LFPs and spiking activity can add to our understanding of the transformation of neural signals from one processing stage to the next (Kreiman et al. 2006; Nielsen et al. 2006). One assumption in comparing LFPs with single cell activity is that spiking activity will show response modulations prior to LFPs only in those brain areas where the processing occurs. In the brain areas receiving this information from other regions, the response modulations in the LFPs will be seen before or

simultaneously with the modulations in the spiking activity (Nielsen et al. 2006; Monosov et al. 2008).

Another reason to measure LFPs in addition to single unit spiking activity is that the fMRI BOLD response seems to correlate more strongly with LFPs than with spiking activity (Logothetis et al. 2001; Viswanathan and Freeman 2007), possibly because the LFPs, as does the BOLD response, reflect an energetically expensive activity (Logothetis et al. 2001; Rauch et al. 2008). LFPs recorded in monkeys could thus be an important link between monkey single cell and human EEG and fMRI data (Logothetis and Wandell 2004; Woodman et al. 2007).

Despite the great opportunities provided by the simultaneous recordings of LFPs and spiking activity, as yet, only few studies, especially in IT cortex, took advantage of this possibility. Nielsen et al. (2006) studied the effect of occlusion of parts of a scene with different behavioral relevance[4] on neuronal responses in IT cortex with single cells and LFPs. They found a dissociation between LFPs and spiking activity as a function of the anatomical recording area: For the spiking activity, a preference for the diagnostic over the nondiagnostic objects was observed in both the posterior and anterior parts of IT. For the LFPs, however, this preference for diagnostic parts was only found in the anterior recording part of IT. Kreiman et al. (2006) showed that LFPs in IT are stimulus selective and scale- and position-invariant. Compared to the spiking activity, the selectivity of LFPs was less pronounced: fewer sites showed stimulus selectivity and the selectivity was less sharp. In general, Kreiman et al. (2006) did not find a correlation between the LFPs stimulus selectivity and the single unit stimulus selectivity measured with the same electrode.

[4] Note that the behavioral relevance might be confounded with contrast level in this study.

THE PRESENT DISSERTATION

In this dissertation, I will present several studies which are aimed at exploring one of the above-mentioned experience-related effects on tuning of IT neurons. The three following parts of this dissertation deal, respectively, with effects of stimulus distribution statistics, effects of categorization learning and effects of adaptation. After the third empirical part, I will bring this dissertation to a close in Chapter 5 with a presentation of the general conclusions which can be drawn from the previous chapters. In this final chapter, I will also propose some directions for future experimental investigations.

FIRST PART: VALIDITY OF THE RSVP TECHNIQUE AND ADAPTATION TO CHANGES IN THE STIMULUS STATISTICS

Given recent demonstrations in the fly visual system and the guinea pig inferior colliculus (Brenner et al. 2000; Dean et al. 2005, respectively) of an adaptive rescaling of neuronal responses when the variance of the stimulus distribution is altered, we examined whether the tuning of IT neurons adapts to the properties of the stimulus distribution other than the mean in the first part (Chapter 2) of this dissertation. To this end, we measured the responses of single IT neurons to a set of shapes that varied parametrically along a single dimension. The neurons were tested in two successive blocks using stimuli that differed in stimulus variance and density between blocks. One important prerequisite to manipulate the stimulus distribution properties is the use of parameterized sets of stimuli because they allow examining how the neuronal responses to stimuli are related to the parametric variation built into the stimulus sets (e.g. Op de Beeck et al. 2001; Sigala and Logothetis 2002; Brincat and Connor 2004; Kayaert et al. 2005).

To study the effects of changes in the stimulus distribution statistics, we opted to use the Rapid Serial Visual Presentation (RSVP) paradigm. In RSVP, images are presented sequentially and continuously at a high pace with each image replacing the previous one at the same location. Although Keysers et al. (2001) and Földiák et al. (2004) pioneered the use of the RSVP paradigm to examine the selectivity of neurons in the superior temporal sulcus (STS) for sharply differing, complex images, this paradigm has rarely been used in combination with single-cell recordings in the higher visual cortex. As a high number of stimuli are presented repeatedly, this paradigm might be more sensitive to adaptive effects than classical testing paradigms. The validity of the RSVP technique to study shape selectivity for parametric sets, however, is not obvious since the differences among the shapes in such sets are much smaller compared to the stimulus differences employed in previous studies using RSVP (Keysers et al. 2001; Földiák et al. 2004; Kiani et al. 2005). As a result, we first wanted to determine whether the RSVP technique is a useful tool for this purpose.

SECOND PART: EFFECTS OF CATEGORIZATION LEARNING

In the second part of this dissertation (Chapter 3), we reexamined the effects of category learning of complex shapes on the neuronal representation in IT cortex. Contrary to previous studies (Op de Beeck et al. 2001; Sigala and Logothetis 2002; Freedman et al. 2003), which reported diverse and conflicting results, we incorporated the possibility to disentangle pre-learned stimulus selectivity effects from learned category-related effects in two ways.

First, we recorded the responses of IT neurons in two monkeys before and after categorization learning. Before categorization learning, we recorded the responses of single IT neurons while presenting all shapes randomly

intermixed in an RSVP paradigm while the monkeys were passively fixating. After categorization training, we again recorded the responses of single IT neurons to the shapes while the monkeys were categorizing the images. Second, we counterbalanced the relevant categorization dimension across animals: In between the two recording phases, we trained the monkeys to group the stimuli into two categories with curvature and aspect ratio as the relevant dimension for the first and second monkey, respectively.

We chose to manipulate the shape dimensions aspect ratio and curvature because these were previously shown to be largely separable in human psychophysical studies (e.g. Op de Beeck et al. 2003; Wagemans et al. 2006). This separability of the dimensions[5] is important as a human psychophysical study (Op de Beeck et al. 2003) reported a dimension-specific gain in perceptual similarity induced by categorization learning for shapes varying along separable, but not integral dimensions. This effect of separability could possibly also explain the discrepancy between the results of Op de Beeck et al. (2001) and Sigala and Logothetis (2002): in the latter study, separable dimensions were manipulated whereas in the former study, integral dimensions were employed.

THIRD PART: ADAPTATION EFFECTS

The main research questions in the third and last empirical part of this dissertation (Chapter 4) are related to the effects of adaptation on the stimulus selectivity or tuning of IT neurons. These issues could not be addressed in the study of Sawamura et al. (2006) since they only presented one test stimulus.

[5] Separable dimensions can be attended to separately. By contrast, for integral dimensions, it is difficult, if not impossible, to ignore variations along one dimension while attending to the other (Garner 1976). Classical examples of separable dimensions are size and brightness, whereas saturation and brightness are classical examples of integral dimensions (Garner 1976; Foard and Kemler 1984; Melara et al. 1993).

A prerequisite to measure neuronal tuning functions, however, is the use of sets of stimuli that vary systematically according to a particular parameter so one can plot the neuronal responses as a function of the parametric values. As mentioned before, it is possible to measure tunings of IT neurons by using shapes that vary systematically along particular shape dimensions (e.g. Op de Beeck et al. 2001; Kayaert et al. 2005).

Using a fully crossed design in which all stimuli could serve as an adapter and as a test stimulus and in which all possible combinations of these stimuli were presented, we could assess the effect of adaptation on the tuning of IT neurons as a function of the similarity between the adapter and the test stimulus, both with single-cell spiking activity and Local Field Potentials (LFPs). Knowledge about this effect is crucial in order to interpret fMR-A results. A common assumption here is that the effect of adaptation reduces with increasing dissimilarity between adapter and test stimulus (Jiang et al. 2006). It is also important to know the degree to which the adaptation and its effect on selectivity depend on the stimulus effectiveness, i.e. on how strongly the stimuli drive the neuron. According to a model linking fMR-A to neuronal tuning (Piazza et al. 2004), the degree of adaptation demonstrated by a neuron is proportional to the strength of its initial response to a stimulus.

Changes in selectivity following adaptation can be used to distinguish two models of adaptation (Grill-Spector et al. 2006): the '*fatigue*' model (Grill-Spector and Malach 2001) and the '*sharpening*' model (Desimone 1996; Wiggs and Martin 1998). The fatigue model predicts that stimulus repetition reduces the response in proportion to the original response, but predicts no change in selectivity with adaptation. The sharpening model, by contrast, predicts that adaptation causes a sharpening of the tuning curves, thus an increased selectivity after adaptation. This results in a sparser representation of the stimuli.

REFERENCES

Afraz SR, Kiani R, Esteky H. Microstimulation of inferotemporal cortex influences face categorization. *Nature* 442: 692-695, 2006.

Anderson B, Mruczek REB, Kawasaki K, Sheinberg D. Effects of familiarity on neural activity in monkey inferior temporal lobe. *Cereb Cortex* Advanced Access: doi:10.1093/cercor/bhn015, 2008.

Ashby FG, Noble S, Filoteo J, Waldron EM, Ell SW. Category learning deficits in Parkinson's disease. *Neuropsychology* 17: 115-124, 2003.

Baker CI, Behrmann M, Olson CR. Impact of learning on representation of parts and wholes in monkey inferotemporal cortex. *Nat Neurosci* 5: 1210-1215, 2002.

Baylis GC, Rolls ET. Responses of neurons in the inferior temporal cortex in short term and serial recognition memory tasks. *Exp Brain Res* 65: 614-622, 1987.

Brenner N, Bialek W, de Ruyter van Steveninck R. Adaptive rescaling maximizes information transmission. *Neuron* 26: 695-702, 2000.

Brincat SL, Connor CE. Underlying principles of visual shape selectivity in posterior inferotemporal cortex. *Nat Neurosci* 7: 880-886, 2004.

Brown MW, Wilson FAW, Riches IP. Neuronal evidence that inferomedial temporal cortex is more important than hippocampus in certain processes underlying recognition memory. *Brain Res* 409: 158-162, 1987.

Brown RG, Marsden CD. Internal versus external cues and the control of attention in Parkinson's disease. *Brain* 111: 323-345, 1988.

Chen CM, Lakatos P, Shah AS, Mehta AD, Givre SJ, Javitt DC, Schroeder CE. Functional anatomy and interaction of fast and slow visual pathways in macaque monkeys. *Cereb Cortex* 17: 1561-1569, 2007.

Clifford CWG, Rhodes G. (Eds.) *Fitting the mind to the world.* Oxford University Press, 2005.

Cruikshank SJ, Rose HJ, Metherate R. Auditory thalamocortical synaptic transmission in vitro. *J Neurophysiol* 87: 361-384, 2002.

Dawson DR, Killackey HP. The organization and mutability of the forepaw and hindpaw representations in the somatosensory cortex of the neonatal rat. *J Comp Neurol* 256: 246-256, 1987.

Dean I, Harper NS, McAlpine D. Neural population coding of sound level adapts to stimulus statistics. *Nat Neurosci* 8: 1684-1689, 2005.

Dean I, Robinson BL, Harper NS, McAlpine D. Rapid neural adaptation to sound level statistics. *J Neurosci* 28: 6430-6438, 2008.

Dean P. Effects of inferotemporal lesions on the behavior of monkeys. *Psychol Bull* 83: 41-71, 1976.

Desimone R. Neural mechanisms for visual memory and their role in attention. *Proc Natl Acad Sci USA* 93: 13494-13499, 1996.

DiCarlo JJ, Maunsell JHR. Anterior inferotemporal neurons of monkeys engaged in object recognition can be highly sensitive to object retinal position. *J Neurophysiol* 89: 3264-3278, 2003.

Fahy FL, Riches IP, Brown MW. Neuronal activity related to visual recognition memory: long-term memory and the encoding of recency and familiarity information in the primate anterior and medial inferior temporal cortex and rhinal cortex. *Exp Brain Res* 96: 457-472, 1993.

Fairhall AL, Lewen GD, Bialek W, de Ruyter van Steveninck R. Efficiency and ambiguity in an adaptive neural code. *Nature* 412: 787-792, 2001

Foard CF, Kemler Nelson DG. Holistic and analytic modes of processing: The multiple determinants of perceptual analysis. *J Exp Psychol Gen* 113: 94-111, 1984.

Földiák P, Xiao DK, Keysers C, Edwards R, Perrett DI. Rapid serial visual presentation for the determination of neural selectivity in area STSa. *Prog Brain Res* 144: 107-116, 2004.

Freedman DJ, Riesenhuber M, Poggio T, Miller EK. A comparison of primate prefrontal and inferior temporal cortices during visual categorization. *J Neurosci* 23: 5235-5246, 2003.

Freedman DJ, Riesenhuber M, Poggio T, Miller EK. Experience-dependent sharpening of visual shape selectivity in inferior temporal cortex. *Cereb cortex* 16: 1631-1644, 2006.

Garner WR. Interaction of stimulus dimensions in concept and choice processes. *Cognitive Psychol* 8: 98-123, 1976.

Goodale MA, Milner AD. Separate pathways for perception and action. *Trends neurosci* 15: 20-25, 1992.

Grill-Spector K, Malach R. fMR-adaptation: a tool for studying the functional properties of human cortical neurons. *Acta Psychologica* 107: 293-321, 2001.

Grill-Spector K, Henson R, Martin A. Repetition and the brain: neural models of stimulus-specific effects. *Trends Cogn Sci* 10: 15-23, 2006.

Gross CG, Schiller PH, Wells C, Gerstein GL. Single-unit activity in temporal association cortex of the monkey. *J Neurophysiol* 30: 833–843, 1967.

Gross CG, Bender DB, Rocha-Miranda CE. Visual receptive fields of neurons in inferotemporal cortex of the monkey. *Science* 166: 1303-1306, 1969.

Henson RN, Rylands A, Ross E, Vuilleumier P, Rugg MD. The effect of repetition lag on electrophysiological and hemodynamic correlates of visual object priming. *Neuroimage* 21: 1674-1689, 2000.

Hubel DH, Wiesel TN. Functional architecture of macaque monkey visual cortex. *Phil Trans R Soc Lond B* 278: 377-409, 1977.

Iwai E, Mishkin M. Further evidence on the locus of the visual area in the temporal lobe of the monkey. *Exp Neurol* 25: 585-594, 1969.

Jiang X, Rosen E, Zeffiro T, VanMeter J, Blanz V, Riesenhuber M. Evaluation of a shape-based model of human face discrimination using FMRI and behavioral techniques. *Neuron* 50: 159-172, 2006.

Juergens E, Guettler A, Eckhorn R. Visual stimulation elicits locked and induced gamma oscillations in monkey intracortical and EEG-potentials, but not in human EEG. *Exp Brain Res* 129: 247-259, 1999.

Kaur S, Lazar R, Metherate R. Intracortical pathways determine breadth of subthreshold frequency receptive fields in primary auditory cortex. *J Neurophysiol* 91: 2551-2567, 2004.

Kayaert G, Biederman I, Op de Beeck H, Vogels R. Tuning for shape dimensions in macaque inferior temporal cortex. *Eur J Neurosci* 22: 212-224, 2005.

Kéri S, Kalman J, Rapcsak SZ, Antal A, Benedek G, Janka Z. Classification learning in Alzheimer's disease. *Brain* 122: 1063-1068, 1999.

Keysers C, Xiao DK, Földiák P, Perrett DI. The speed of sight. *J Cogn Neurosci* 13: 90-101, 2001.

Kiani R, Esteky H, Tanaka K. Differences in onset latency of macaque inferotemporal neural responses to primate and non-primate faces. *J Neurophysiol* 94: 1587-1596, 2005.

Kim DS, **Ronen I**, **Olman C**, **Kim SG**, **Ugurbil K**, **Toth LJ.** Spatial relationship between neuronal activity and BOLD functionalMRI. *Neuroimage* 21: 876-885, 2004.

Kobatake E, Wang G, Tanaka K. Effects of shape-discrimination training on the selectivity of inferotemporal cells in adult monkeys. *J Neurophysiol* 80: 324-330, 1998.

Komatsu H, Ideura Y. Relationships between color, shape, and pattern selectivities of neurons in the inferior temporal cortex of the monkey. *J Neurophysiol* 70: 677-694, 1993.

Komatsu H. The neural mechanisms of perceptual filling-in. *Nat Rev Neurosci* 7: 220-231, 2006.

Kreiman G, Hung CP, Kraskov A, Quirogq RQ, Poggio T, DiCarlo JJ. Object selectivity of local field potentials and spikes in the macaque inferior temporal cortex. *Neuron* 49: 433-445, 2006.

Krekelberg B, Boynton GM, van Wezel RJA. Adaptation: from single cells to BOLD signals. *Trends Neurosci* 29: 250-256, 2006.

Li L, Miller EK, Desimone R. The representation of stimulus familiarity in anterior inferior temporal cortex. *J Neurophysiol* 69: 1918–1929, 1993.

Logothetis NK, Pauls J, Poggio T. Shape representation in the inferior temporal cortex of monkeys. *Curr Biol* 5: 552-563, 1995.

Logothetis NK, Sheinberg DL. Visual object recognition. *Annu Rev Neurosci* 19: 577-621, 1996.

Logothetis NK, Pauls J, Augath M, Trinath T, Oeltermann A. Neurophysiological investigation of the basis of the fMRI signal. *Nature* 412: 150-157, 2001.

Logothetis NK, Wandell BA. Interpreting the BOLD signal. *Annu Rev Physiol* 66: 735-769, 2004.

Maccotta L, Buckner RL. Evidence for neural effects of repetition that directly correlate with behavioral priming. *J Cogn Neurosci* 16: 1625-1632, 2004.

McMahon DBT, Olson CR. Repetition suppression in monkey inferotemporal cortex: relation to behavioural priming. *J Neurophysiol* 97: 3532-3543, 2007.

Melara RD, Marks LE, Potts BC. Primacy of dimensions in color perception. *J Exp Psychol Human* 19: 1082-1104, 1993.

Miller EK, Gochin PM, Gross CG. Habituation-like decrease in the responses of neurons in inferior temporal cortex of the macaque. *Vis Neurosci* 7: 357-362, 1991a.

Miller EK, Li L, Desimone R. A neural mechanism for working and recognition memory in inferior temporal cortex. *Science* 254: 1377-1379, 1991b.

Miller EK, Desimone R. Parallel neuronal mechanisms for short-term memory. *Science* 263: 520-522, 1994.

Missal M, Vogels R, Li CY, Orban GA. Shape interactions in macaque inferior temporal neurons. *J Neurophysiol* 82: 131-142, 1999.

Mitzdorf U. Current source-density method and application in cat cerebral cortex: investigation of evoked potentials and EEG phenomena. *Physiol Rev* 65: 37-100, 1985.

Mitzdorf U. Properties of the evoked potential generators: current source-density analysis of visually evoked potentials in the cat visual cortex. *Int J Neurosci* 33: 33-59, 1987.

Monosov IE, Trageser JC, Thompson KG. Measurements of simultaneously recorded spiking activity and local field potentials suggest that spatial selection emerges in the frontal eye field. *Neuron* 57: 614-625, 2008.

Mruczek RE, Sheinberg DL. Context familiarity enhances target processing by inferior temporal cortex neurons. *J Neurosci* 27: 8533-8545, 2007.

Mukamel R, Gelbard H, Arieli A, Hasson U, Fried I, Malach R. Coupling between neuronal firing, field potentials, and fMR1 in human auditory cortex. *Science* 309: 951-954, 2005.

Murray EA, Bussey TJ, Hampton RR, Saksida LM. The parahippocampal region and object identification. *Ann NY Acad Sci* 911: 166-174, 2000.

Naccache L, Dehaene S. The priming method: imaging unconscious repetition priming reveals an abstract representation of number in the parietal lobes. *Cereb Cortex* 11: 966-974, 2001.

Nielsen KJ, Logothetis NK, Rainer G. Dissociation between local field potentials and spiking activity in macaque inferior temporal cortex reveals diagnosticity-based encoding of complex objects. *J Neurosci* 26: 9639-9645, 2006.

Niessing J, Ebisch B, Schmidt KE, Niessing M, Singer W, Galuske RAW. Hemodynamic signals correlate tightly with synchronized gamma oscillations. *Science* 309: 948-951, 2005.

Norman KA, Polyn SM, Detre GJ, Haxby JV. Beyond mind-reading: multi-voxel pattern analysis of fMRI data. *Trends Cogn Sci* 10: 424-430, 2006.

Op de Beeck H, Vogels R. Spatial sensitivity of macaque inferior temporal neurons. *J Comp Neurol* 426: 505-518, 2000.

Op de Beeck H, Wagemans J, Vogels R. Inferotemporal neurons represent low-dimensional configurations of parameterized shapes. *Nat Neurosci* 4: 1244-1252, 2001.

Op de Beeck H, Wagemans J, Vogels R. The effect of category learning on the representation of shape: dimensions can be biased but not differentiated. *J Exp Psychol Gen* 132: 491-511, 2003.

Op de Beeck HP, Wagemans J, Vogels R. Effects of perceptual learning in visual backward masking on the responses of macaque inferior temporal neurons. *Neuroscience* 145: 775-789, 2007.

Piazza M, Izard V, Pinel P, Le Bihan D, Dehaene S. Tuning curves for approximate numerosity in the human intraparietal sulcus. *Neuron* 44: 547-555, 2004.

Rauch A, Rainer G, Logothetis NK. The effect of a serotonin-induced dissociation between spiking and perisynaptic activity on BOLD functional MRI. *Proc Natl Acad Sci USA* 105: 6759-6764, 2008.

Riches IP, Wilson FAW, Brown MW. The effects of visual stimulation and memory on neurons of the hippocampal formation and neighboring parahippocampal gyrus and inferior temporal cortex of the primate. *J Neurosci* 11: 1763-1779, 1991.

Riesenhuber M, Poggio T. Neural mechanisms of object recognition. *Curr Opin Neurobiol* 12: 162-168, 2002.

Ringo JL. Stimulus specific adaptation in inferior temporal and medial temporal cortex of the monkey. *Behav Brain Res* 76: 191-197, 1996.

Sakai K, Miyashita Y. Neuronal tuning to learned complex forms in vision. *Neuroreport* 5: 829-832, 1994.

Sawamura H, Orban GA, Vogels R. Selectivity of neuronal adaptation does not match response selectivity: a single cell study of the fMRI adaptation paradigm. *Neuron* 49: 307-318, 2006.

Schacter DL, Buckner RL. Priming and the brain. *Neuron* 20: 185-195, 1998.

Schwartz EL, Desimone R, Albright TD, Gross CG. Shape recognition and inferior temporal neurons. *Proc Natl Acad Sci USA* 80: 5776-5778, 1983.

Sharpee TO, Sugihara H, Kurgansky AV, Rebrik SP, Stryker MP, Miller KD. Adaptive filtering enhances information transmission in visual cortex. *Nature* 439: 936-942, 2006.

Sigala N, Logothetis NK. Visual categorization shapes feature selectivity in the primate temporal cortex. *Nature* 415: 318-320, 2002.

Smirnakis S, Berry MJ, Warland D, Bialek W, Meister M. Adaptation of retinal processing to image contrast and spatial scale. *Nature* 386: 67-73, 1997.

Sobotka SS, Ringo JL. Investigation of long term recognition and association memory in unit responses from inferotemporal cortex. *Exp Brain Res* 96: 28-38, 1993.

Sobotka S, Ringo JL. Mnemonic responses of single units recorded from monkey inferotemporal cortex, accessed via transcommissural versus direct pathways: a dissociation between unit activity and behavior. *J Neurosci* 16: 4222-4230, 1996.

Tanaka K, Saito HA, Fukada Y, Moriya M. Coding visual images of objects in the inferotemporal cortex of the macaque monkey. *J Neurophysiol* 66: 170-189, 1991.

Tanaka K. Inferotemporal cortex and object vision. *Annu Rev Neurosci* 19: 109-139, 1996.

Tovée MJ, Rolls ET, Azzopardi P. Translation invariance in the responses to faces of single neurons in the temporal visual cortical areas of the alert macaque. *J Neurophysiol* 72: 1049-1060, 1994.

Ungerleider LG, Mishkin M. Two cortical visual systems. In *Analysis of Visual Behavior* (edited by Ingle DJ) pp. 549-586. Cambridge: MIT Press, 1982.

Ungerleider LG, Gaffan D, Pelak VS. Projections from inferior temporal cortex to prefrontal cortex via the uncinate fascicle in rhesus monkeys. *Exp Brain Res* 76: 473-484, 1989.

Van der loos H, Woolsey TA. Somatosensory cortex: Structural alterations following early injury to sense organs. *Science* 179: 385-398, 1973.

van Turennout, M Ellmore T, Martin A. Long-lasting cortical plasticity in the object naming system. *Nature Neurosci* 3: 1329-1334, 2000.

Viswanathan A, Freeman RD. Neurometabolic coupling in cerebral cortex reflects synaptic more than spiking activity. *Nat Neurosci* 10: 1308-1312, 2007.

Vogels R, Sary G, Orban GA. How task-related are the responses of inferior temporal neurons. *Vis Neurosci* 12: 207-214, 1995.

Vogels R, Orban GA. Coding of stimulus invariances by inferior temporal neurons. *Prog Brain Res* 112: 195-211, 1996.

Vogels R. Categorization of complex visual images by rhesus monkeys. Part 2: single-cell study. *Eur J Neurosci* 11: 1239-1255, 1999.

von Bonin G, Bailey P. *The neocortex of Macaca mulatta*. University of Illinois Press: Urbana, 1947.

Wagemans J, Ons B, Gillebert CR, Op de Beeck H. Effects of categorization learning on perceived shape similarity in humans. *Soc Neurosci Abstr* 438: 22, 2006.

Webster MJ, Bachevalier J, Ungerleider LG. Connections of inferior temporal areas TEO and TE with parietal and frontal cortex in macaque monkeys. *Cereb Cortex* 4: 470-483, 1994.

Wiesel TN, Hubel DH. Single cell responses in striate cortex of kittens deprived of vision in one eye. *J Neurophysiol* 26: 1003-1017, 1963.

Wiesel TN, Hubel DH. Comparison of the effects of unilateral and bilateral eye closure on cortical unit responses in kittens. *J Neurophysiol* 28: 1029-1040, 1965.

Wiggs CL, Martin A. Properties and mechanisms of perceptual priming. *Curr Opin Neurobiol* 8: 227-233, 1998.

Woodman GF, Kang MS, Rossi AF, Schall JD. Nonhuman primate event-related potentials indexing covert shifts of attention. *Proc Natl Acad Sci USA* 104: 15111-15116, 2007

Xiang JZ, Brown MW. Differential neuronal encoding of novelty, familiarity and recency in regions of the anterior temporal lobe. *Neuropharmacol* 37: 657-676, 1998.

Yi D, Kelley TA, Marois R, Chun MM. Attentional modulation of repetition attenuation is anatomically dissociable for scenes and faces. *Brain Research* 1080: 53-62, 2006.

CHAPTER 2
PROPERTIES OF SHAPE TUNING OF MACAQUE INFERIOR TEMPORAL NEURONS EXAMINED USING RAPID SERIAL VISUAL PRESENTATION

Journal of Neurophysiology, 2007, 97, 2900-2916[1,2]

We used rapid serial visual presentation (RSVP) to examine the tuning of macaque inferior temporal cortical (IT) neurons to five sets of 25 shapes each that varied systematically along predefined shape dimensions. A comparison of the RSVP technique using 100-ms presentations with that using a longer duration showed that shape preference can be determined with RSVP. Using relatively complex shapes that vary along relatively simple shape dimensions, we found that the large majority of neurons preferred extremes of the shape configuration, extending the results of a previous study using simpler shapes and a standard testing paradigm. A population analysis of the neuronal responses demonstrated that, in general, IT neurons can represent the similarities among the shapes at an ordinal level, extending a previous study that used a smaller number of shapes and a categorization task. However, the same analysis showed that IT neurons do not faithfully represent the physical similarities among the shapes. The responses to the two-part shapes could be predicted, virtually perfectly, from the average of the responses to the respective two parts presented in isolation. We also showed that IT neurons adapt to the stimulus distribution statistics. The neural shape discrimination improved when a shape set with a narrower stimulus range was presented, suggesting that the tuning of IT neurons is not static but adapts to the stimulus distribution statistics, at least when stimulated at a high rate with a restricted set of stimuli.

---

[1] This paper was co-authored by Elsie Premereur and Rufin Vogels

[2] The authors are indebted to Steve Raiguel and three anonymous reviewers for critical comments on an earlier draft of this manuscript.

INTRODUCTION

Visual object recognition and categorization are extremely difficult for artificial vision systems, although they seem to be accomplished effortlessly by the brain. In macaques, these processes are thought to depend on the highest stage of the ventral stream: the inferior temporal (IT) cortex (Dean 1976; Logothetis and Sheinberg 1996). Single IT neurons can be strongly selective for object attributes such as shape, texture, and color, while remaining tolerant to some transformations such as object position and scale (for a review, see Logothetis and Sheinberg 1996; Riesenhuber and Poggio 2002; Tanaka 1996).

In contrast with its extensive use in behavioral research (e.g., Chun and Potter 1995; Potter and Levi 1969; Subramaniam et al. 2000), the rapid serial visual presentation (RSVP) paradigm has rarely been used in combination with single-cell recordings in the higher visual cortex. In RSVP, images are presented sequentially and continuously (with no interstimulus interval or ISI) with each image replacing the previous one at the same location on the screen. Keysers et al. (2001) and Földiák et al. (2004) pioneered the use of the RSVP paradigm to examine the selectivity for complex images of neurons in the superior temporal sulcus (STS). Although an increasing presentation rate resulted in a flattening of the neuronal tuning, the stimulus-coding ability of the population of STS neurons recorded was preserved even at the highest presentation rates (14 ms/image), suggesting that RSVP is a useful technique for studying the stimulus selectivity of STS neurons with a large number of stimuli. However, in that and another study (Kiani et al. 2005) using RSVP, stimuli were highly complex and differed sharply.

In studying the stimulus selectivity of IT cells, several researchers (e.g., Brincat and Connor 2004; Kayaert et al. 2005a; Op de Beeck et al. 2001;

Sigala and Logothetis 2002) opted for the use of parametric shape configurations principally because it allows examining how the responses of IT neurons to complex stimuli are related to the parametric variation built into the stimulus sets. The use of all shapes to search for and test responsive neurons is a prerequisite for obtaining an unbiased measure of the responses and tuning of an IT neuron population to a set of parameterized shapes. However, the total experimental time available is limited when using the conventional presentation techniques, thus limiting the number of stimuli that could be presented in most of these studies. This drawback to use parametric shape sets can be overcome by the application of the RSVP paradigm because it allows the presentation of many stimuli. Thus one aim of the present study was to determine whether the RSVP technique is useful for studying the shape selectivity of IT neurons using parameterized sets of shapes (Kayaert et al. 2005a; Op de Beeck et al. 2001). The validity of the RSVP technique to study shape selectivity for parametric sets is not obvious since the differences among the shapes in such sets are much smaller than the stimulus differences employed in the previous IT studies using RSVP (Földiák et al. 2004; Keysers et al. 2001; Kiani et al. 2005).

Kayaert et al. (2005a) recorded from IT cells while showing simple shapes (e.g., a rectangle or triangle) parametrically manipulated along simple shape dimensions (e.g., taper or axis curvature). They found systematic response modulation along these simple dimensions with the largest response, on average, to the extreme values along a given dimension. The findings of Kayaert et al. (2005a), which suggest monotonic tuning in IT cortex for simple shapes, raise questions concerning the tuning curves for other, more complex shapes. Op de Beeck et al. (2001) used more complex shapes, but their squared configurations, consisting of merely eight shapes, did not allow disentangling preferences for extreme values on a given dimension from preferences for intermediate values along that dimension. Because of the

nature of their configuration, every shape corresponded a priori to an extreme value on a dimension. Hence in a first experiment, our primary aim was to examine the neural representation in IT cortex of complex shapes that vary systematically along shape dimensions using the RSVP paradigm. The application of the RSVP method provided an opportunity to increase the number of shapes per configuration. Thanks to this, we could also examine the extent to which the similarity among complex shapes is also represented on an ordinal and metrical level in IT cells when configurations are used that consist of a larger number of shapes than those employed by Op de Beeck et al. (2001).

As in the Kayaert et al. (2005a) study, the major portion of the neurons recorded in the present study showed a preference for the extreme values of the parametric space, at least within the range of values tested. One important issue, discussed by Kayaert et al. (2005a), is the degree to which the tuning for the extremities of the space is due to the repeated presentation of a restricted set of stimuli, i.e., the statistics of the stimulation history. Recent work has demonstrated that early visual and auditory neurons adapt to recent stimulus statistics so that information transmission is enhanced (e.g., Brenner et al. 2000; Dean et al. 2005; Fairhall et al. 2001; Sharpee et al. 2006; Smirnakis et al. 1997). Similar adaptive mechanisms might be operating at higher levels of the visual system or the effects of such adaptive mechanisms at earlier levels of the visual system could be inherited in IT. It is known that the responses of IT neurons can depend on previous stimulus presentations, e.g., stimulus repetition commonly reduces the responses of IT neurons (Baylis and Rolls 1987; Gross et al. 1967, 1969; Miller et al. 1991a; Riches et al. 1991; Sobotka and Ringo 1993), even with intervening presentations of other stimuli (e.g., Brown et al. 1987; Miller et al. 1991b; Sawamura et al. 2006). Because a high number of stimuli are presented repeatedly in RSVP, this paradigm might be more sensitive to adaptive effects than classical

testing paradigms in which one stimulus is presented per trial after acquisition of fixation and the intertrial interval is relatively long. This also implies that RSVP might be a useful technique with which to demonstrate the effect of stimulus statistics on neuronal tuning. Given recent demonstrations of an adaptive rescaling of neuronal responses in the fly visual system (Brenner et al. 2000) and guinea pig inferior colliculus (Dean et al. 2005) when the variance of the stimulus distribution is altered, we used RSVP to examine whether the tuning of IT neurons adapts to the properties of the stimulus distribution other than the mean. Note that the manipulation of stimulus distribution properties is possible only when parameterized sets of stimuli are used. Thus in a second experiment, we measured the responses of IT neurons to a set of shapes that varied along a single dimension. The neurons were tested in two successive blocks using stimuli that differed in stimulus variance and density between blocks. Parts of the results of the present study have been published in abstract form (De Baene and Vogels 2005).

METHODS

SUBJECTS

Two male rhesus monkeys (*Macaca mulatta*; *monkeys J* and *B*) served as subjects. Before conducting the experiments, aseptic surgery under isoflurane anesthesia was performed to attach a fixation post to the skull and to stereotactically implant a plastic recording chamber. The recording chambers were positioned dorsal to IT, allowing a vertical approach, as described by Janssen et al. (2000). During the course of the recordings, we took a structural magnetic resonance (MRI) image, with a copper sulfate filled tube inserted in the grid at one of the recording positions. The recording positions were

estimated by comparing this MRI with depth readings of the white and gray matter transitions and of the skull base during the recordings.

All animal care and experimental and surgical procedures followed national and European guidelines and were approved by the K.U. Leuven Ethical Committee for animal experiments.

STIMULI

All shapes (maximum size: 7.1°) were filled with pixel noise and were presented foveally in continuous rapid random sequences at a rate of 100 ms/image on a gray background on a monitor positioned 60 cm from the monkeys (60-Hz frame rate; 1,024 x 768 pixels). A trial started after 250 ms of stable fixation and ended when the monkey broke fixation or when every stimulus had been presented twice (for *experiment 1*) or 20 times (for *experiment 2*). Different visual stimuli were used in each experiment (see following text).

Experiment 1.

We generated five parametric sets in which shapes were varied systematically along two dimensions, permuting into 25 combinations of values of the two dimensions per set in a circular configuration (see Figure 1). The range of the dimensions of the parametric configurations was restricted in two ways. First, within a set, the pixel-based dissimilarities (cf. see following text, *Eq. 3*) between the shapes along a given dimension had to be largely similar to the pixel-based dissimilarities between the shapes along the other dimension. Second, these pixel-based dissimilarities, as calculated per set, had to be similar across sets.

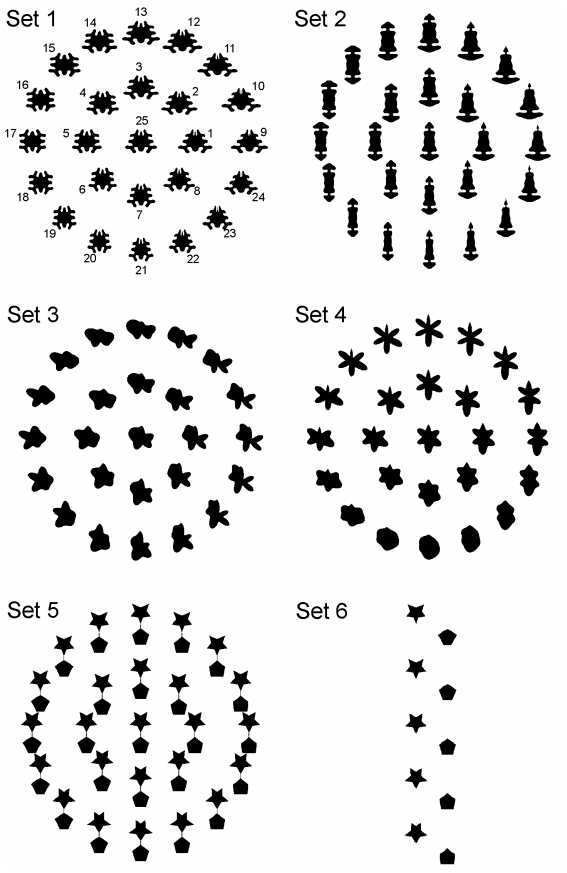

Figure 1. Visual stimuli *experiment 1.* The parametric configurations consisted of 5 sets of 25 shapes each. For each of these 5 stimulus sets, the parametric configuration of the stimuli was circular. The manipulated dimensions for *sets 1* and *2* were taper and aspect ratio (respectively, horizontal and vertical axis). The amplitude of 2 radial frequency components were varied in *sets 3* and *4.* In *set 5,* the taper of the bottom and the top part (respectively, vertical and horizontal axis) of the shape was manipulated. The isolated upper parts of the shapes on the vertical axis of *set 5* together with the isolated lower parts of the shapes on the horizontal axis of *set 5* constituted *set 6.*

For *sets 1* and *2,* the dimensions *taper* and *aspect ratio* were manipulated. The amplitude of two radial frequency components were varied in s*ets 3* and *4,* whereas the taper of the bottom and the top part of a two-part shape were independently manipulated in *set 5.* The isolated upper parts of the stimuli on the vertical axis of *set 5* as well as the isolated lower parts of the stimuli on the horizontal axis of *set 5* constituted a sixth set (Figure 1). The shapes of *set 6* were presented at the same positions as when presented in combination (*set 5*). The resulting 135 stimuli were presented in a random order.

Experiment 2.

In *experiment 2,* the parametric dimension showing the maximal response modulation in *experiment 1* was chosen for each of the five circular parametric sets of *experiment 1* (i.e., without *set 6*). Based on these five dimensions, we created two one-dimensional configurations of nine shapes each per set (Figure 2) and labeled these the "narrow-range" and the "wide-range" configurations. The parametric distances between the subsequent stimuli of the wide-range configurations were chosen such that no additional features were introduced for the shapes at the extremes. The narrow-range configurations were obtained by halving parametric distances between subsequent stimuli in the wide ranges. This resulted in a fourfold increase in variance and in an increase in the mean (pixel-based) dissimilarity (cf. following text, *Eq. 3*) between stimuli in the wide-range sets compared with the narrow-range sets, as well as in a lower density of the wide-range stimulus configurations.

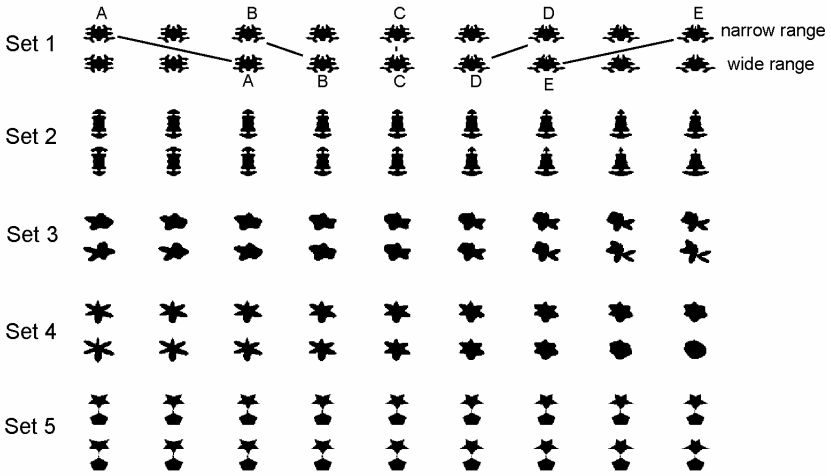

Figure 2. Visual stimuli *experiment 2.* For each of the 5 shape sets of *experiment 1,* 2 range configurations of each 9 shapes were generated for the parametric dimension showing maximal response modulation in *experiment 1.* The wide-range configurations were derived from the narrow-range configurations by doubling the parametric distance between the stimuli of these narrow-range configurations. The shapes denoted by the letters A to E are common to both ranges. Identical, matching stimuli are connected (—).

PROCEDURE

In both experiments, eye position was monitored through the pupil position using an infrared eye tracking system (ISCAN, EC-240A) at a sampling rate of 120 Hz. Monkeys were rewarded with a drop of fruit juice at an increasing pace as long as they kept their gaze within 3° (*monkey J*) or 1.5° (*monkey B*) of a black fixation target (0.17° diam) in the center of the display.

Experiment 1.

We searched for responsive neurons by presenting the 135 stimuli in a random order at a continuous rate (no ISI) of 3.3 images/s (27 neurons) or 10 images/s (57 neurons) in trials of maximally 270 stimuli while the monkey was passively fixating.

We visualized the responses of the cell in a peristimulus time histogram (PSTH) averaged over trials and all stimuli. If this PSTH showed that the cell responded, we continued presenting the stimuli for ~15 min. If the PSTH indicated that the cell did not respond to any of the stimuli, we abandoned this cell and searched for another. All 27 neurons that were initially tested with the slow presentation rate of 3.3 images/s (stimulus presentation duration = 300 ms) were subsequently tested with the short, standard 100-ms presentation times, allowing a comparison of the responses for the two presentation rates.

Experiment 2.

Search test. We searched for responsive neurons with the nine stimuli of every shape set presented for 300 ms, randomly intermixed, with an ISI of 700 ms. For half of the recorded cells, the wide-range configurations were used in the search test; for the other half, the narrow-range configurations

were used. When we found a neuron responsive to ≥1 of these 45 stimuli (based on the visual inspection of the PSTHs), the shape set with the largest neuronal responses was selected for the subsequent test.

RSVP test. The stimuli from the selected shape set with the same range configuration as that in the search task were presented randomly intermixed at a rate of 10 images/s (with no ISI) in trials of no more than 180 stimuli for a total duration of ~15 min. Afterward, the stimuli of the other range configuration of the same shape set were presented in a similar fashion for ~30 min. The second range was presented twice as long as the first range. This enables us to examine the temporal evolution of the adaptation to the stimulus statistics even when this adaptation process was slow. The order of the wide- and narrow-range configurations was counterbalanced across neurons.

RECORDINGS

Standard extracellular recordings were performed with Tungsten microelectrodes, lowered in a guiding tube, into the lower bank of the superior temporal sulcus and lateral convexity of IT during a passive fixation task. The signals of the electrode were amplified and filtered using conventional single-cell recording equipment. Spikes from individual neurons were isolated on-line using Plexon software (Plexon, Dallas, TX). The timing of the single units and the stimulus and behavioral events were stored with 1-ms resolution on a personal computer for later off-line analysis.

DATA ANALYSIS AND TESTS

In both *experiments 1* and *2,* the response of the neuron was defined as the mean number of spikes in a 50- to 200-ms analysis window relative to stimulus onset. Alternative analysis windows (50–250 ms and 100–200 ms)

showed highly similar results. The first three stimuli of every trial were excluded from all analyses because the responses of the majority of the recorded neurons were characterized by a burst at the start of every trial, lasting for ~300 ms (i.e., the total presentation duration of 3 stimuli at a rate of 100 ms/image). The last stimulus of every trial was also excluded from all analyses. This last stimulus differed from all others in the trial in that it was not followed by any other stimulus, excluding any potential backward masking effect that could have been present for all other stimuli.

Experiment 1.

All analyses were performed on those neurons showing shape selectivity within one or more shape sets. The shape selectivity of the neurons was examined by assessing the statistical significance of the observed variance of neuronal mean responses to stimuli within a shape set by using a permutation test. The range of variances per shape set expected by chance was determined by calculating new variances from the data after permuting the order of the stimuli within each trial while maintaining the actual spike counts. A distribution of 1,000 permuted variances was generated, representing the distribution of variances that would have been expected to occur by a chance association between stimulus and neuronal firing. If the observed variance of the neuronal mean responses to stimuli within a shape set was larger than the 95th percentile of the values in its own variance distribution, that neuron was considered to be shape selective within that shape set ($p < 0.05$, 1-tailed). The shape selectivity for the 10 shapes of *set 6* (the isolated parts of the shapes on the axes of *set 5*) was also tested with this permutation test.

As a measure of the selectivity for the shapes of a set, we computed the depth of selectivity (DOS) (Rainer and Miller 2000) for every neuron and shape set.

This measure of the degree of tuning of a neuron to a given stimulus set is defined as

$$[n-(\sum R_i / R_{\max})]/(n-1) \quad (1)$$

where n = number of shapes of a set, R_i = mean firing rate to i^{th} shape and R_{max} = max{R_i}. The DOS can vary between 0 (when the neuron responds equally to all shapes) and 1 (when there is a response to only one shape).

To estimate the reliability of our procedures in measuring the degree of selectivity, we employed an odd-even split half method. First we computed for each neuron the DOS indices separately for the odd and even repetitions of the stimuli and correlated these DOS indices across neurons. Because the split-half correlation is based on only half of the data, this was corrected by computing the Spearman-Brown split-half coefficient (Lord and Novick 1968):

$$r_{sb} = 2r_{xy}/(1+r_{xy}) \quad (2)$$

where r_{sb} = corrected split-half reliability coefficient and r_{xy} = correlation between the DOS-indices for the odd and even repetitions.

To investigate whether the population responses of IT neurons can reveal low-dimensional representations of similarity in the parametrically configured shapes, we compared the within-set configurations obtained from position corrected pixel-based similarities with the neuronal representation space in IT cortex. Pixel-based similarities between two shapes were computed for each of 99x99 relative positions. The positions of one shape corresponded to a 99x99-square grid (step size = 1 pixel) that was centered on the other shape. As the pixel-based dissimilarity measure, we computed the Euclidean distance between the gray-level values of the pixels of two shapes. This

procedure was done for each of the 99x99 relative positions, according to the formula

$$[(\sum_i^n (G_i^1 - G_i^2)^2)/n]^{1/2} \quad (3)$$

where G^1 and G^2 = gray levels of pixel i for shape 1 and 2 and n = number of pixels. The similarity of a stimulus pair was defined as the smallest value of the 99 × 99 positions.

The representation of shape similarities at the neuronal population level was analyzed by computing the Euclidean distance between a pair of stimuli *i* and *j* in the multidimensional space spanned by the responses of all neurons

$$[(\sum_{n=1:p} |\mathrm{Resp}_i(n) - \mathrm{Resp}_j(n)|^2)/p]^{1/2} \quad (4)$$

where n = cell number and p = number of recorded cells.

For each stimulus group, the different sets of similarity data were analyzed with nonmetric multidimensional scaling (MDS) using Statistica software.

To determine whether a systematic relationship existed between responses to the nine stimuli on the axes of *set 5* (further referred to as the compound stimuli; there are 5 stimuli per axis, but the 2 orthogonal axes have the central stimulus in common, producing 9 distinct stimuli) and responses to the isolated parts of these stimuli (further referred to as the constituent stimuli; *set 6*), we performed a linear regression analysis per cell with the responses to the compound stimuli as the dependent variable and with the sums of the responses to the respective constituent stimuli as the predictor variable. Additionally, we ran the same regression analysis after pooling the responses of all cells showing shape selectivity for the 10 constituent stimuli to examine

the relationship between the responses to the constituent stimuli and to the compound stimuli at a population level. In these regression analyses, a slope of 0.5 would indicate that the responses to the compound stimuli are the averages of the responses to the constituent stimuli, presented in isolation, whereas a slope of 1.0 indicates that the responses to the compound stimuli are the sum of the responses to the constituent stimuli.

We examined the temporal dynamics of both the selectivity among the shapes from different stimulus sets and discrimination among the shapes within one stimulus set at a population level using an information-theoretic approach (cf. Sugase et al. 1999). According to this approach, each predictable piece of information associated with an occurrence of a neuronal response [$I(S;R)$] is quantified as the decrease in entropy of the stimulus occurrence [$H(S)$]

$$I(S;R) = H(S) - H(S \mid R) = \sum\nolimits_s - p(s) \log p(s) - \left\langle \sum\nolimits_s - p(s \mid r) \log p(s \mid r) \right\rangle_r \quad (5)$$

where S = set of stimuli s, R = set of signals r (i.e. spike counts), p(s|r) = conditional probability of stimulus s given an observed spike count r and p(s) = *a priori* probability of stimulus s. The brackets indicate the average of the signal distribution p(r).

The use of a small number of trials induces an upward bias in the estimation of transmitted information. To correct for this, we subtracted the first-order correction term ($C1$) from the value calculated using *Eq. 5*, as $C1$ represents almost all the error due to limited sampling (Panzeri and Treves 1996)

$$C_1 = \frac{1}{2N \ln 2} \{ \sum\nolimits_s \widetilde{B}_s - B - (S-1) \} \quad (6)$$

where N = total number of stimulus presentations, $\widetilde{B}_S$ = number of non-zero response bins for the presentations of stimulus s, B = total number of bins and S = number of stimuli. Thus, the corrected transmitted information, Ic, is defined as follows:

$$I_c = I(S;R) - C_1 \tag{7}$$

To examine the time course of the transmitted information, we computed the neuronal responses using sliding windows of different durations. The results shown in Figure 9 are based on a window duration of 50 ms and the middle of the window was moved in 8-ms steps beginning 5 ms after the stimulus onset, up to 277 ms. These values are identical to those used by Sugase et al. (1999), facilitating a comparison of our with their results. A shorter time window of 10 ms produced highly similar results. The temporal evolution of the selectivity among shapes from different sets was examined by computing, for each time window, the information transmitted by the neuronal responses to four randomly selected stimuli, each from a different set (for the selection of the 4 stimulus sets, see following text), using *Eq. 7.* This was repeated 1,000 times. The temporal dynamics of the discrimination among the shapes of one stimulus set was examined by computing, again per time window, the information transmitted by the neuronal responses to four randomly selected stimuli from within that set. This was also repeated 1,000 times per set. This procedure permits excluding a potential bias due to a different number of stimuli or a different number of trials when comparing the transmitted information for stimuli within one set with the transmitted information for stimuli from different sets.

For both selectivity between sets and within sets, the information latency was measured from the stimulus onset to the center of the first of at least three consecutive windows for which the information differed significantly (using a

paired *t*-test) from the information in the window with the center at 5 ms after stimulus onset. The peak was defined as the center of the window in which the transmitted information, averaged across cells, reached a maximum. Stimulus sets were chosen for this selectivity time course analysis based on a cluster analysis (Ward's method; Statistica) of the neural similarity matrix of all neurons and all stimuli (see RESULTS). This clustering algorithm starts from a configuration with as many clusters as stimuli and groups similar stimuli in a series of steps (starting with the most similar ones) until all stimuli are clustered together.

Experiment 2.

All analyses were performed on those neurons showing shape selectivity in the RSVP test for at least one of the two range configurations, as tested by a one-way ANOVA ($p < 0.05$) for each range configuration (of 9 stimuli each).

To compare the neuronal selectivity at the population level for the shapes from the narrow- and wide-range configurations, the stimuli were first ranked based on the difference between the mean response to stimuli A and B, averaged across the two ranges, and the mean response to stimuli D and E of both ranges (see Figure 2 for definitions of stimuli A, B, etc.). If the former average response was larger than the latter, the stimuli were ranked in ascending order (i.e., A B C D E). If the opposite was true, a descending ranking was used (i.e., E D C B A). The same ranking was used for the nine stimuli. The responses to the nine stimuli of the wide- and narrow-range configurations were fitted with a second-order polynomial least-squares fit.

For all further analyses, we focused on the shapes common to the two ranges, i.e., the A to E stimuli of Figure 2, to study the effect of stimulus context on the responses and selectivity of our cells. For every cell, the depth of selectivity index (DOS, *Eq. 1*) was calculated for both the narrow and wide

range to quantify the degree of selectivity for the common shapes. To show the evolution of the neuronal selectivity over time, the data were subdivided into blocks of 10 presentations per stimulus and for each range configuration, DOS indices were calculated per block.

To quantify the neuronal ability to discriminate among shapes, we employed receiver operator characteristic (ROC) analysis (e.g., Cohn et al. 1975; Vogels and Orban 1990). For each neuron, ROC curves were generated by computing the distribution of the responses in the different presentations of a stimulus and then computing the proportion of spikes that exceeded a particular response criterion (in steps of 1 spike). The ROC analysis was done using the middle stimulus C and one of the extreme stimuli, either A or E (i.e., the one ranked as having the maximum response for that cell), of *experiment 2*. The area under the ROC curve generated by the neuronal response distributions for this pair of stimuli yields a score for the neuronal discrimination ability. Perfect discrimination results in an area of 1; random discrimination produces an area of 0.5. Because we were interested in discriminability per se, the lowest value -chance performance- is 0.5. Thus values < 0.5 were corrected by subtracting these from 1.

To examine whether the stimulus statistics altered the amount of information carried by the responses of the cells, the information transmitted by the neuronal responses regarding the presentation of shapes A to E (in a 50- to 200-ms time window) was quantified per cell for both the narrow and the wide range using *Eq. 7*.

RESULTS

EXPERIMENT 1

We recorded from 84 neurons (67 from *monkey J;* 17 from *monkey B*) using the RSVP procedure with a 100 ms/image presentation rate. Eighty neurons showed shape selectivity within one or more shape sets as measured with a permutation test (see METHODS), resulting in a significant response modulation for a total of 240 shape sets. For each cell, there was an average of 76.52 presentations per stimulus (minimum = 12, maximum = 151).

Across animals, the recording positions were estimated to range from 12 to 16 mm anterior to the external auditory meatus and included the lower bank of the superior temporal sulcus and the cortical convexity lateral to the anterior middle temporal sulcus.

Comparison of short and long presentation rates.

For 27 of the 80 cells that were selective at a 100-ms presentation rate, stimuli were first presented in an RSVP procedure using 300-ms presentation duration before using the regular 100-ms/image presentation rate. Thus for this sample of neurons, one can correlate the shape selectivity for the fast, 100-ms and slow, 300-ms presentation durations. For both presentation rates, responses were computed using the 50- to 200-ms analysis window. We analyzed the responses to the shapes of those sets (n = 83) for which there was a significant modulation for the standard, fast presentation rate. To qualitatively compare the responses for the two presentation rates, for each neuron, the 25 stimuli within a set were ranked according to the size of their responses in the 300-ms presentation condition. The same ranking was then used to order the stimuli presented at 100 ms/image. As shown in Figure 3*A*, the mean response in the 100-ms/image presentation rate condition, averaged

across neurons, decreased as a function of stimulus rank. A general linear model (GLM) repeated-measures ANOVA with rank as within-neuron factor showed that this modulation for the 100-ms/image sequences was significant [$F(24,1968) = 29.71$, $p < 0.001$], indicating that the overall ranking was preserved at this fast presentation rate. A similar overall preservation of shape rank was obtained when the stimuli were ranked using the responses of the fast presentation rate [Figure 3*B*; $F(24, 1968) = 30.39$, $p < 0.001$]. To quantify the similarity of the selectivity patterns under both presentation duration conditions, we correlated for each neuron the responses to the 25 shapes in the fast presentation rate with those to the same shapes in the slow presentation rate.

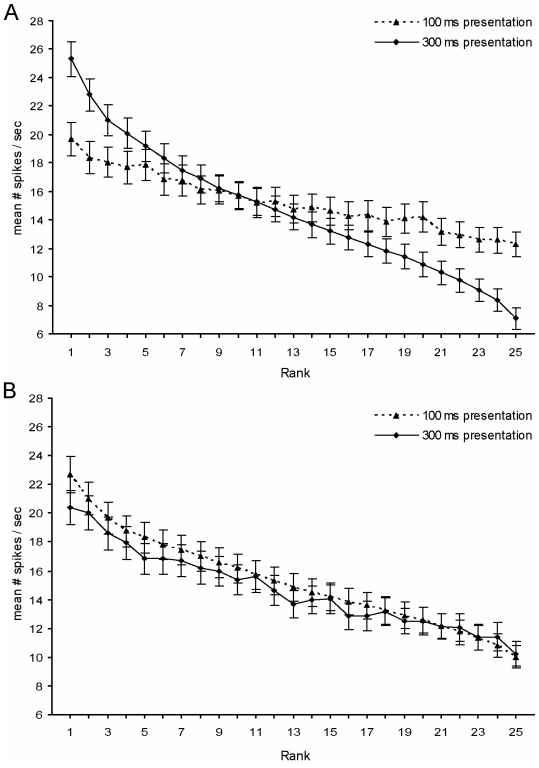

Figure 3. Ranking by response strength of all shapes of the sets showing significant response modulation ($n = 83$) averaged across all 27 cells for which the stimuli were presented both at a 300-ms/image rate (— with SEs) and at a 100-ms/image rate (- - - with SEs). *A*: shape ranking obtained from the neuronal responses in the 300-ms presentation duration condition was used to order the responses to the stimuli presented at the 100-ms/image presentation rate. *B*: shapes were first ranked based on the neuronal responses in the 100-ms presentation duration condition (- - - with SEs). This ranking was then used to order the responses to the stimuli when presented for 300 ms (— with SEs).

The median percent of variance in the response pattern measured at the fast presentation rate that could be explained by the response pattern measured at the slow rate was 0.32 (1st quartile = 0.13; 3rd quartile = 0.56), which corresponds to a correlation coefficient of 0.57. The preceding correlation analysis (as well as the ranking) was performed on the 25 stimuli of a set for which the neuron responded selectively. When the responses to all 135 stimuli were correlated instead, the median correlation between responses to the fast and slow rates was even higher: $r = 0.75$ (explained variance = 0.57).

The degree of shape selectivity within a set, as measured by the depth of selectivity (DOS; see METHODS), obtained at the fast presentation rate was highly correlated with that for the slow rate: $r = 0.81$ (explained variance = 0.66). Although highly correlated, the DOS for the slowest rate was significantly higher than for the 100-ms/image rate (averages of 0.45 and 0.34, respectively; Wilcoxon matched pairs test, $p < 0.001$). The Spearman-Brown split-half reliability coefficients (see METHODS) for the DOS indices were 0.89 and 0.96 for the slow and fast presentation rate conditions, respectively. The drop in selectivity with increasing presentation pace cannot be attributed to a possible higher noise level for the fast presentation rate condition because the Spearman-Brown split-half reliability coefficient for the fast presentation rate condition was not lower than that for the slow presentation rate condition. This difference in DOS, however, was due to smaller responses to the best shapes and larger responses to the nonpreferred shapes in the fast presentation condition. This can be appreciated by comparing the responses for stimulus ranks 1 and 25 for the 300-ms presentation duration in Figure 3*A* with those for the 100-ms presentation duration of Figure 3*B* (stimulus rank 1: 25 vs. 23 spikes/s; stimulus rank 25: 7 vs. 10 spikes/s). This suggests an underestimation of the degree of stimulus selectivity at the fastest presentation pace.

Note that the ranking curves for the fast and slow presentation of Figure 3 are more similar for the fast rate reference ranking (Figure 3*B*) than when the slow rate is used as a reference (Figure 3*A*). This can be explained as follows. Given the imperfect correlation of the responses in the two presentation conditions, the ranking curve for the slow rate will flatten if the shape ranks are based on the fast rate (compare — in Figure 3, *A* and *B*). Also, the ranking curve for the fast rate will flatten when the slow rate is used as the reference (compare - - - in Figure 3, *B* and *A*). Given the higher selectivity for the slow compared with the fast rate, the flattened curve for the slow rate will become somewhat similar to the ranking curve for the fast rate when the latter is used as reference (Figure 3*B*), whereas the curves for the two rates become more dissimilar when the slow rate is used as a reference (Figure 3*A*).

Tuning within parametric shape spaces.

Most of the neurons recorded showed a preference (i.e., the largest response) for the extreme values of the parametric space (see Figure 4 for a representative neuron).

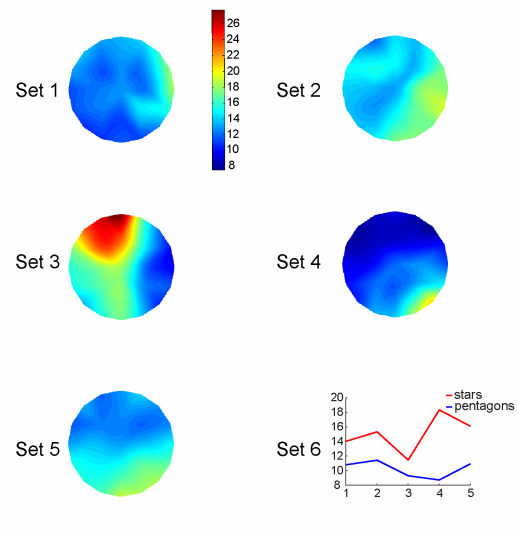

Figure 4. Schematic representation of the mean response strength (mean number of spikes in hertz counted in a 50- to 200-ms time window after stimulus onset) of an example neuron to all shapes of the shape sets. The ordering of the shapes is the same as in Figure 1 for *sets 1–5*. For *set 6,* the shapes are ordered from top to bottom (i.e. for both the stars and the pentagons, stimulus 1 is the upper shape shown for *set 6* in Figure 1; stimulus 5 is the lower one).

Instead of showing a uniform distribution across the parametric shape space, the neuronal shape preferences across the population of recorded neurons were concentrated at the extremes of the stimulus dimensions (Figure 5*A*). This preference for the extremes was significantly higher than expected by chance: in 215 of the 240 tested shape sets, the maximum response was for an extreme value of the parametric configuration [$p < 0.001$ as tested with a Binomial test over all sets; null hypothesis with expected relative frequency = 0.64 (16/25 extreme stimuli); all $p < 0.002$ for separate Binomial tests per parametric set].

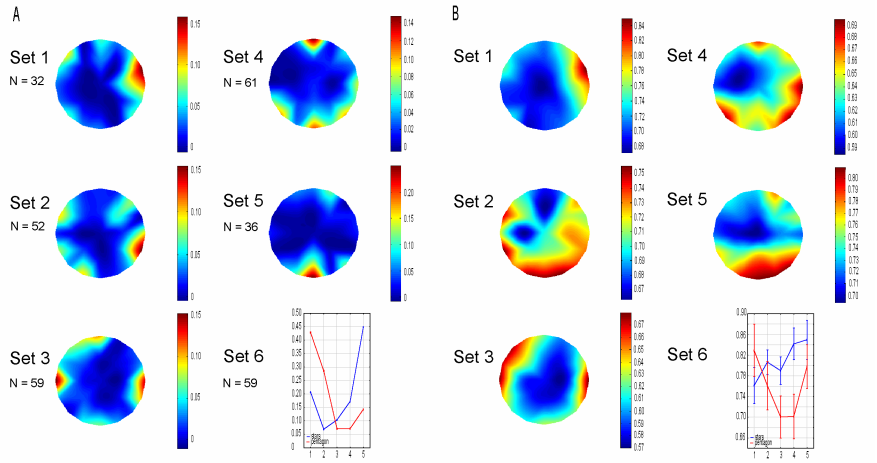

Figure 5. Population responses. Every row shows the results for a different shape set (from *set 1* to *set 6,* as labeled in Figure 1). *A*: distribution of the relative frequency of the preferred shape (shape producing the maximum response) for each of the sets. Only cells showing a significant modulation for that set are included (number of cells per set is shown). *B*: schematic representation of the mean normalized responses to all shapes per set, averaged over all cells showing a significant modulation for that set. Responses were normalized to the maximum response per cell. For *set 6,* the SE is shown for each stimulus.

We further tested whether the mean normalized responses of the cells showing shape selectivity for that shape set were uniformly distributed using a one-way ANOVA per shape set. For each set, the analyses showed that the mean responses were not uniformly distributed over cells ($p < 0.01$ for *sets 2* and *4;* $p < 0.001$ for *sets 1, 3,* and *5*). Indeed Figure 5*B* shows that the

neurons responded more strongly to the extreme values of a shape configuration.

The tuning for the extremities of the shape configuration was present for each of the five shape spaces and thus not just for the simple shape dimensions (aspect ratio and taper; shape *sets 1, 2,* and *5*) manipulated by Kayaert et al. (2005a). However, it should be noted that the radial frequency components we manipulated resulted in a systematic variation in the degree of indentation along the horizontal and vertical dimensions of *sets 3* and *4,* respectively. It is apparent from the response profiles that the latter change resulted in the strongest modulation.

We used the responses of the 80 neurons to those shape sets with significant modulation (240 sets) to compute the neuronbased (dis)similarity between each pair of stimuli. To determine how the neurons represent the similarities among the shapes, we analyzed the neural-based Euclidean distances (see METHODS) between the stimuli using MDS and compared the obtained neural-based configurations with the parametric, position corrected pixel-based stimulus configurations (Figure 6). Note that the pixel-based configurations preserved the stimulus order of the parametric configurations (Figure 1) and, in addition, showed that the physical distances among the shapes were similar along the two dimensions in each of the five configurations. Two-dimensional configurations explained most of the variance in the neural similarities for *stimulus sets 1–5* [averaged across monkeys: 86% (n = 32 neurons), 91% (n = 52), 88% (n = 59), 87% (n = 61) and 92% (n = 36) for *stimulus sets 1–5,* respectively].

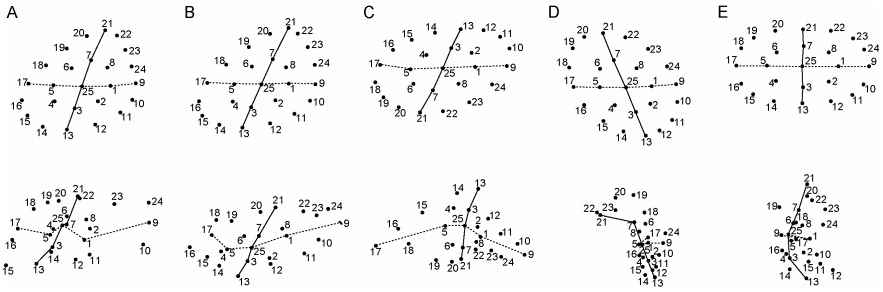

Figure 6. Multidimensional scaling (MDS-derived 2-dimensional) configurations of stimuli for *sets 1–5.* The numbers refer to the stimuli as they are labeled in Figure 1 (*set 1*). - - - and —, stimuli positioned on the horizontal and vertical meridian, respectively, of the parametric configurations (Figure 1). *Top panels:* configurations based on the position-corrected pixel-based similarity between stimuli. *Bottom panels:* configurations based on the neural-based similarity between stimuli. To aid in a visual comparison of the pixel-based with the neuron-based configurations, the latter were Procrustes transformed (i.e., a combination of translation, scaling, rotation, and reflection). *A–E*: configurations for *sets 1–5,* respectively.

An inspection of the configurations shown in Figure 6 clearly suggests that single stimulus dimensions unrelated to shape, such as area, cannot solely explain the observed stimulus selectivity. If, for example, this selectivity could be explained solely by area, for both *sets 1* and *2,* shapes 1, 5, 9, 17, and 25 (see Figure 1) should be clustered together, shape 11 should be clustered with shape 15, and shape 19 should be clustered together with shape 23. The configurations of Figure 6 clearly show that this is not the case.

The stimulus order in the neuron-based two-dimensional (2D) configurations matched the order of the pixel-based configurations for *sets 2* and *3.* The neuron-based 2D configuration for *stimulus set 1* deviated from that of the pixel-based configuration for two stimulus pairs, again demonstrating a good overall fit between physical and neural similarities. Note that for *set 3,* the neurons represented the horizontal dimension, i.e., "indentation", more acutely than the vertical one, which fits the distribution of the tuning shown in Figure 5*A*. An even more striking difference in sensitivity for the two radial frequency dimensions was present for *stimulus set 4.* For the latter stimulus set, the sensitivity along the horizontal dimension was much weaker

than along the vertical, indentation dimension, resulting in a highly anisotropic distribution of the stimuli in the two-dimensional space. However, note that along the vertical dimension, the stimulus order is relatively well preserved, indicating that the neurons represent variations along this dimension at the ordinal level.

Stimulus set 5 is a special case because the shapes were compound stimuli consisting of two shapes, each of which was varied systematically along one dimension. Figure 6*E* shows the 2D configuration for *shape set 5* and indicates that there was an overall correspondence between the parametric space and the neural configuration, albeit not as clear as that for *sets 1–3.* Also this set displayed a strong difference in sensitivity for the two stimulus dimensions: the neurons were more sensitive to variations along the vertical "star" dimension than along the horizontal "pentagon" dimension.

Comparison of responses to two-part shapes and their single parts.

An important question regarding the shapes in *set 5* is how the responses to these two-parts shapes relate to the responses to the single parts, i.e., the constituent stimuli. We quantified this relationship for 59 neurons that showed significant shape selectivity for the 10 constituent stimuli (*set 6;* see METHODS) or for the compound stimuli (*set 5*) as tested with a permutation test. Figure 7*A* shows a scatter plot for one of these cells in which the responses to the nine compound stimuli are plotted against the sum of the responses to the constituent stimuli presented in isolation. The responses to the compound stimuli were much smaller than the sum of the responses to the constituent stimuli, indicating a strongly nonadditive relationship between responses to the two-part and single shapes. The slope of the regression line relating the sum of the responses to the constituent stimuli and the responses to the compound stimuli was 0.51. Thus for this neuron, the responses to the

compound stimuli were very close to the average of the responses to the constituent stimuli presented in isolation. As expected from such averaging, the responses to the two-part shape were significantly lower than the responses to the part eliciting the best response when presented alone [paired *t*-test; $t(8) = 2.34$, $p < 0.05$; Figure 7*B*] and significantly higher than the responses to the part eliciting the worst response [paired *t*-test; $t(8) = -7.14$, $p < 0.001$; Figure 7*C*] when presented alone.

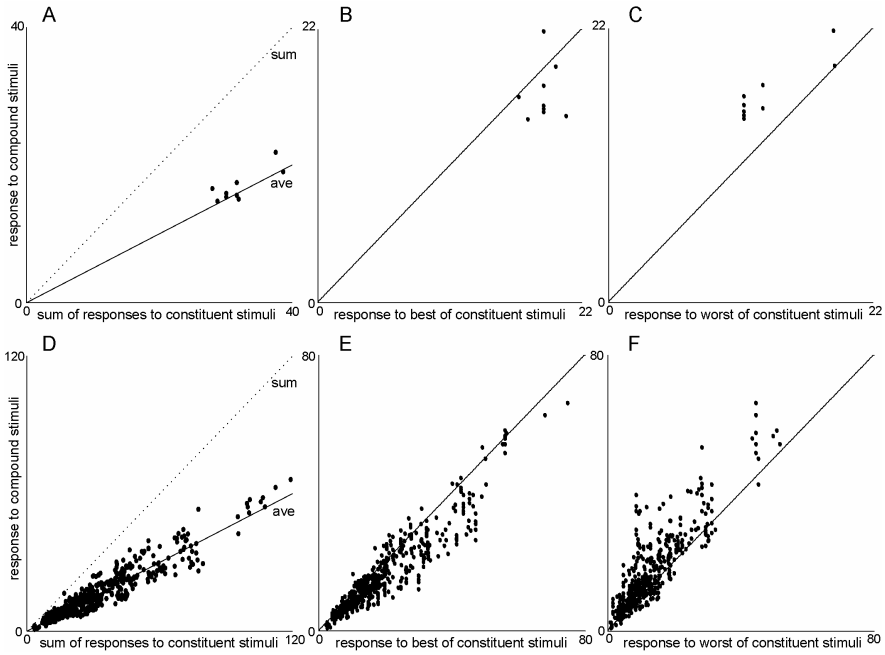

Figure 7. Responses to compound, 2-part shapes as a function of the responses to their respective constituent parts. *A* and *D*: responses to compound stimuli (in spike/s) are plotted against the sum of the responses to the constituent stimuli presented in isolation. - - - and —, respectively, the sum (slope = 1) and the average (slope = 0.5) of the responses to the constituent stimuli. *B* and *E*: responses to compound stimuli are plotted against the best of responses of the respective constituent stimuli. *C* and *F*: responses to compound stimuli are plotted against the worst of responses of the respective constituent stimuli. *A–C*: example data from a single cell. Each point corresponds to a different 2-part shape. *D–F*: scatter plots showing the responses of all 59 neurons showing response modulation for *set 5* or 6 ($n = 9$ 2-part shapes X 59 neurons).

For the population of 59 neurons, the mean slope of the regressions was 0.47 ± 0.51 (SD), suggesting that this averaging effect was present at the

population level. To examine this further, we pooled the data from all 59 neurons and performed the regression analysis on the pooled data. As shown in Figure 7*D*, the responses to the compound stimuli were highly correlated with the sum of responses to the constituent stimuli presented alone (r = 0.94). The slope of the regression for the pooled data set was 0.51, which indicates that the responses of a population of IT neurons to the compound stimuli can be predicted, virtually perfectly, as the average of its responses to the constituent stimuli presented in isolation. Again as expected, the responses to the compound stimuli were significantly lower than the responses to the respective best constituent shape [paired t-test; $t(530) = 5.44$, $p < 0.001$; Figure 7*E*] and significantly higher than the responses to the respective worst constituent shape [paired t-test; $t(530) = -7.26$, $p < 0.001$; Figure 7*F*].

As discussed in detail by Zoccolan et al. (2005), who reported a similar averaging effect, shifts in attention might explain such an effect. According to this attention hypothesis, the mean response to the compound stimuli will correspond to the average of the responses to the constituent stimuli presented in isolation if the attention of the monkey was directed toward one part (e.g., upper part) for approximately half of the presentations and the other part (e.g., lower part) for the rest of the presentations. This hypothesis assumes that the response distribution across all presentations of each compound stimulus is drawn more or less equally from the distributions of responses to the two constituent shapes. Thus the attention hypothesis predicts that the variance of the distribution of responses to each compound stimulus equals the variance of the distribution that is obtained by combining the response distributions to the constituent shapes when the latter are presented in isolation. Following Zoccolan et al. (2005), we computed the Fano factors, i.e., the ratio of the response variance to the mean response, for the response distributions of each of the compound shapes (observed Fano factor) and compared those to the

Fano factors computed for the distributions obtained by combining the responses to the constituent shapes, i.e., the response distributions predicted by the attention hypothesis. In performing this analysis for all 59 neurons, we found that the observed mean Fano factor (1.42) was significantly smaller than the value predicted by the attention hypothesis [1.69; paired *t*-test, $t(530) = 12.16$, $p < 0.001$]. When only those compound stimuli were included for which the responses of the neuron to the respective two constituent stimuli differed by a factor of two or more (i.e., where 1 constituent stimulus was much more effective than the other), similar results were found [observed mean Fano factor = 1.34 vs. Fano factor predicted by the attention hypothesis = 1.87; paired *t*-test, $t(101) = 8.84$, $p < 0.001$]. These results indicate that the reported average effect is not likely to be merely the result of shifts in attention.

Time course of shape selectivity.

The RSVP paradigm is similar to reverse correlation paradigms that have been used to examine the time course of e.g., orientation and spatial frequency selectivities in earlier visual areas such as V1 (e.g., Bredfeldt and Ringach 2002; Ringach et al. 1997, 2003). As in the latter studies, the present RSVP data can be used to examine the time course of shape selectivity. Because we used different shape sets, we can compare the time course of the selectivity for the shapes belonging to different sets with that of the selectivity for the shapes of a single set. If shapes from different sets are, at least on average, less similar than shapes from the same set, we could use this characteristic to address the question of whether the onset of selectivity depends on shape similarity because we would therefore expect earlier between-set than within-set selectivity.

To assess whether this prerequisite of greater within-set versus between-set similarity had been met, we first performed a hierarchical cluster analysis on the neuron-based similarities that were computed between all possible pairs of stimuli using the responses of all 80 neurons (neural-based Euclidean distances; see METHODS). As shown in Figure 8, all stimuli from *set 1* were assigned to the same cluster before being clustered with stimuli from other shape sets. The stimuli from *set 2* were also clustered together first as well as the stimuli from *set 5*. However, the stimuli of *sets 3* and *4* were not cleanly assigned to two separate clusters. Some stimuli from both sets were clustered with one another before being clustered with other stimuli from their respective sets. This is illustrated in more detail in Figure 8, *inset,* in which the shapes of the different sets that were clustered are indicated by colored squares. Interestingly, the clustered shapes of the two sets are similar regarding their "blobby" nature. When either *set 3* or *4* was excluded from the cluster analysis, the results showed the expected clustering: all stimuli from a set were first assigned to the same cluster before being clustered with stimuli from the other three sets. Therefore, to examine whether the onset of selectivity is earlier for the between-set compared with the within-set selectivity and to meet the prerequisite of larger within-set versus between-set similarity, we excluded *shape set 4* from further analyses (exclusion of *set 3* instead of *set 4* resulted in highly similar findings).

The temporal dynamics of the selectivity within and between shape sets was examined at the population level by evaluating the information about the stimuli that was available in the neuronal responses using a 50-ms sliding window, in steps of 8 ms (highly similar results were found using a 10-ms sliding window and steps of 5 ms). Figure 9 shows the time course of the mean transmitted information measures computed within each of the four sets and between the four sets. The average between-sets transmitted information was, as expected, larger than the within-set transmitted information.

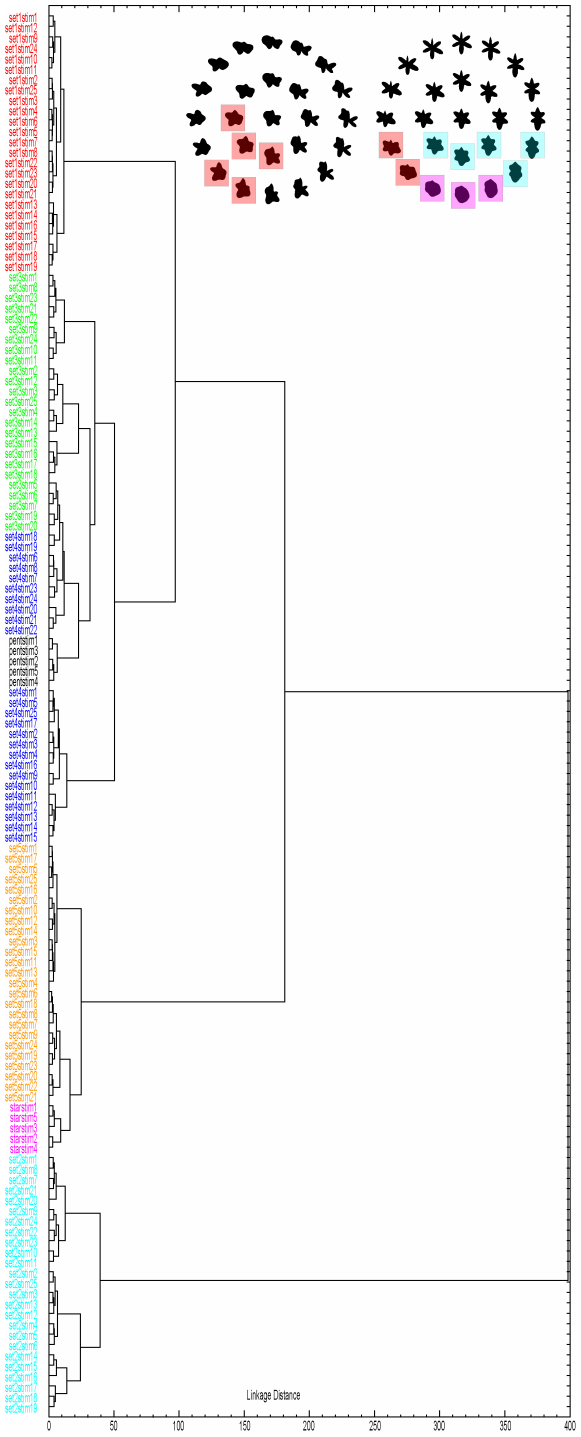

Figure 8. Results of a hierarchical cluster analysis on the responses of 80 cells for the 135 shapes of *experiment 1*. Stimuli presented in the same color belong to the same shape set (i.e. *set 1* = red; *set 2* = turquoise; *set 3* = green; *set 4* = blue; *set 5* = orange; stars = pink; pentagons = black). Stimuli of *sets 1, 2,* and *5* were first clustered together with all other stimuli of their respective set before being clustered with stimuli from other sets. Stimuli from *sets 3* and *4,* however, were not successfully assigned to 2 separate clusters: some stimuli were first clustered with stimuli from the other set before being clustered with other stimuli from their respective set. *Inset*: schematic representation of shapes of *sets 3* and *4*. Shapes of both sets that were clustered together are indicated by the same color: in the first step, the shapes in red are clustered together. In the next step, these red shapes are clustered together with the blue shapes. Finally, the purple shapes join the others in a single cluster.

Note that at the population level, the average within-set transmitted information differed among sets with *sets 1* and *5* showing the least information and *sets 2* and *3* the most. This fits with the larger number of neurons showing shape selectivity as assessed by the permutation test (see preceding text) for *sets 2* and *3* compared with *sets 1* and *5.* To compare the within and between sets transmission rates, we analyzed both the latencies and the peaks of the curves. The between-sets information peaked at 149 ms. The information for *set 2* peaked at the same time, whereas for the other shape sets, the peak was reached slightly later (at 173 ms, 157 ms and 173 ms for *sets 1, 3,* and *5,* respectively, resulting in a mean within-sets peak of 163 ms). The latency for the between-set transmitted information was 69 ms, whereas the latencies for the within-sets information were 109, 77, 85, and 109 ms for *sets 1-3* and *5,* respectively (resulting in a mean within-set latency of 95 ms).

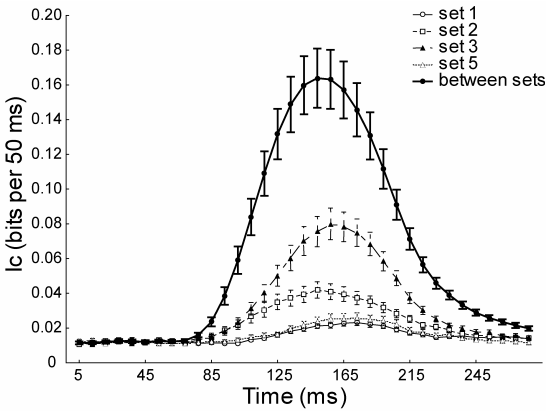

Figure 9. Transmitted information of the neuronal population computed within and between shape sets (between sets: thick solid line; *set 1*: solid line; *set 2*: dashed line; *set 3*: dash dot line; *set 5*: dotted line; maximum information transmission rate possible = 2 bits). The transmitted information (mean of 80 neurons, with SEs) is plotted against the center of the 50-ms sliding window (in steps of 8 ms).

Similar results were obtained if the within-sets transmission rates were computed on only those cells showing significant response modulation (instead of on all 80 recorded cells). The latencies for the within-sets transmitted information were 101, 77, 85, and 109 ms (mean within-sets latency = 93 ms), whereas the peaks were reached after 173, 149, 157, and

165 ms for *sets 1-3* and *5,* respectively (mean within-sets peak = 161 ms). When we compare these values to the between set latency and peak of 69 and 149 ms, respectively, then it is clear that although overall the within-set selectivity takes somewhat longer to develop than the between-set selectivity, this difference can be rather small [minimum latency difference of 8 ms (*set 2*) and minimum peak difference of 0 ms (*set 2*)].

EXPERIMENT 2

We recorded from 46 neurons (26 from *monkey J;* 20 from *monkey B*), 40 of which showed shape-selectivity within at least one of the two range configurations. For 22 neurons, the wide-range configuration was presented first. For the remaining 18 cells, the narrow-range configuration was presented first. For the stimuli of the first-presented configurations, an average of 808.31 presentations per stimulus was obtained per cell (minimum = 595, maximum = 961). For the stimuli of the configurations presented second, 1,513.48 presentations were shown on average per cell (minimum = 590, maximum = 4,027).

Across animals, the recording positions were estimated to range from 12 to 16 mm anterior to the external auditory meatus. All neurons, except one that was recorded from the lower bank of the STS, were from the cortical convexity lateral to the anterior middle temporal sulcus or from the lip of the STS (area TEm) (Seltzer and Pandya 1978).

Comparison of RSVP and slow, intermittent stimulus presentation.

As in *experiment 1,* we wanted to check whether stimulus selectivity is preserved at the fast RSVP rate of 100 ms/image. Each neuron was tested in the search test using the same stimuli as in the subsequent RSVP condition. In that search test, stimuli were presented for 300 ms with an ISI of ≥ 700 ms.

These are standard procedures for testing the responses of visual neurons. As for *experiment 1,* we used a ranking procedure to qualitatively compare the selectivity in the two testing procedures. It is important to note that in the search test, a minimum number of trials were presented per stimulus, just enough to check which shape set elicited the best responses. We compared the responses in the two testing procedures for those neurons (n = 39) for which in the search test, the stimuli were presented at least twice (median number of presentations = 3; 1st quartile = 2; 3rd quartile = 4). For both testing procedures, the responses were quantified using an identical 50- to 200-ms analysis window. We therefore ranked the responses to the stimuli of a given shape set in the RSVP test according to the responses in the search test. As shown in Figure 10, the responses to the stimuli presented in the RSVP test monotonically decreased as a function of the stimulus rank determined in the search test. This effect of stimulus rank was significant [repeated-measures ANOVA; $F(8,304) = 10.01$, $p < 0.001$], demonstrating that, at the population level, the stimulus preference at the 100-ms/image RSVP rate was overall similar to that obtained when using the intermittent presentations.

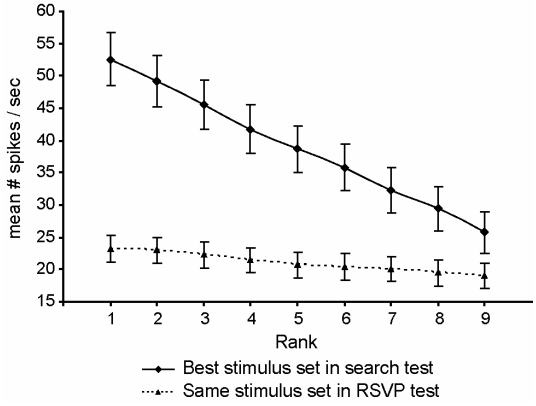

Figure 10. *Experiment 2*: ranking of the 9 shapes of the shape set with best neuronal responses in the search test by response strength (— with SEs). This stimulus rank, determined from the neuronal responses in the search test, was used to order the responses to the stimuli of the same shape set (with the same range) measured in the rapid serial visual presentation (RSVP) test (- - - with SEs).

Note that the average response level was considerably lower for the RSVP than for the intermittent presentations. The stronger forward and backward masking and stronger repetition suppression (see following text) in the RSVP compared with the slow intermittent presentations are the most likely factors contributing to this difference in the overall responsiveness.

To quantify the similarity of the selectivity patterns under both presentation duration conditions, we correlated for each neuron the responses to the nine shapes in the search test with those to the same shapes in the RSVP test. The median correlation coefficient was 0.52 which corresponds to a median explained variance of 0.27 (1st quartile = 0.03; 3rd quartile = 0.70).

The DOS indices obtained in the search test correlated significantly with those obtained in the RSVP test [$r = 0.35$ ($p < 0.05$; $n = 39$)]. The Spearman-Brown split-half reliability coefficients for the DOS-indices were 0.87 and 0.97 for the search test and RSVP test, respectively. Thus the low correlation between the DOS of the search and RSVP tests is not due to a low reliability of the DOS measure in the tests but reflects a genuine change in the degree of selectivity. The mean DOS for the search test was significantly higher than for the RSVP test (0.32 and 0.18, respectively; Wilcoxon matched pairs test, $p < 0.001$).

Effect of stimulus statistics on stimulus selectivity. We performed analyses on the stimuli common to the two range configurations (stimuli A-E in Figure 2) to study the effect of the stimulus distribution statistics, i.e., stimulus context, on the responses and selectivity of all tested cells. First, we performed a repeated-measures ANOVA on the neuronal responses for these common shapes with order of sets as a between-neurons variable (wide range first or narrow range first) and stimulus rank and range (wide or narrow) as within-neurons variables.

Stimulus rank was determined as described in METHODS. As expected from the stimulus ranking procedure, the main effect of rank was significant [$F(4,152) = 24.77$, $p < 0.001$]. There was no main effect of range ($F < 1$), but more importantly, the interaction range x rank was significant [$F(4,152) = 7.53$, $p < 0.001$], indicating a difference in selectivity between the sets with different ranges.

To elaborate on this result, we compared the slopes of the polynomial fits to the population responses ($n = 40$ neurons) for the nine stimuli (Figure 11*A*): the slope of the polynomial fit for the narrow range was steeper than the slope of the polynomial fit for the wide range (narrow range: $y = 0.29x^2 - 3.87x + 32.03$; wide range: $y = 0.10x^2 - 1.82x + 27.35$), indicating that the narrower range increased the selectivity of the same shapes. The polynomial fits for the two set orders are shown separately in Figure 11*A, insets*. For both orders, the slope of the polynomial fit for the narrow range was steeper than the slope of the polynomial fit for the wide range (narrow range first: narrow range: $y = 0.21x^2 - 2.89x + 28.67$; wide range: $y = 0.04x^2 - 1.15x + 25.93$; wide range first: narrow range: $y = 0.38x^2 - 4.86x + 35.39$; wide range: $y = 0.16x^2 - 2.50x + 28.77$). Additional repeated-measures ANOVAs on the neuronal responses for the common shapes for both orders separately with stimulus rank and range (wide or narrow) as within-neurons variables confirmed that, for both orders, the main effect of rank and the interaction range x rank were significant [wide range first: rank: $F(4,84) = 19.25$, $p < 0.001$, range x rank: $F(4,84) = 4.78$, $p < 0.002$; narrow range first: rank: $F(4,68) = 8.07$, $p < 0.001$, range x rank: $F(4,68) = 3.31$, $p < 0.02$], whereas the main effect of range did not reach significance [$F < 1$ and $F(1,17) = 2.42$, $p > 0.10$ for, respectively, the wide range and narrow range first]. Note that the overall response level appears to depend on the order (compare Figure 11*A, insets a* and *b*), but statistical testing showed that this interaction between range and order did not reach significance [range x order: $F(1,38) = 2.77$, $p > 0.10$]. In fact, there was

no significant main effect of order of sets ($F < 1$), and no interaction-effects with order were significant (rank x order: $F < 1$; range x rank x order: $F < 1$).

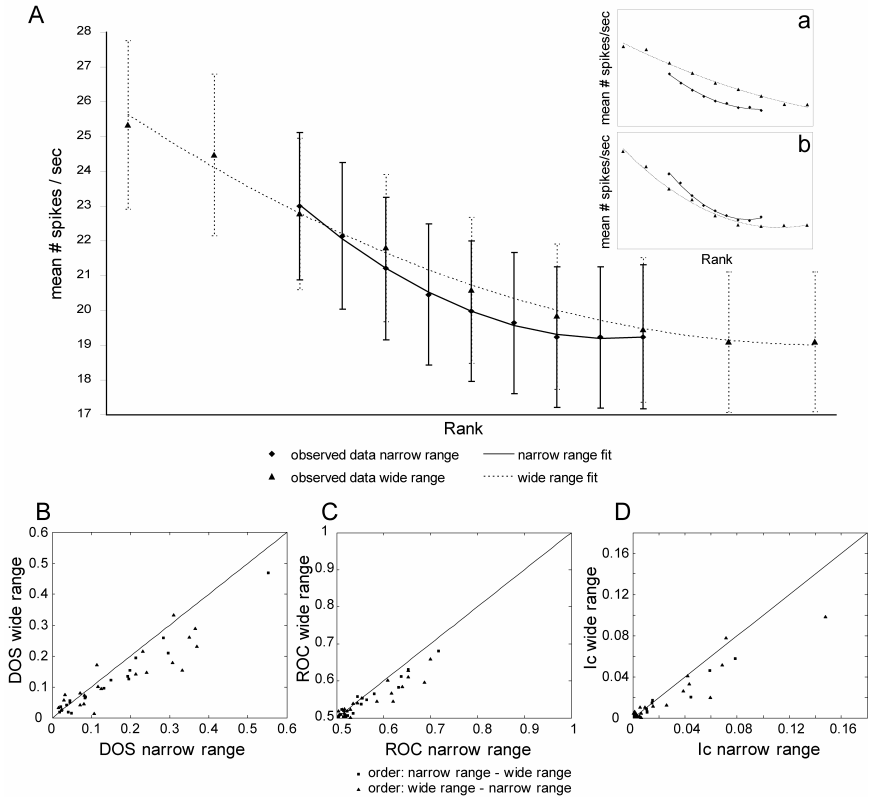

Figure 11. Shape selectivity compared for 2 stimulus ranges (*experiment 2*) at the population level. *A*: comparison of the ranked responses to stimuli from the 2 range configurations (narrow range: ■ wide range: ▲ both with SEs). — and - - -, 2nd-order polynomial fit for the narrow ($R^2 = 0.998$) and wide range ($R^2 = 0.993$), respectively. Second-order polynomial fits for the split data, based on whether the narrow range or the wide range was tested first, are shown in the *insets Aa* and *Ab,* respectively (narrow range first: R^2 narrow range = 0.995, R^2 wide range = 0.988; wide range first: R^2 narrow range = 0.994, R^2 wide range = 0.993). *B*: depth of selectivity (DOS) indices for the wide-range configuration as a function of the DOS indices for the narrow-range configuration. Each point represents 1 neuron. ■, neurons for which the narrow-range configuration was presented before the wide-range configuration. ▲, neurons for which the opposite stimulation order was used. —, equal DOS indices for both range configurations. *C*: ROC values for the wide-range configuration are plotted against the ROC values for the narrow-range configurations. For both ranges, ROC analyses were performed using 1 of the extreme stimuli (either A or E, depending on which 1 was ranked as having the maximum response) and the middle stimulus (*C*). Same conventions as in *B*. *D*: information transmission rates (*Ic*'s) for the wide-range configuration are plotted against the *Ic*'s for the narrow-range configurations (maximum information transmission rate possible = 2.32 bits). Same conventions as in *B*.

This difference between selectivities for the two range configurations could also be demonstrated by the significantly smaller (Wilcoxon matched pairs test, $p < 0.001$) DOS index for the wide range (mean = 0.12) compared with the narrow range (mean = 0.16; Figure 11*B*). A separate analysis for the two set orders excluded the possibility that the difference in the DOS indices of the two range configurations is merely a presentation order effect: for each presentation order, the DOS index for the wide-range configuration was significantly smaller compared with the narrow range (Wilcoxon matched pairs test, narrow range first: $p < 0.01$; wide range first: $p < 0.05$; Figure 11*B*).

To show that not only is selectivity increased for the narrower range configuration but that the discriminability of the shapes is also improved, we employed ROC analysis. The goal of the ROC analysis was to measure the ability of the neurons to discriminate between the middle stimulus C and one of the extreme stimuli A or E (Figure 2), depending on which of both stimuli was ranked as having the best response. The ROC analysis takes into account not only mean differences in firing rate - as the DOS index does - but also considers the variability of the spike counts for the presentations of a stimulus. For each range configuration, this analysis was applied to the responses of each cell to the stimuli C and A or E of Figure 2. The ROC values obtained for the narrow-range configuration were significantly larger than for the wide-range configuration (Wilcoxon matched pairs test, $p < 0.001$), indicating that the discriminability of the same shapes was larger for the narrow-range stimulus distribution than for the wide-range stimulus distribution (Figure 11*C*). A separate analysis for the two orders excluded the possibility that the difference in the ROC values of the two range configurations is merely a presentation order effect: for each presentation order, the mean ROC value for the wide-range configuration was significantly smaller compared with the narrow range (Wilcoxon matched pairs test, both orders: $p < 0.01$; Figure 11*C*).

If discriminability of the shapes is improved for the narrow-range configuration over the wide range, one would expect the neurons to transmit more information about the stimuli in the narrow-range configuration as well. For both range configurations, we calculated the information available in the neuronal responses to the five stimuli common to the two configurations in a 50- to 200-ms time window. A Wilcoxon matched pairs test showed that significantly more information was indeed transmitted by the neurons in the narrow-range compared with the wide-range configuration ($p < 0.02$; mean *Ic* narrow range = 0.025 bits; mean *I*c wide range = 0.018 bits; Figure 11*D*).

If the increase in selectivity for the narrow compared with the wide range results from an adaptation to the stimulus statistics, one would expect this difference to evolve during stimulus exposure. Thus we computed DOS indices in succeeding blocks of 10 presentations per stimulus and did this for the first 30 blocks. These analyses, examining the evolution of the DOS index over time, were performed on the stimuli common to the two range configurations (A-E of Figure 2). A GLM repeated-measures ANOVA with range (wide or narrow) and presentation block as within-neurons variables showed a significant main effect of range [$F(1,39) = 5.51$, $p < 0.05$], confirming a selectivity difference between the two range sets. The main effect of presentation block was also significant [$F(29,1131) = 26.72$, $p < 0.001$], showing a decrease in selectivity with an increasing number of presentations of the stimuli. Importantly, the interaction between range and presentation block was significant [$F(29,1131) = 2.54$, $p < 0.001$], revealing a different evolution of the neuronal selectivity over time for the two range configurations. To evaluate this interaction, we performed post hoc comparisons (Bonferroni test) between the two ranges for every presentation block. Initially, there were no significant differences between the ranges (*blocks 1-7*: $p = 1$). After ~70 presentations/stimulus (*block 8*), the first difference began to appear: the DOS for the narrow-range set was larger than

for the wide-range set ($p < 0.05$). Up to 150 presentations, most blocks showed this pattern (*block 10*: $p < 0.001$; *block 12* up to 14: $p < 0.01$; but *block 9*: $p > 0.5$ and *block 11*: $p > 0.14$). After >150 presentations, the differences in DOS between the two ranges failed to reach significance (*block 15*: $p > 0.07$; *block 16* up to 30: $p = 1$), although the DOS indices were still consistently greater for the narrow compared with the wider range. Thus as shown in Figure 12, the higher DOS for the narrow compared with the wide range was not present from the start but evolved during the successive presentations, suggesting that this effect indeed resulted from an adaptation to the stimulus statistics.

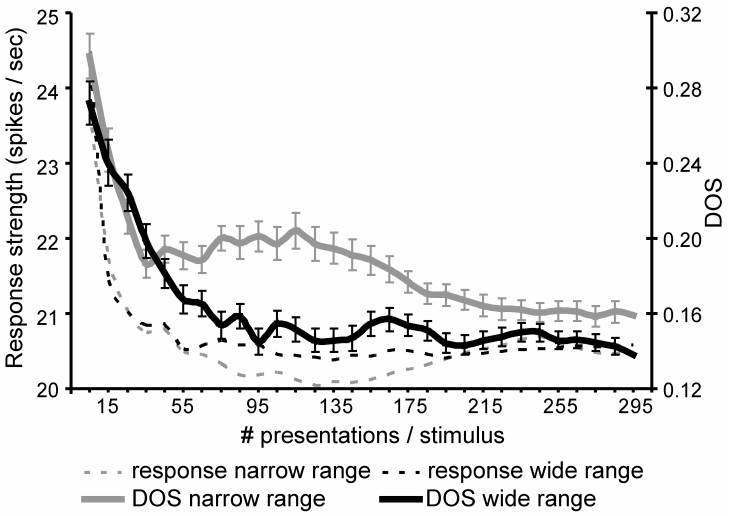

Figure 12. Temporal evolution of the DOS index and the response strength for the narrow- and wide-range configurations (*experiment 2*). The computations were performed for the first 300 presentations/stimulus in succeeding blocks of 10 presentations/stimulus for the common shapes of the 2 range configurations (shapes A–E as labeled in Figure 2). Population data for the narrow- and wide-range configuration are depicted by gray and black lines, respectively. The evolution of the response strength (in the range depicted on the left *y* axis) is represented by dotted lines. The evolution of the DOS index (in the range depicted on the right *y* axis) is represented by solid lines (with SEs).

Using the same subdivision in presentation blocks of the data, we also analyzed the evolution in time of the neuronal mean response strengths of the common shapes (A-E; Figure 2) of the two range configurations (Figure 12)

using a GLM repeated-measures ANOVA with range (wide or narrow) and presentation block as within-subjects variables. Neither the main effect of range, nor the interaction effect of range x presentation block reached significance ($F < 1$ for both). The main effect of presentation block was significant [$F(29,1131) = 9.00$, $p < 0.001$]): the neuronal responses to the stimuli decreased with repetition, an effect typical for IT neurons (Baylis and Rolls 1987; Gross et al. 1967, 1969; Miller et al. 1991a; Riches et al. 1991; Sobotka and Ringo 1993).

DISCUSSION

The present study used RSVP to investigate the tuning of macaque IT cortical neurons to shapes that varied systematically along predefined shape dimensions. A comparison of the RSVP technique using 100-ms presentations with that using longer presentation durations and an ISI showed that the shape preference can indeed be determined using RSVP. Using relatively complex shapes that vary along relatively simple shape dimensions, we found that the large majority of neurons preferred the extremes of the shape configuration, extending the results of a previous study using very simple shapes and standard stimulation procedures (Kayaert et al. 2005a). In addition, a population analysis using MDS showed that for some stimulus sets, the neurons can represent the similarities among the shapes at an ordinal level, extending a previous study that used a much smaller number of shapes and a categorization task (Op de Beeck et al. 2001). However, the same analysis demonstrated that the IT neurons do not faithfully represent the physical similarities among the shapes: the sensitivity of IT neurons can depend strongly on the particular stimulus dimension. We also showed that the IT neurons adapt to properties of the stimulus distribution other than the mean. The degree of shape discrimination by a population of neurons

depended on the stimulus distribution statistics. Although the latter effect was small, it was significant and suggests that the tuning of IT neurons is not fixed but adapts to the stimulus statistics at least when stimulated at a high rate with a restricted set of stimuli. The implications of these and other findings of the present study will be discussed in more detail in the following text.

RSVP VERSUS TRADITIONAL TESTING

RSVP-methods have been used in the retina, LGN, and early visual areas with success (e.g., Berry et al. 1997; Jones and Palmer 1987; Reid and Shapley 2002; Ringach et al. 1997). In these studies, stimuli were shown for short durations (< 50 ms) without ISIs, and regression methods (reverse correlation) were used to obtain receptive field maps and stimulus selectivities. Fewer studies have employed this method in higher visual cortex, especially in the ventral visual stream. Studies using backward masking in IT (Kovács et al. 1995; Rolls and Tovee 1994) showed that although the response level declines with decreasing stimulus onset asynchrony, the stimulus preference is preserved. This suggests that fast RSVP can be used to show the stimulus preferences of IT neurons and indeed, subsequent studies by Keysers and colleagues (2001) demonstrated that the stimulus preference of STS neurons is relatively well preserved for fast RSVP sequences. We show in the present study that even for stimuli that are much more similar than those used by Keysers et al. (2001), the shape preference at fast RSVP sequences correlate with those obtained using longer presentation durations (*experiment 1*) or standard testing procedures (*experiment 2*). This suggests that RSVP is a useful method for studying the shape tuning of IT neurons.

However, four caveats should be taken into account when using RSVP to study the shape selectivity of IT neurons. First, pilot work using presentation

durations shorter than 100 ms produced less reliable results and weaker responses, but this might have been specific to the sort of stimuli used. Thus one should perform control studies with longer stimulus durationswhen using presentation times < 100 ms in IT. Second, we found that the degree of stimulus selectivity was on average somewhat smaller with shorter presentations; this agrees with the finding of Keysers et al. (2001) that increasing the presentation rate results in a flattening of the neuronal tuning. These results thus imply that RSVP might underestimate the degree of shape selectivity. Third, RSVP implies the occurrence of forward and backward masking effects as well as effects of repetition. Each of these three factors will result in decreased responses, and the suppression arising from repetition is likely to be stronger when stimulus similarity within the stimulus sets is larger. The latter is a likely explanation for the large difference in response levels between the standard and RSVP paradigms that we observed for the highly similar shapes of *experiment 2*. Such repetition-based suppression effects can be reduced by using interleaved presentations of highly different stimulus sets as we did in *experiment 1*. Fourth, adaptation to stimulus statistics might be more prominent when RSVP is used, given the high number of repeated presentations of a given stimulus set within a short time span. Indeed, we could demonstrate effects of the stimulus distribution on the measured neuronal selectivity (*experiment 2*) although the significant effects were relatively small and restricted to the degree of shape selectivity and did not extend to shape preference. Thus in general, the present data suggest that although the RSVP method is well suited to studying stimulus preferences (stimulus ranking), estimates of the degree of selectivity (tuning bandwidth) should be made with some caution because these appear to depend on the specifics of the measurement procedure.

TUNING FOR EXTREMITIES OF SHAPE CONFIGURATIONS

The very large majority of neurons responded most strongly to a shape located at an extremity of the explored shape spaces. This sort of tuning for extremities was observed for each of the five shape sets in *experiment 1*. Tuning for the extremities of parametric shape spaces has been described before by Kayaert et al. (2005a), but in that study, the stimuli were much simpler (variations of a triangle and rectangle) than in the present investigation. The present study shows that tuning for extremities is also present for complex shapes when dimensions such as taper, aspect ratio, and "indentation" (amplitude of Fourier descriptor) are varied, at least within the stimulus range explored in the present study.

Kayaert et al. (2005a) suggested that IT neurons show dimension-specific shape tuning and tend to prefer the extremes of these dimensions, i.e., monotonic tuning. Similar monotonic tunings have been reported in IT neurons for faces varying along dimensions such as caricaturization, aspect ratio, and inter-eye distance (Freiwald et al. 2005; Leopold et al. 2006). As yet, the significance of tunings for extremities is unclear (for further discussion, see Kayaert et al. 2005a; Leopold et al. 2006). One might conjecture that IT neurons represent shapes in terms of their distance with respect to extremities along specific shape dimensions. One issue to consider regarding the interpretation of the observed stronger responses for extreme stimuli is that the employed stimuli are likely to be suboptimal for the tested IT neurons. The critical question here is why the extreme stimuli are less suboptimal than the other stimuli given the likely high-dimensional space in which IT neurons are tuned. A satisfactory answer to this important question will require a full description of the nature of the tuning functions of IT neurons as well as knowledge about the relative position and range of the stimulus set with respect to these tuning functions.

The possibility cannot be excluded that IT neurons learn the stimulus statistics of the parametric shape spaces and thus that the observed tunings depend on the stimulation history and the specific stimulus spaces. *Experiment 2* demonstrated that the responses of IT neurons can indeed be modified by changes in input statistics. These effects were small in comparison to the degree of monotonic tuning, but stimulus statistics might exert a more profound effect with more extensive daily repetition of the same stimulus spaces as is the common practice in single-cell recording experiments.

The MDS results clearly show that IT neurons are more sensitive for some stimulus variations (e.g., indentation; stimulus *sets 3* and *4*) than for others. This is in agreement with previous studies using calibrated sets of shapes (Kayaert et al. 2005a,b). This sort of differential sensitivity for stimulus dimensions is difficult to explain by stimulation-history-dependent mechanisms because the stimulation frequency was equal for the different dimensions. This does not mean that IT tunings are not modifiable by experience: indeed, several studies show that the degree of selectivity of IT neurons is greater for extensively trained than for novel stimuli (Baker et al. 2002; Freedman et al. 2006; Kobatake et al. 1998).

RESPONSES TO TWO-PART SHAPES AND THEIR SINGLE PARTS COMPARED

The shapes of *set 5* consisted of two parts connected by a thin line, similar to the stimuli used by Baker et al. (2002). Using these so-called “baton stimuli”, Baker et al. (2002) found nonlinear interactions between the constituent parts of the compound stimuli in animals that were trained to discriminate between the compound shapes. In our study, the responses to the two-part shapes could be predicted surprisingly well from the responses to the constituent

shapes (*set 6*) presented at the same visual field locations. In fact, the response to the two-parts shapes was the average of the individual responses to the constituent shapes, which agrees extremely well with Zoccolan et al. (2005). In both studies, the constituent shapes were relatively small (~2°), both shapes were presented close to each other and short presentation durations (100 ms) were employed (although with a 100-ms ISI in the Zoccolan et al. study) while the monkeys were passively fixating. So it appears that under the behavioral conditions and for the small stimulus variations used in our and the Zoccolan et al. study (2005), the shape interactions do not depend on shape identity but depend mainly on response. However, Missal et al. (1999) found that in some IT neurons, shape interactions can depend on the shape. In that study though, the interacting shapes differed more than in the present study, were much larger and were presented at greater eccentricities. The role of these stimulus factors needs to be addressed in further studies. The animals in ours and the Zoccolan et al. study were not trained to discriminate between the compound stimuli. This might be of importance because Baker et al. (2002) demonstrated that the response and selectivity for compound shapes can be affected by the training history of the subjects.

TIME COURSE OF SHAPE SELECTIVITY AND SHAPE SIMILARITY

Sugase et al. (1999) and Matsumoto et al. (2004) investigated how well single IT responses could categorize stimuli consisting of geometric shapes and monkey or human faces with various expressions. At the population level, global categorization (i.e., categorizing the stimuli as shapes, monkey faces, or human faces) started in the earliest part of the responses, whereas fine categorization (i.e., categorization within a global category, e.g., based on facial expression) occurred, on average, 51 ms later. Tsao et al. (2006) obtained similar results by comparing face categorization (faces vs. objects)

and face identification. We examined whether this difference in the time of onset of stimulus selectivity is also present when the stimuli differ in only shape but not in other features and are not biologically relevant categories (such as faces). If the difference in the onset of stimulus selectivity in between- versus within-categories is merely related to average differences in similarity, then one should observe a similar effect for groups of shapes, although in the latter case, all stimuli belong to the global biologically irrelevant category of geometrical shapes. We defined the shape categories using cluster analysis of the neural responses. We found that shape categories thus defined were differentiated slightly faster than the individual shapes of a single set. Because the procedure that we used to compute the latencies differed from the one used by Sugase et al. (1999), we can compare only the relative difference in the onset of stimulus selectivity in between- versus

within-categories between both studies. The average between- versus within-category latency difference (26 ms, minimum: 8 ms, maximum: 40 ms) found in the present study was only half the mean latency difference of 51 ms between the global and fine categorization reported by Sugase et al. (1999). It cannot be excluded that this discrepancy between ours and Sugase et al.'s result might be due to a possible smaller difference in the average similarity between stimuli from the same versus a different category in our study. This conjecture is difficult to verify given the large dissimilarities between the stimulus sets of the two studies.

The shape selectivity peaked at about 150 ms, which fits the peak of the shape discrimination of IT neurons reported by Rollenhagen and Olson (2000) and obtained with a classical testing paradigm. However, it lies between the two values obtained by Tsao et al. (2006) for face categorization (133 ms) and identification (192 ms) and is later than the human versus animals face classification obtained in IT using a similar RSVP technique (Kiani et al.

2005). Thus it is possible that biologically relevant stimuli are discriminated faster by IT neurons than abstract, meaningless shapes, but this should be examined with stimuli calibrated for contrast, luminance and other low-level confounding variables.

ADAPTATION TO STIMULUS DISTRIBUTION STATISTICS

Experiment 2 is to our knowledge the first demonstration that the measured tuning of IT neurons is influenced by the stimulus distribution statistics: extensive stimulation using very similar stimuli increased the selectivity of IT neurons for these stimuli compared with stimulation with less similar stimuli. This suggests that the selectivity of IT neurons is not fixed but can be dynamically adjusted based on the input statistics. Note that this effect occurred for highly familiar stimuli and thus differs from changes in selectivity observed with the introduction of novel stimuli (Rolls et al. 1989).

Adaptation to input statistics is seen in the visual system of widely different animal species, such as the fly (Brenner et al. 2000) or the guinea pig (Dean et al. 2005). The time course as well as the size of our effect differs, however, from that observed in the fly visual system (Fairhall et al. 2001). The latter adapts much faster (over a time scale of seconds) and to much a larger degree than that seen in IT, suggesting different underlying mechanisms. The end-result, however, is qualitatively similar: an adaptive rescaling of the input with respect to the stimulus range. Further studies are needed to determine whether IT neurons adapt to other measures of the stimulus distribution such as the mean or higher-order statistics, and whether similar adaptive effects are observed using other stimulation protocols (e.g., with ISIs).

Our experimental design does not allow disentangling the effect of variance from that of the density of the stimuli in a block because we kept the number of stimuli constant in the two ranges. In the narrow-range condition, shapes

are packed at higher density and thus are more similar than in the wide-range condition. Repetition suppression for a particular stimulus may depend on the mean similarity of that stimulus to other recently presented stimuli and because the mean similarity was larger for the narrow compared with the wide range, stronger repetition suppression in the narrow condition might have caused the increased selectivity in the latter condition. However, as shown in Figure 12, there was no clear difference in either the time course or size of the overall response decrease between the two ranges, which does not fit with stronger repetition suppression in the narrow compared with the wide range. One could argue, however, that the change in selectivity results from a similarity-based repetition suppression mechanism that depends on the last one to five or so presentations: by nature of the design, these will have a greater average similarity for the narrow compared with the wide range. Such an explanation runs counter to the observation, shown in Figure 12, that the difference in selectivity between the two ranges needs $\geq$ 50 stimulus presentations to develop. However, it cannot be excluded that similarity-based repetition suppression on a longer time scale produces the observed differences in selectivity between the two ranges. Indeed, whatever the underlying mechanisms, the present data suggest that the observed change in selectivity takes quite a number of presentations to develop, implying a relatively slow adaptation to a change in the input statistics.

Although the effect of stimulus statistics on selectivity was significant, it was rather small. This is a comforting observation since any large effect of stimulus set statistics on neural measures would produce serious methodological problems in assessing neuronal selectivity. Nevertheless, one should be aware of such issues, especially when using high-rate stimulations of frequently reoccurring stimuli.

REFERENCES

Baker CI, Behrmann M, Olson CR. Impact of learning on representation of parts and wholes in monkey inferotemporal cortex. *Nat Neurosci* 5: 1210-1215, 2002.

Baylis GC, Rolls ET. Responses of neurons in the inferior temporal cortex in short term and serial recognition memory tasks. *Exp Brain Res* 65: 614-622, 1987.

Berry MJ, Warland D, Meister M. The structure and precision of retinal spike trains. *Proc Natl Acad Sci USA* 94: 5411-5416, 1997.

Bredfeldt CE, Ringach DL. Dynamics of spatial frequency tuning in macaque V1. *J Neurosci* 22: 1976-1984, 2002.

Brenner N, Bialek W, de Ruyter van Steveninck R. Adaptive rescaling maximizes information transmission. *Neuron* 26: 695-702, 2000.

Brincat SL, Connor CE. Underlying principles of visual shape selectivity in posterior inferotemporal cortex. *Nat Neurosci* 7: 880-886, 2004.

Brown MW, Wilson FAW, Riches IP. Neuronal evidence that inferomedial temporal cortex is more important than hippocampus in certain processes underlying recognition memory. *Brain Res* 409: 158-162, 1987.

Chun MM, Potter MC. A two-stage model for multiple target detection in rapid serial visual presentation. *J Exp Psychol Hum Percept Perform* 21: 109-127, 1995.

Cohn TE, Green DG, Tanner WP. Receiver operating characteristics analysis: application to the study of quantum fluctuation effects in optic nerve of *Rana pipiens*. *J Gen Physiol* 66: 583-616, 1975.

De Baene, W, Vogels, R. Tuning of macaque inferior temporal neurons to parameterized shapes in a rapid serial visual presentation (RSVP) paradigm. *Soc Neurosci Abstr* 16: 620, 2005.

Dean I, Harper NS, McAlpine D. Neural population coding of sound level adapts to stimulus statistics. *Nat Neurosci* 8: 1684-1689, 2005.

Dean P. Effects of inferotemporal lesions on the behavior of monkeys. *Psychol Bull* 83: 41-71, 1976.

Fairhall AL, Lewen GD, Bialek W, de Ruyter van Steveninck R. Efficiency and ambiguity in an adaptive neural code. *Nature* 412: 787-792, 2001.

Földiák P, Xiao DK, Keysers C, Edwards R, Perrett DI. Rapid serial visual presentation for the determination of neural selectivity in area STSa. *Prog Brain Res* 144: 107-116, 2004.

Freedman DJ, Riesenhuber M, Poggio T, Miller EK. Experience-dependent sharpening of visual shape selectivity in inferior temporal cortex. *Cereb Cortex* 16: 1631-1644, 2006.

Freiwald, WA, Tsao, DY, Tootell, RBH, Livingstone, MS. Single-unit recording in an FMRI-identified macaque face patch. II. Coding along multiple feature axes. *Soc Neurosci Abstr* 6: 362, 2005.

Gross CG, Bender DB, Rocha-Miranda CE. Visual receptive fields of neurons in inferotemporal cortex of the monkey. *Science* 166: 1303-1306, 1969.

Gross CG, Schiller PH, Wells C, Gerstein GL. Single-unit activity in temporal association cortex of the monkey. *J Neurophysiol* 30: 833-843, 1967.

Janssen P, Vogels R, Orban GA. Selectivity for 3D shape that reveals distinct areas within macaque inferior temporal cortex. *Science* 288: 2054-2056, 2000.

Jones JP, Palmer LA. The two-dimensional spatial structure of simple receptive fields in cat's visual cortex. *J Neurophysiol* 58: 1187-1211, 1987.

Kayaert G, Biederman I, Op de Beeck H, Vogels R. Tuning for shape dimensions in macaque inferior temporal cortex. *Eur J Neurosci* 22: 212-224, 2005a.

Kayaert G, Biederman I, Vogels R. Representation of regular and irregular shapes in macaque inferotemporal cortex. *Cereb Cortex* 15: 1308-1321, 2005b.

Keysers C, Xiao DK, Földiák P, Perrett DI. The speed of sight. *J Cogn Neurosci* 13: 90-101, 2001.

Kiani R, Esteky H, Tanaka K. Differences in onset latency of macaque inferotemporal neural responses to primate and non-primate faces. *J Neurophysiol* 94: 1587-1596, 2005.

Kobatake E, Wang G, Tanaka K. Effects of shape-discrimination training on the selectivity on inferotemporal cells in adult monkeys. *J Neurophysiol* 80: 324-330, 1998.

Kovács G, Vogels R, Orban GA. Cortical correlate of pattern backward masking. *Proc Natl Acad Sci USA* 92: 5587-5591, 1995.

Leopold DA, Bondar IV, Giese MA. Norm-based face encoding by single neurons in the monkey inferotemporal cortex. *Nature* 442: 572-575, 2006.

Logothetis NK, Sheinberg DL. Visual object recognition. *Annu Rev Neurosci* 19: 577-621, 1996.

Lord, FM, Novick, MR. *Statistical Theories of Mental Test Scores.* Reading, MA: Addison-Wesley, 1968.

Matsumoto N, Okada M, Sugase-Miyamoto Y, Yamane S, Kawano K. Population dynamics of face-responsive neurons in the inferior temporal cortex. *Cereb Cortex* 15: 1103-1112, 2004.

Miller EK, Gochin PM, Gross CG. Habituation-like decrease in the responses of neurons in inferior temporal cortex of the macaque. *Vis Neurosci* 7: 357-362, 1991a.

Miller EK, Li L, Desimone R. A neural mechanism for working and recognition memory in inferior temporal cortex. *Science* 254: 1377-1379, 1991b.

Missal M, Vogels R, Li CY, Orban GA. Shape interactions in macaque inferior temporal neurons. *J Neurophysiol* 82: 131-142, 1999.

Op de Beeck H, Wagemans J, Vogels R. Inferotemporal neurons represent low-dimensional configurations of parameterized shapes. *Nat Neurosci* 4: 1244-1252, 2001.

Panzeri S, Treves A. Analytical estimates of limited sampling biases in different information measures. *Network* 7: 87-107, 1996.

Potter MR, Levi EI. Recognition memory for rapid sequence of pictures. *J Exp Psychol* 81: 10-15, 1969.

Rainer G, Miller EK. Effects of visual experience on the representation of objects in the prefrontal cortex. *Neuron* 27: 179-189, 2000.

Reid RC, Shapley R. Space and time maps of cone photoreceptor signals in macaque lateral geniculate nucleus. *J Neurosci* 22: 6158-6175, 2002.

Riches IP, Wilson FAW, Brown MW. The effect of visual stimulation and memory on neurons of the hippocampal formation and neighboring parahippocampal gyrus and inferior temporal cortex of the primate. *J Neurosci* 11: 1763-1779, 1991.

Riesenhuber M, Poggio T. Neural mechanisms of object recognition. *Curr Opin Neurobiol* 12: 162-168, 2002.

Ringach DL, Hawken MJ, Shapley R. Dynamics of orientation tuning in macaque primary visual cortex. *Nature* 387: 281-284, 1997.

Ringach DL, Hawken MJ, Shapley R. Dynamics of orientation tuning in macaque V1: the role of global and tuned suppression. *J Neurophysiol* 90: 342-352, 2003.

Rollenhagen JE, Olson CR. Mirror image confusion in single neurons of macaque inferotemporal cortex. *Science* 287: 1506-1508, 2000.

Rolls ET, Baylis GC, Hasselmo ME, Nalwa V. The effect of learning on the face selective responses of neurons in the cortex in the superior temporal sulcus of the monkey. *Exp Brain Res* 76: 153-164, 1989.

Rolls ET, Tovee MJ. Processing speed in the cerebral cortex and the neurophysiology of visual masking. *Proc Biol Sci* 257: 9-15, 1994.

Sawamura H, Vogels R, Orban GA. Selectivity of neuronal adaptation does not match response selectivity: a single-cell study of the FMRI adaptation paradigm. *Neuron* 49: 307-318, 2006.

Seltzer B, Pandya DN. Afferent cortical connections and architectonics of the superior temporal sulcus and surrounding cortex in the rhesus monkey. *Brain Res* 149: 1-24, 1978.

Sharpee TO, Sugihara H, Kurgansky AV, Rebrik SP, Stryker MP, Miller KD. Adaptive filtering enhances information transmission in visual cortex. *Nature* 439: 936-942, 2006.

Sigala N, Logothetis NK. Visual categorization shapes feature selectivity in the primate temporal cortex. *Nature* 415: 318-320, 2002.

Smirnakis S, Berry MJ, Warland D, Bialek W, Meister M. Adaptation of retinal processing to image contrast and spatial scale. *Nature* 386: 67-73, 1997.

Sobotka SS, Ringo JL. Investigation of long term recognition and association memory in unit responses from inferotemporal cortex. *Exp Brain Res* 96: 28-38, 1993.

Subramaniam S, Biederman I, Madigan SA. Accurate identification but no priming and chance recognition memory for pictures in RSVP sequences. *Vis Cogn* 7: 511-535, 2000.

Sugase Y, Yamane S, Ueno S, Kawano K. Global and fine information coded by single neurons in the temporal visual cortex. *Nature* 400: 869-873, 1999.

Tanaka K. Inferotemporal cortex and object vision. *Annu Rev Neurosci* 19: 109-139, 1996.

Tsao DY, Freiwald WA, Tootell RBH, Livingstone MS. A cortical region consisting entirely of face-selective cells. *Science* 311: 670-674, 2006.

Vogels R, Orban GA. How well do response changes of striate neurons signal differences in orientation: a study in the discriminating monkey. *J Neurosci* 10: 3543-3558, 1990.

Zoccolan D, Cox DD, DiCarlo JJ. Multiple object response normalization in monkey inferotemporal cortex. *J Neurosci* 25: 8150-8164, 2005.

CHAPTER 3
EFFECTS OF CATEGORY LEARNING ON THE STIMULUS SELECTIVITY OF MACAQUE INFERIOR TEMPORAL NEURONS

Learning and Memory (in press)[1,2]

Primates can learn to categorize complex shapes, but as yet it is unclear how this categorization learning affects the representation of shape in visual cortex. Previous studies that have examined the effect of categorization learning on shape representation in macaque inferior temporal (IT) cortex have produced diverse and conflicting results that are difficult to interpret owing to inadequacies in design. The present study overcomes these issues by recording IT responses before and after categorization learning. We employed parameterized shapes that varied along two shape dimensions. Monkeys were extensively trained to categorize the shapes along one of the two dimensions. Unlike previous studies, our paradigm counterbalanced the relevant categorization dimension across animals. We found that categorization learning increased selectivity specifically for the category-relevant stimulus dimension (i.e. an expanded representation of the trained dimension) and that the ratio of within-category response similarities to between-category response similarities increased for the relevant dimension (i.e. category tuning). These small effects were only evident when the learned category-related effects were disentangled from the pre-learned stimulus selectivity. These results suggest that shape-categorization learning can induce minor category-related changes in the shape tuning of IT neurons in adults, suggesting that learned, category-related changes in neuronal response mainly occur downstream from IT.

---

[1] This paper was co-authored by Bart Ons, Johan Wagemans and Rufin Vogels

[2] The authors are indebted to Steve Raiguel and five anonymous reviewers for critical comments on an earlier draft of this manuscript.

INTRODUCTION

Lesion (Dean 1976), microstimulation (Afraz et al. 2006) and single cell studies (Gross et al. 1969; Logothetis and Sheinberg 1996; Tanaka 1996) indicate that the inferior temporal (IT) cortex is involved in the processing of features necessary for the identification and categorization of objects. Single cell studies of category encoding by IT neurons (Vogels 1999b; Sigala and Logothetis 2002; Freedman et al. 2003; Kiani et al. 2007) reported that, while some single IT neurons responded selectively to exemplars of a particular category, these *single* IT neurons still showed selectivity for different exemplars within that category. The output of a *population* of IT neurons can be used to classify exemplars of different categories (Thomas et al. 2001; Kayaert et al. 2005; Kiani et al. 2007) suggesting a population-coding of features that is biased towards category-relevant distinctions between stimuli. Here we address the question of whether this sort of category-related bias in IT neuronal sensitivity can be induced by categorization learning. Indeed, the tuning of IT neurons could be susceptible to categorization learning, as neuronal responses in IT cortex can reflect the perceptual similarity across stimuli (Kayaert et al. 2003; Op de Beeck et al. 2001) and the latter can be affected by categorization (Goldstone 1994; Goldstone et al. 2001; Livingston et al. 1998).

Previous studies of the effect of categorization learning on the tunings of IT neurons have obtained diverse results. Sigala and Logothetis (2002) reported enhanced selectivity for shape features that were relevant (compared to irrelevant) for the categorization. However, the relatively large effect of categorization-relevant feature selectivity could merely be due to stimulus selectivity, unrelated to categorization learning, since no pre-training selectivity measurements were obtained, and the diagnostic features were identical in both monkeys. Freedman et al. (2003) found that responses to

shapes within a learned category were slightly more similar than responses to shapes from different categories. However, this small effect could also have resulted from physical differences amongst the stimuli rather then differences in category membership. Finally, Op de Beeck et al. (2001) found no effect of a learned categorization rule upon the selectivities of IT neurons. A possible explanation for the discrepancy between the Op de Beeck et al. and Sigala and Logothetis studies could be that Sigala and Logothetis manipulated separable dimensions while Op de Beeck et al. employed integral dimensions. Separable dimensions, but not integral dimensions, can be attended to separately (Garner 1976). Indeed, a human psychophysical study (Op de Beeck et al. 2003) found that categorization learning induced a dimension-specific gain in perceptual similarity for shapes that varied along separable, but not integral, dimensions. Given these discrepant results, we revisited the effect of categorization learning on IT shape selectivity. We controlled for pre-learned stimulus-selectivity effects by measuring the selectivities of IT neurons both before and after learning, and by counterbalancing the relevant categorization dimensions across animals. We manipulated shape dimensions that had previously been shown to be separable in human psychophysical studies (e.g. Op de Beeck et al. 2003; Wagemans et al. 2006).

RESULTS

Before starting the categorization training, we measured pre-training "baseline" IT responses to 4 different parametric sets of 16 shapes each. In each set, the 16 shapes differed along a "curvature" and "aspect ratio" dimension (Figure 1). Responses were measured using a rapid serial visual presentation (RSVP) paradigm while the monkeys were passively fixating.

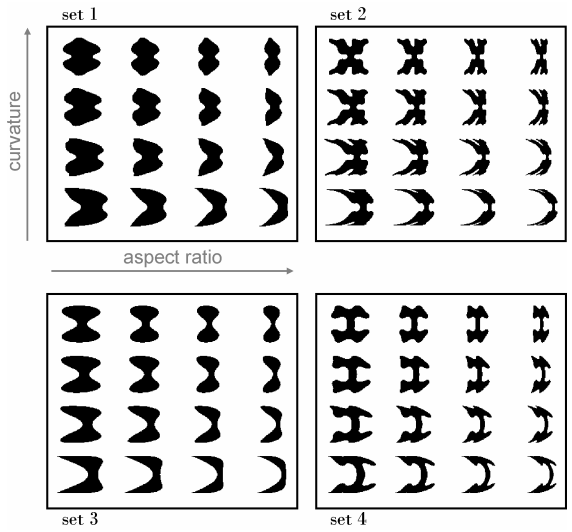

Figure 1. Visual stimuli. The square parametric configurations consisted of 4 sets of 16 shapes each. The manipulated dimensions were curvature and aspect ratio (vertical and horizontal axis, respectively). Curvature was modulated by manipulating the turning angle of the tangents at the shape ends on the vertical axis. Aspect ratio was modulated by manipulating shape width.

In a subsequent categorization training phase, one monkey was trained to group stimuli into 2 categories based on the curvature dimension (monkey C; training duration: 53 days); the other monkey was trained to use the aspect ratio dimension (monkey A; training duration: 80 days) to categorize the shapes. After this training phase, we recorded IT responses while the monkeys were categorizing the shapes (post-training recordings).

BEHAVIORAL RESULTS

The behavioral results of the two monkeys during the last 10 days of training (Figure 2) indicate that both animals were fairly adept at categorizing the shapes that were used in the post-training recordings. While shapes close to the extreme parametric values (0 or 100%) were categorized almost perfectly, these subjects reached a performance level of about 85% correct for shapes with moderate parametric values (around 33 and 66%).

Averaged over all post-training recording sessions, monkey C, who used curvature as the relevant dimension, reached a performance of 98% in categorizing the 16 shapes of Figure 1. For the position- and size-control

shapes (see Materials and Methods), categorization was correct in 99% and 97% of the trials respectively. Monkey A, who used aspect ratio as the relevant dimension, categorized the 16 shapes correctly on 97% of the trials. He reached a performance of 96% for the position control shapes and 95% for the size control shapes. Thus. both animals performed with a high accuracy in the categorization task during the recording-sessions.

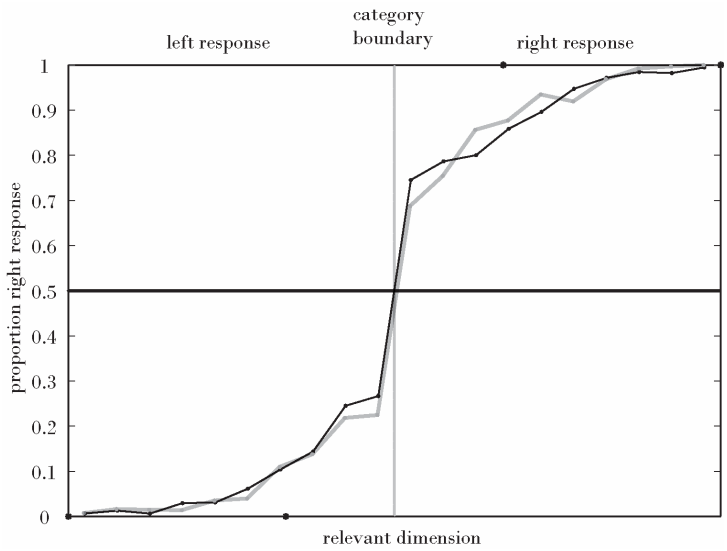

Figure 2. Behavioral performance during the last 10 days of the categorization training phase. The X-axis indicates the parametric values along the relevant dimension, with the black markers on the 0, 33, 66 and 100% values. The Y-axis represents the average proportion of rightward saccades. The gray solid line in the middle shows the category boundary. Shapes on the left of this boundary were associated with a leftward saccade; shapes on the right with a rightward saccade. The gray and black curves show the mean performance of monkey C and monkey A respectively, averaged in 20 consecutive bins, for the shapes with random parametric values used during the last 10 days of training.

NEURONAL RESULTS

Neuronal results

Database.

Pre-training recording phase. We recorded from 214 neurons (109 cells in monkey C; 105 cells in monkey A), 201 of which showed significant shape selectivity within one or more shape sets (101 cells in monkey C; 100 cells in monkey A). This resulted in a significant response modulation for 479 non-rotated shape sets, as tested with a permutation test (see Materials and Methods). For each cell, there was an average of 98.66 presentations per stimulus (minimum = 36; maximum = 152).

Post-training recording phase. We recorded from 137 neurons (70 cells in monkey C, 67 in monkey A) using the same stimulus centering as in the pre-training recording phase (center type 1; see Materials and Methods). All of these neurons were responsive to at least one set, as tested with a split-plot design analysis of variance (ANOVA; Kirk, 1995). These 137 responsive cells provided us with 283 sets for which a significant response occurred (further denoted as *responsive sets*). For 215 of these 283 sets, there was significant shape selectivity (further denoted as *selective sets*). We recorded an additional 100 responsive neurons (48 and 52 cells in monkey C and monkey A, respectively) using stimuli positioned according to center type 2 (see Materials and Methods), This resulted in 206 responsive sets, 123 of which were shape selective. Additionally, we recorded from 44 responsive neurons using center type 2 in the left hemisphere of monkey A resulting in 74 selective sets of a total of 94 responsive sets.

As all further analyses were performed on trials with a correct response, only sets with at least 1 (for the computation of the Depth of Selectivity (DOS)) or

2 (for category tuning indices) correct trials for each stimulus were included. As a consequence, 2 responsive sets (both selective; center type 1) were excluded from further analyses. This resulted in an average of 8.84 correct trials per stimulus per cell (minimum = 4; maximum = 15).

Comparison of pre- and post-training.

When comparing pre- and post-training data, we only included neurons in the analysis that showed a significant shape selectivity for stimulus sets recorded using the same centering (type 1) in the two training phases.

Effect of categorization learning on selectivity along relevant and irrelevant dimensions. To examine whether categorization training affected the degree of selectivity for the relevant and irrelevant dimensions, we computed the Depth Of Selectivity (DOS) index using the mean responses for the 4 values of a dimension, irrespective of the 4 values of the other dimension. The larger the DOS, the greater the selectivity. We performed an ANOVA on the DOS values for the pre-and post-training phase. The variables *shape set* (sets 1 to 4), *recording phase* (before or after categorization training) and *monkey* (monkey C or A) were included as between-neurons variables. *Category dimension* (aspect ratio or curvature) was included as a within-neuron variable. The main effect of recording phase was significant ($F(1,676)$=86.40, $p < .001$). More interestingly, the three-way interaction between category dimension, monkey, and recording phase was significant ($F(1,676)$=13.86, $p < .001$). The four-way interaction between category dimension, monkey, recording phase and shape set was not significant ($F(3,676)=1.34$, $p > .25$). Figure 3A shows that categorization training resulted in a selectivity increase for both dimensions, but this increase was larger for the relevant dimension than for the irrelevant dimension, and this observation held for both monkeys.

Thus categorization enhanced the selectivity more for the relevant dimension than for the irrelevant dimension (Figure 3B and 3C).

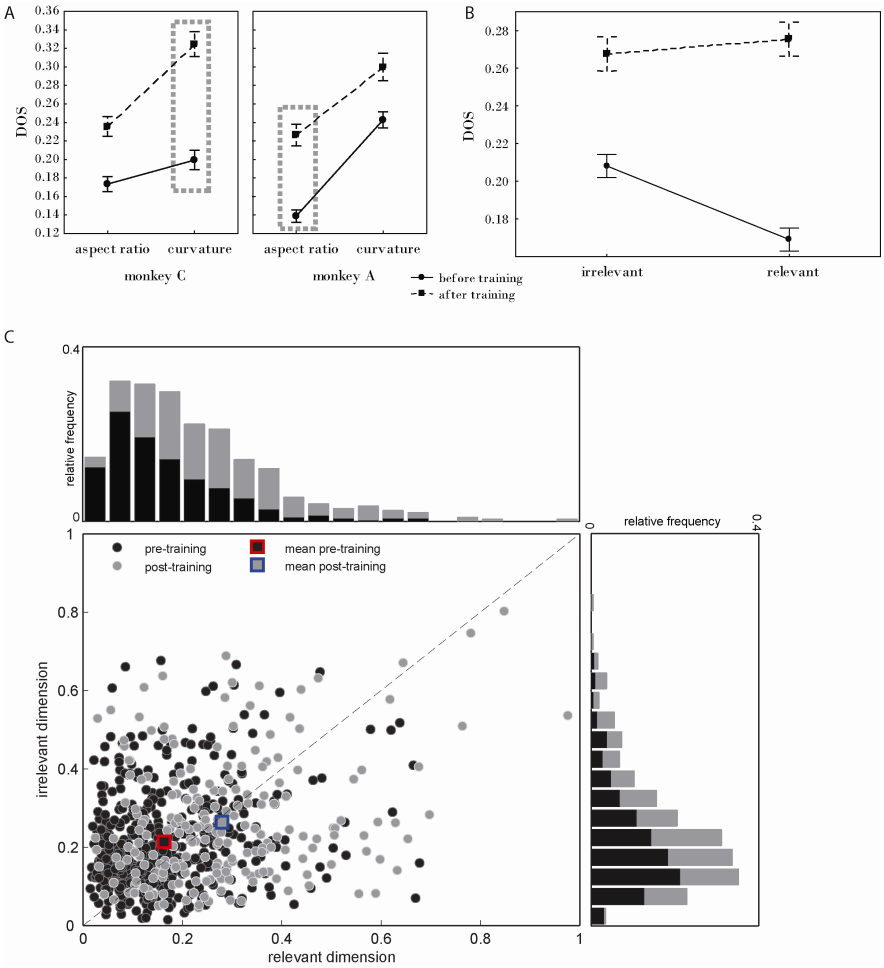

Figure 3. Effect of categorization learning on degree of selectivity. In panel A, the DOS indices compared before and after categorization training are shown. The results for the monkey C using curvature as the relevant dimension are shown in the left panel; in the right panel, the results for monkey A using aspect ratio as the relevant dimension are shown. The results before and after training are depicted by dotted and solid lines, respectively (with SEs). In panel B, the DOS indices compared before and after categorization training for the relevant and irrelevant dimension, pooled across the two monkeys are shown. The results before and after training are depicted by dotted and solid lines, respectively (with SEs). In panel C, the DOS indices for the irrelevant dimension are plotted against the DOS indices for the relevant dimension, both for the data obtained before (black dots) and after categorization training (gray dots). Means are indicated by the colored symbols. In the marginal histograms, the relative frequencies of the DOS indices for the relevant and irrelevant dimension are shown. The indices obtained before training are depicted by black and gray bars, respectively. Grey dotted rectangles outline the results for the relevant dimension for each monkey.

Indeed, the percent of neurons with a greater DOS for the relevant compared to the irrelevant dimension was larger after (54%) compared to before training (33%; difference: $p < .001$, Binomial test; Figure 3C). Highly similar, statistically significant results were found when the best-worst selectivity index employed by Sigala and Logothetis (2002) was used instead of the DOS index. The latter selectivity index was defined as the difference between the maximum and the minimum response for a given dimension divided by their sum. Furthermore, similar statistical significant effects were obtained using a best-worst index normalized by trial-to-trial variability. For this, the differences between the maximum response (averaged across presentations of the same stimulus) for a set and the minimum mean response for the same value along the relevant or irrelevant dimension were computed followed by a division by the mean trial-to-trial standard deviation of the responses for the best and worst conditions.

Effect of categorization learning on strength of category tuning. The above analyses determined whether categorization learning induced categorization-dimension-specific changes in selectivity. Another possible categorization-learning induced change in selectivity is related to the difference in responses to shapes belonging to the same versus different learned categories. Do neurons respond more similarly to shapes that belong to the same category than to shapes that belong to different categories? To examine this, we computed a category tuning index (see Materials and Methods) for each neuron. The category tuning index assesses the similarity between responses to shapes of the same category versus shapes of different categories, taking into account trial-to-trial variations in response strength (computed on d'; see Materials and Methods). The larger the category tuning index, the more similar are the responses of neurons to shapes of the same category compared to shapes belonging to different categories. We employed an ANOVA on the category tuning index values in the pre-and post-training phase. As between-

neurons variables, we included *shape set* (set 1 to 4), *recording phase* (before or after categorization training) and *monkey* (monkey C or A). *Category dimension* (aspect ratio or curvature) was included as a within-neuron variable. The three-way interaction between category dimension, monkey and recording phase reached significance ($F(1,673)$=3.89, $p < .05$). The four-way interaction between category dimension, monkey, recording phase and shape set was not significant ($F(3,673)=1.84$, $p > .13$). Inspection of Figure 4A showed that the category tuning index increased with training for the relevant but not for the irrelevant dimension. This observation was confirmed by post-hoc comparisons (Fisher LSD tests): for monkey C, the training effect was significant for the category tuning index along the relevant curvature dimension ($p < .05$). For the category tuning index along the aspect ratio dimension, however, there was no significant training effect ($p > .11$). The opposite was true for monkey A ($p < .001$ and $p > .89$ for the training effect along the aspect ratio and curvature dimension, respectively). Thus categorization learning affected the category tuning along the relevant dimension but not along the irrelevant dimension (Figure 4B and 4C). The distribution of the category tuning index also changed significantly with training for the relevant but not for the irrelevant dimension ($p < .01$ and $p > .18$, respectively, Kolmogorov-Smirnov test; Figure 4C). Similar trends were found when the analyses were applied using absolute response differences without normalizing by the response variance (as Freedman et al. (2003) did) instead of using d' values.

As the category tuning index reflects the ratio of within-category response differences (WCD's) to between-category response differences (BCD's), we zeroed in on the effect of training on both of these factors. To examine this, we employed an ANOVA on the between- and within category differences in the pre-and post-training phase, taking into account trial-to-trial variations in response strength (computed on d'). As between-neurons variables, we

included *shape set* (set 1 to 4), *recording phase* (before or after categorization training) and *monkey* (monkey C or A). *Category dimension* (relevant or irrelevant) and *category difference* (between or within) were included as within-neuron variables.

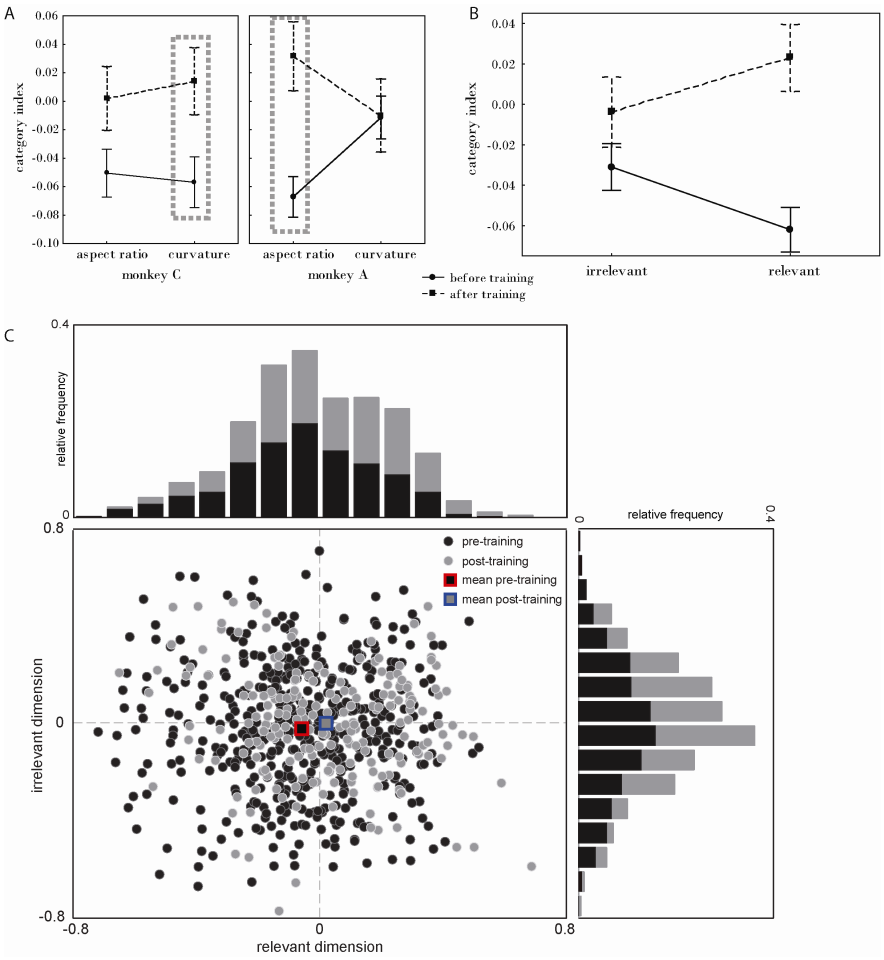

Figure 4. Effect of category learning on category tuning A: Category tuning indices along the curvature and aspect ratio dimensions compared before and after categorization training. The results for the monkey using curvature as the relevant dimension are displayed on the left; on the right, the results for the monkey using aspect ratio as the relevant dimension are shown. The data obtained before and after training are depicted by dotted and solid lines, respectively (with SEs). In panel B, the category tuning indices compared before and after categorization training for the relevant and irrelevant dimension, pooled across the two monkeys, is shown. The data obtained before and after training are depicted by dotted and solid lines, respectively (with SEs). In panel C, the category tuning indices for the irrelevant dimension are plotted against the category tuning indices for the relevant dimension. Same conventions as in Figure 3.

The three-way interaction between category dimension, category difference and recording phase was significant ($F(1,673)=7.34$, $p < .01$). The training increased the between-category differences more for the relevant (post-pre training difference in mean between-category d': 0.62) than for the irrelevant dimension (d' difference: 0.57). For the within-category differences, the opposite was true: the increase for the relevant dimension (d' difference: 0.53) was smaller than for the irrelevant dimension (d' difference: 0.56). Thus, with training, responses to shapes from the same category became more similar and responses to shapes from different categories became less similar.

Comparison of responses for the relevant and irrelevant dimension after training.

We also analyzed the post-training data separately, asking whether there was an interaction of stimulus dimension and monkey on the degree of selectivity and the category tuning index. These analyses are similar to those in previous studies that did not employ pre-training measures. The results reported below are for the selective sets only. Including all responsive sets did not change the results in any substantial way.

Selectivity along the relevant and irrelevant dimensions after training. To examine whether selectivity for the relevant dimension was enhanced compared to the irrelevant dimension in the post-training recording phase, we performed an ANOVA on the DOS values for all selective sets in the post-training phase with *category dimension* (aspect ratio or curvature) as a within-neuron variable and *shape set* (set 1 to 4), *center type* (type 1 or 2) and *monkey* (monkey C or A) as between-neurons variables. The interaction between dimension and monkey did not reach significance ($F(1,394)$=1.80, $p > .17$), indicating that the selectivity for the relevant dimension was not significantly enhanced compared to the irrelevant dimension. This was the

case for both center types (DOS index for relevant dimension minus DOS index for irrelevant dimension: center type 1= .008; center type 2= -.034). The results for the best-worst selectivity index used by Sigala and Logothetis (2002) were, again, very similar.

Strength of category tuning along the relevant versus irrelevant dimension after training. To examine whether the strength of the category tuning was greater along the relevant dimension than along the irrelevant dimension after training, we employed an ANOVA on the category tuning index values for all selective sets in the post-training phase. As between-neurons variables, we included *shape set* (set 1 to 4), *center type* (type 1 or 2) and *monkey* (monkey C or A). *Category dimension* (aspect ratio or curvature) was included as a within-neuron variable. Although the interaction between dimension and monkey did not reach significance ($F(1,387)$=1.29, $p > .25$), the category tuning along the relevant dimension was greater compared to the irrelevant dimension, which was the case for both center types (category tuning for relevant dimension minus category tuning for irrelevant dimension: center type 1 =.027; center type 2 = .019). A highly similar pattern of non-significant results was found when the analysis was applied using the absolute response differences, as Freedman et al. (2003) did, instead of using the d' values.

DISCUSSION

We examined the effects of categorization learning for shapes upon the selectivity of IT neurons for these shapes while we controlled for pre-learning stimulus selectivity effects versus learned category-related effects by recording the neuronal selectivity before and after categorization learning as

well as by counterbalancing the relevant categorization dimensions across animals.

Unlike previous studies, our design allowed us to simultaneously examine two different possible effects of categorization learning on the tunings of IT neurons. First, IT neurons showed an increased sensitivity for shapes that varied along the trained dimension compared to shapes that varied along the irrelevant dimension. This categorization-relevant selectivity effect was relatively small and could only be demonstrated when comparing pre- and post-training data. Sigala and Logothetis (2002) reported a much stronger effect of categorization training on shape tuning. In the present study, only 55% of the cells showed a larger selectivity (as quantified by the best-worst selectivity index employed by Sigala and Logothetis) for the relevant compared to the irrelevant dimension after training, which is much smaller than the ~75% found by Sigala and Logothetis (2002; quantified after visual inspection of the results in their Figure 4a and b). The discrepancy between the size of the effects in the present and the latter study is unlikely to be due to differences in the amount of training. Another reason for the discrepancy between the two studies might be that Sigala and Logothetis had only post-training data and the dimensions actually relevant to the categorization were not counterbalanced across monkeys. Without proper counterbalancing, our results could have been as follows: If curvature had been the relevant dimension for both monkeys, the selectivity for this relevant dimension would have been larger than for the irrelevant aspect ratio dimension for 68% of the cells when using post-training data or 69% of the cells when using pre-training data. These proportions are close to those reported by Sigala and Logothetis (2002). However, if aspect ratio would have been the relevant dimension for both monkeys, only 32% (post-training) or 31% (pre-training data) of the cells would have shown this result pattern. This exercise shows that without proper counterbalancing of the trained dimension, the

contribution of a genuine learning effect to the observed selectivity is impossible to assess. Thus, it is possible that if Sigala and Logothetis had counterbalanced the trained dimensions across their subjects, the size of the categorization effect on selectivity would have been much smaller and comparable to that of the present study.

The present results disagree with Op de Beeck et al. (2001) who did not find an effect of categorization rules on IT response tunings. However, training was somewhat less extensive (~ 6 to 8 weeks) than that in the present study and, likely more critical, integral but not separable dimensions (as in the present study and in Sigala and Logothetis (2002)) were manipulated. Perhaps category selective effects on IT tuning occur only for separable dimensions, in line with a psychophysical study of category learning effects (Op de Beeck et al. 2003).

In addition to the dimension-specific change in degree of selectivity, we observed a general increase in selectivity when comparing pre- and post training selectivity measures. As the procedures of the pre- and post-training recordings differed in several aspects (e.g. fixation vs categorization, different presentation durations), it is impossible to determine the source of the overall difference in selectivity between the pre- and post-training phases. De Baene et al. (2007) reported that a RSVP task with a fast presentation rate (100 ms/image) can lead to an underestimation of the degree of stimulus selectivity. This suggests that the overall increase in selectivity with categorization training that was observed in the present study, can be, at least partially, explained by an initial underestimation of the stimulus selectivity caused by the use of a fast presentation rate RSVP task. However, given previously reported effects of learning on overall shape selectivity (Kobatake et al. 1998; Miyashita et al. 1993; Baker et al. 2002; Freedman et al. 2006), it seems very likely that at least part of the difference in selectivity observed

before and after the training is due to a genuine effect of categorization learning on shape selectivity. Note that the different paradigms when searching and testing responsive neurons before and after training cannot explain the dimension-specific changes in selectivity because the relevant dimension was counterbalanced across animals.

Dimension-specific changes in perceptual sensitivity have been observed after categorization learning in humans using similar (Op de Beeck et al. 2003) or identical shapes (Wagemans et al. 2006) as those used in our study, and in monkeys using other shapes (Sigala et al. 2002). In those behavioral studies, the subjects were performing a task that was different from the trained categorization task when testing their perceptual sensitivity. In our study (as in other single cell categorization studies (e.g. Vogels 1999b; Sigala and Logothetis 2002; Op de Beeck et al. 2001; Freedman et al. 2003)) the animals were performing the categorization task during the post-training recordings, which raises the possibility that the selectivity change is only present when the animals are doing the categorization. Such a task-related selectivity change may reflect category-dimension specific attention as postulated in exemplar-based models of categorization (e.g. Nosofsky 1986; Kruschke 1992). Note though that the present study would be the first one to show such stimulus dimension-dependent attention effect in the ventral visual stream, since previously studies that specifically examined such attention effects on tuning failed to find it (Mirabella et al. 2007; see Vogels 2007). Although the tuning changes observed in the present study agree with the attentional effect postulated in categorization models, it is possible that the dimension-specific selectivity effect is task-independent, and thus might, at least partially, underlie the task-independent changes in behavioral sensitivities that result from categorization learning. To ascertain this, post training RSVP measures would have been necessary which were unfortunately not possible in the present study (see Materials and Methods).

Second, IT neurons responded more similarly to shapes belonging to the same category than to shapes belonging to different categories. Since the categorization-related effect is a change in the similarity of the IT responses to shapes that belong to the same versus different categories and thus differs from a dimension-specific change in shape selectivity (see above), it is difficult to see how this category effect can be explained by an increased attention to the relevant dimension. However, since the two categories were associated with two different behavioral responses, one could argue that the category effect does not reflect a task-independent change in shape tuning, but instead reflects the upcoming behavioral response. Previous studies that used the same task as we have did not find evidence for such behavioral response-related responses in IT cortex (Op de Beeck et al. 2001; Baker et al. 2002; Koida and Komatsu 2007; also see Mogami and Tanaka 2006). Given the lack of clear evidence for behavioral response-related effects in these IT studies, it is very unlikely that the category effect that we observed is related to the behavioral response.

During the categorization training, a small region around the category boundary was spared which resulted in a slight difference in stimulus statistics for the two monkeys. As a consequence, an unsupervised learning process could have led to a clustering of responses according to the two categories. Although we cannot exclude a possible contribution of this unsupervised learning to the observed category effect, it is very unlikely that it is its sole or main cause. Indeed, the trained shapes near the category boundary were very similar as is evident from the poor classification performance for these shapes in both animals (about 70% correct classifications).

Whatever the cause of the category tuning effect, it is numerically rather small. Freedman et al. (2003) reported a similar, small effect of categorization

learning upon category tuning of IT neurons (after > 6 months of training (D. Freedman, personal communication)), although, unlike that in our study, their effect could have been due to pre-training stimulus selectivities. Recent human fMRI studies did not find evidence for such category-related tuning in area LOC (believed to be the human homologue of monkey area IT (Denys et al. 2004)) using an adaptation protocol (Jiang et al. 2007) or pattern classification tool (Li et al. 2007). However, effects as small as those observed in the present study may easily be missed with fMRI. Given the modest size of the category-related tuning effect in IT, the question arises as to which area(s) more strongly encode the category membership of a stimulus after learning. Freedman et al. (2003) observed much stronger category tuning effects in prefrontal than in IT neurons when animals performed categorization in the context of a working memory task. Also, several human functional imaging studies of categorization (Jiang et al. 2007; Li et al. 2007; Vogels et al. 2002; for review see Keri (2003) and Ashby and Maddox (2005)) reported activation in prefrontal cortex during categorization. A recent study by Freedman and Assad (2006) reported strong category-related information in a working memory task in the intra-parietal sulcus. Because motion stimuli were used in this study, it remains unclear whether the parietal areas play a role in categorization tasks in general (thus also when static shapes are used), or only when categorizing motion stimuli (Li et al. 2007). Several functional imaging studies in humans also suggest an involvement of the striatum in categorization (Li et al. 2007; Vogels et al. 2002; for review see Keri (2003) and Ashby and Maddox (2005)). As the striatum can integrate the outputs of multiple IT neurons (Cheng et al. 1997), a striatal role in categorization is indeed possible. Note that we cannot exclude that at least part of the effect of category learning on the tuning of IT neurons is caused by feedback from one of the category-selective areas.

The present study suggests that shape-categorization learning in adults induces only minor category-related changes in the shape tuning of IT neurons. These changes are such that, at least when post-training responses during categorization are compared to pre-training responses in a fixation task, the representation of the categorization relevant stimulus features are enhanced and that the responses of the neurons are somewhat more similar for exemplars that belong to the same, compared to different, categories (Figure 3 and 4, respectively). Our data support a two-stage model of categorization in adults in which IT neurons are tuned to exemplars, although in a category-biased way, while learned categories become explicitly represented in extra-visual cortical regions that read-out IT. Note that the two-stage model proposed here differs from the HMAX model (Riesenhuber and Poggio 1999; Jiang et al. 2007) by allowing a category related, biased object representation in IT, which is not present in HMAX. It is possible that during development, i.e. in animals younger than the ones used in the present study, categorization learning has much stronger category-related effects on the feature representations in the visual cortex and shapes the category-biased representation as was found by e.g. Kiani et al. (2007) for animate versus inanimate objects.

MATERIALS AND METHODS

SUBJECTS

Two male rhesus monkeys (*Macaca mulatta*; Monkey C and A) served as subjects. Before conducting the experiments, we performed aseptic surgery under isoflurane anesthesia to attach a plastic head-fixation post to the skull and to stereotactically implant a plastic recording chamber. To allow a vertical approach, we positioned the recording chambers dorsal to IT (see Janssen et al. 2000).

All animal care and experimental and surgical procedures followed national and European guidelines and were approved by the K.U. Leuven Ethical Committee for animal experiments.

STIMULI

Starting with 4 *"archetypical"* 2D shapes, we generated 4 parameterized two-dimensional shape sets by manipulating the dimensions "curvature" and "aspect ratio" (Figure 1). All archetypical shapes (not shown in Figure 1) were chosen so as to display vertical and horizontal symmetry.

Aspect ratio was defined as the ratio between the width and the height of a stimulus. To manipulate this ratio, we modified the width of the archetypical shapes by a transformation which maintained horizontal and vertical symmetry. Curvature was manipulated by modifying the turning angle of the tangents at the lowest and highest point of the vertical axis of the symmetric archetypes (see Foster and Wagemans 1993).

Before carrying out the aspect ratio transformation, we ran a human psychophysical study (N=6) on the basis of which the aspect ratio of the archetypical stimuli were set so as to be perceptually equal to the aspect ratio

of a rectangle with vertical sides twice the length of the horizontal sides. We performed a second pilot study with human participants (N=5) to calibrate the aspect ratio and curvature transformations to achieve perceptually equidistant steps for both stimulus dimensions (B.Ons, W.De Baene, and J.Wagemans submitted). A third pilot study with human participants (N=3) showed that the introduced shape transformations along the aspect ratio and curvature dimension were fairly perceptual separable, and we were therefore able to combine the two transformations in a linear way to create a two-dimensional stimulus set based on the previously-defined transformations (B.Ons, W.De Baene, and J.Wagemans submitted).

To prevent the possibility that shape categorization might be performed on the basis of shape width instead of aspect ratio, we generated 3 different shape sizes by a scaling transformation. The mean heights of the large, intermediate and small sizes were 9.8° (min = 9.5°; max = 10.1°), 5.6° (min = 5.4°; max = 5.8°) and 3.2° (min = 3.1°; max = 3.3°), respectively. As the turning angle is scale-invariant (Foster and Wagemans 1993), this scaling did not affect the curvature of the shapes. Note that it is still possible that the monkeys might have performed the categorization task on the basis of features that vary with the modulated dimensions, rather than using these dimensions themselves. However, as these changes are intertwined with variations in aspect ratio or curvature, we will use the labels “aspect ratio” and “curvature” for the remainder of this paper.

All shapes were presented on a gray background on a monitor positioned 60 cm from the monkeys (60 Hz frame rate; 1024 x 768 pixels) and were filled with pixel noise. The mean luminance of the shapes and background was equal.

PROCEDURE

Eye position was monitored by virtue of an infrared eye tracking system (ISCAN, EC-240A) at a sampling rate of 120 Hz. An electronic fixation window insured that the monkeys maintained their gaze within 0.8° of a black fixation target (0.17° diameter) that was presented in the center of the display during the trials.

Standard extracellular recordings were performed with Tungsten microelectrodes that were placed using a guiding tube fixed in a Crist (Hagerstown, MD) grid using previously published techniques (De Baene et al. 2007). Recording positions were estimated by comparing depth readings of the white and gray matter transitions, and that of the skull base during electrode penetrations, with structural magnetic resonance (MRI) images taken in between the recordings (using a copper-sulphate-filled tube inserted in the grid at one of the recording positions). In monkey C, we recorded from the left hemisphere; in monkey A, we recorded from the right hemisphere. Across animals, the recording positions in both pre- and post-training recording phases (see below) ranged from 15 to 22 mm anterior to the external auditory meatus and included the lower bank of the superior temporal sulcus (STS), the cortical convexity lateral to the anterior middle temporal sulcus (aMTS) and the lip of the STS (area TEm, Seltzer and Pandya 1978). The distribution of recording locations in the pre- and post-training recording phases largely overlapped. Additionally, in the post-training phase, we recorded from the left hemisphere in monkey A as a control. The recording positions in that hemisphere were within the same range as those for the other hemisphere.

Experimental phases.

We planned 4 experimental phases: a pre-training "baseline" recording using a passive fixation task, a categorization training phase, a post-training recording during categorization and a post-training recording during passive fixation. However, monkey C died from a gastrointestinal disorder after the post-training recordings during categorization, precluding post-training measurements using the passive fixation task. Thus, the experimental design included only 3 phases which will be described below.

Pre-training recordings.

During the pre-training recordings, we used 16 stimuli of intermediate size of each of the 4 sets (= 64 stimuli in total; Figure 1). These stimuli were obtained by combining 4 fixed levels of the curvature parameter with 4 fixed levels of the aspect ratio parameter. The 4 fixed curvature levels were combined with each of the 4 levels of the aspect ratio, as shown in Figure 5.

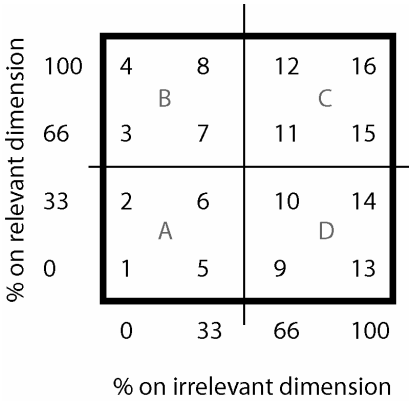

Figure 5. Schematic representation of how the shape sets were constructed. The numbers 1 to 16 indicate the different shapes obtained by combining 4 levels (0, 33, 66 and 100%; 0 and 100% being the extremes of the range tested on this dimension) of the relevant parameter with the same 4 levels of the irrelevant parameter. The letters A, B, C and D represent the 4 different quadrants of the configurations from which the position control shapes were chosen. The category boundary is depicted by the horizontal line.

The 0%, 33%, 66% and 100% aspect ratios of Figure 5 corresponded to respective horizontal expansions of 1.75, 1.32, 0.99 and 0.75 times the archetypical shapes. The four curvature values corresponded to turning angles

of the vertical axis of 3.34, 2.23, 1.29 and 0.52 radians (Figure 5). The ranges used here were imposed by the intrinsic properties of the shape sets themselves. Higher values on any one of these dimensions would have introduced additional features for the respective stimuli. For every shape, a 90° rotated version was generated, resulting in 128 (4 x 16 x 2) different stimuli. All these shapes were filled with 3 different pixel noise patterns, yielding a total of 384 stimuli. The position of the shapes on the screen was determined by the center of the archetypical shape of the respective set. This archetypical shape was centered so that the middle of the shape on the horizontal axis at middle height was at the center of the screen. The curvature and aspect ratio was modulated after this centering. This manner of centering is further referred to as center type 1.

The 384 stimuli were presented in continuous, rapid, random sequences (no interstimulus interval) at a rate of 100 ms/image (as in De Baene et al. 2007). In this passive fixation task, a trial started after 500 ms of stable fixation and ended when the monkey broke fixation or when every stimulus had been presented once. Monkeys were rewarded with a drop of apple juice at an increasing pace until the end of the trial. This procedure was used to search for responsive neurons. If the online-generated peristimulus time histogram (PSTH; averaged across trials and all stimuli) of the responses indicated that the cell did not respond to any of the stimuli, we abandoned this cell and searched for another. Spikes from responsive cells were sampled for about 75 trials.

Categorization learning.

In a second phase, the monkeys were trained to group the stimuli into 2 categories, with curvature and aspect ratio as the relevant dimensions for monkeys C and A, respectively. Each category was associated with a saccade

direction: shapes with parametric values < 50% on the relevant dimension (below horizontal line, Figure 5) were associated with a leftward saccade, shapes with parametric values > 50% (above horizontal line, Figure 5) with a rightward saccade. In this categorization task, a trial started after 500 ms of stable fixation. A stimulus was presented for 300 ms and after another 200 ms of fixation, 2 black target spots (0.71° diameter) appeared to the left and right of the fixation point, at 9° eccentricity, as a response cue. Saccades in the correct direction and within 2000 ms after the onset of the target spots were rewarded with a drop of apple juice. The fixation point and target spots were turned off as the eye trace entered a target window. Trials in which the animal interrupted fixation before target spot onset or failed to saccade to one of the two target spots were counted as aborts, and were not included when computing categorization performance. In contrast to the stimuli in the first recording phase, which were presented at a fixed intermediate size, all shapes in the categorization learning phase were presented at three different sizes (see above). Each shape was presented at a random position within a 3.6° square region centered on the fixation point and was filled with one of three different pixel noise patterns, which were refreshed daily.

The monkeys first learned to categorize the shapes of set 1 (Figure 1). Initially, only eight stimuli per size were presented, i.e. 4 of each extreme level (0 and 100%) of the irrelevant dimension (i.e. shapes 1 to 4 and 13 to 16; shapes numbered as in Figure 5). We increased the number of shapes on a daily basis by adding shapes 8 and 9 on day 2, shapes 7 and 10 on day 3, shapes 5 and 12 on day 4 and shapes 6 and 11 on day 5.

For each remaining day of the training phase, we generated 16 novel shapes for each size, 8 for each category, with random values along the two dimensions. These values were randomly picked from within the limits of the original shape configuration (Figure 1) but excluding a small range (having

an extent of approximately 1/6 of the total tested range) symmetrical around the category boundary of the relevant dimension. The category boundary for curvature was defined as the parametric value at the 50% level, referring to a turning angle of 1.74 radians. The category boundary for aspect ratio was defined as the parametric value generating shapes with a physical aspect ratio of 0.54. The reason for this will be discussed below.

After the fifth day of training, we tested the transfer to the other 3 sets on 3 consecutive days. For each of these sets, 16 transfer stimuli were generated for each of the 3 sizes by combining the 4 fixed levels (0, 33, 66 and 100%) of the curvature parameter with the 4 fixed levels of the aspect ratio parameter (see above). These 48 (3 x 16) transfer stimuli within a set were randomly intermixed with 16 randomly generated stimuli per size of set 1 (each presented 9 times; 3 times per pixel noise pattern), and were presented twice, making up 10% of all trials presented on a given day. These transfer stimuli were always followed by reward, irrespective of the monkey's response (Vogels 1999a). These transfer tests showed that monkey C was able to generalize the learned category boundary to novel sets, while monkey A had difficulty in doing this generalization: Monkey C achieved an average performance of 70% over the 3 novel sets and performed significantly better than chance for all 3 sets (tested with a Binomial test. Mean = 62.5%, $p <$ 0.05 for set 2; Mean = 71%, $p < .001$ for set 3; Mean = 77%, $p < .001$ for set 4). Monkey A attained 61% correct averaged across the 3 novel sets and performed significantly above chance level only for set 3 (tested with a Binomial test; Mean = 60.5%, $p > .05$ for set 2; Mean = 65.5%, $p < .01$ for set 3; Mean = 56%, $p > .05$ for set 4). It is difficult to know whether the difference in the degree of transfer to novel sets shown by two animals simply reflects a distinction between individual subjects or is instead related to the different trained dimensions.

After this transfer test, we presented stimuli from the 4 sets randomly intermixed. From this point on, the 16 shapes with fixed values (per size) of set 2, 3 and 4 were no longer used for the remainder of the training phase (as was already the case for set 1). Instead, every day, we randomly picked 16 new stimuli (8 for each category) per size and per set with values from within the limits of the tested configuration. Again, these values could not lie within a small range symmetrical around the category boundary of the relevant dimension (see above). This range of values was identical for all sets for the curvature dimension. This was because shapes from different sets that had equal parametric curvature values indeed had equal curvature. As the archetypical shapes were calibrated to have perceptually equal aspect ratios, the shapes of different sets differed slightly in their physical aspect ratios. To induce category boundaries that were at an equivalent physical aspect ratio level for any given set, for each set we adapted the range around the boundary from which no values could be picked. The 16 shapes that were used in the post-training recording phase (see further) were assigned to the same category across the 4 sets.

Because monkey C, who performed the categorization task with curvature as the relevant dimension, made very few errors, the range around the category boundary was halved (to 1/12 of the total tested range) for this monkey after the 4^{th} day of performing to criterion level (see below).

Once the monkeys (Monkey C: 16 days; Monkey A: 42 days) had learned to categorize the shapes to criterion performance (90% correct responses averaged across all stimuli of all sets and sizes), the training continued for another 37 or 38 days (for monkey C and monkey A, respectively).

Post-training recordings.

In a third phase, we recorded from IT cortex while the monkeys were performing the categorization task (see above). We searched for responsive neurons with 16 randomly generated stimuli per size for each of the 4 sets (using the same randomization as during the training phase; see above) which were presented with 3 different pixel noise patterns at a random position within a square region of 3.6 deg centered at the fixation point. Every day, we generated new stimuli and renewed the pixel noise patterns. We visualized the responses of the cells in peristimulus time histograms (PSTHs) averaged across trials and shapes. We had a PSTH for each combination of the 4 sets and 3 sizes, resulting in 12 different PSTHs. Based on a visual inspection of these PSTHs, we selected the sets for which a neuron was judged to be responsive, for the subsequent main test. Note that this selection of responsive neurons and stimulus sets was unbiased with respect to the tuning for the curvature or aspect ratio dimensions.

To maximize the data collected on a given recording day, we selected a maximum of 2 shape sets for the subsequent test. If the neuron responded to shapes from more than 2 sets, we randomly chose 2 sets from these possibilities and started the subsequent test with the randomly intermixed presentation of the shapes of these 2 sets. The remaining sets were introduced only in a subsequent test once we had sampled enough trials (i.e. minimally 10 trials per stimulus) for the first two chosen sets. The recording of a cell was aborted when all shapes of all selected sets had been presented about 10 times, when it became impossible to isolate the cell's responses from the other neuronal activity, or when the monkey simply stopped working.

In this main test, we presented, per selected set, the 16 shapes with fixed parametric levels (as in Figure 1 & 5) filled with one pixel noise pattern (which was refreshed every day) at an intermediate size at a fixed position.

Given the inherent difficulty of centering stimuli that vary in curvature and the fact that the animals were trained to categorize the stimuli at randomly chosen positions, we also tested neurons with a second type of centering (in addition to the one used in the pre-training recording phase (center type 1)). This allowed us to generalize the (absence of) effects of categorization on neural selectivity for different positioning of the stimuli (see Results). For this center type 2, the middle of the vertical, curved medial axis was centered on the screen. This center type 2 was used in about half of all cells recorded in the post-training phase and for all cells recorded in the left (control) hemisphere in monkey A. Note that all analyses that compare pre- and post-training responses utilized only data obtained with the same centering (center type 1). The difference between the two types of centering was such that the aspect ratio or curvature transformations were first applied before the shape was centered in center type 2, while the shape was centered before application of the stimulus transformations in center type 1.

In addition to the 16 fixed shapes per selected set, eight catch stimuli per set were added for behavioral control only: 4 size controls and 4 position controls. The size control stimuli included 2 large and 2 small shapes, with random parametric values lying within the limits of the tested configuration and with the constraint that each category was chosen with equal frequency. From each quadrant of the 16-shape configuration (A to D; Figure 5), one shape of intermediate size was presented at a control position. The maximum difference between the position control shapes and their corresponding reference shapes was 1.5°.

DATA ANALYSIS AND TESTS

In both pre- and post-training recordings, the response of the neuron was defined as the mean number of spikes in a 70-200 ms analysis window relative to stimulus onset. The selection of the analysis window was based on an analysis of the monkeys' eye movements during the categorization task in the post-training phase (Figure 6).

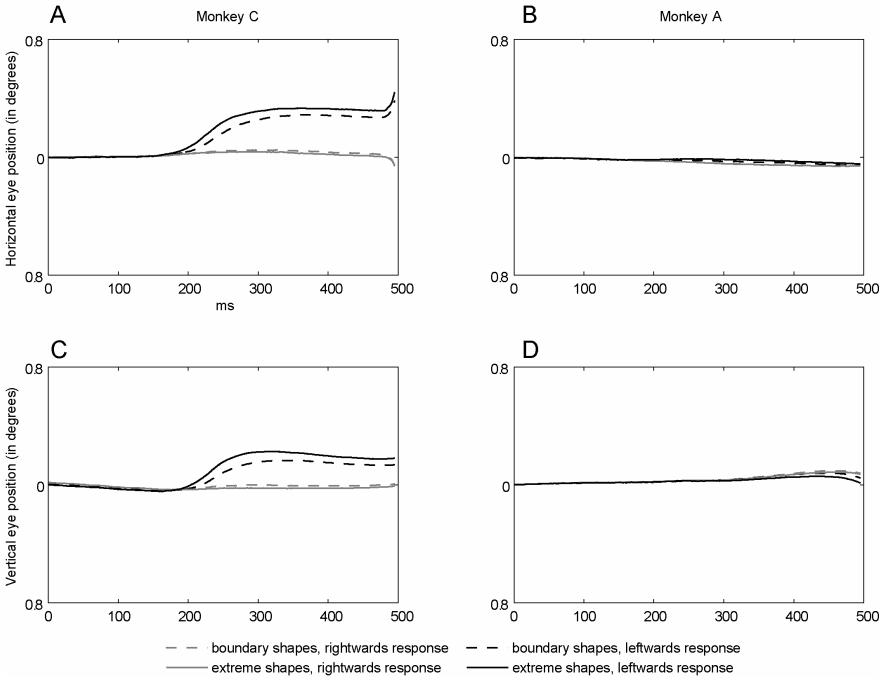

Figure 6. Eye positions averaged over trials for monkey C (A and C) and monkey A (B and D) during the categorization task in the post-training recording phase. In the upper part (A and B), the mean horizontal eye positions (in visual degrees) are displayed. In the lower part (C and D), the mean vertical eye positions are presented. On the X-axis, the stimulus presentation time relative to stimulus onset is plotted; on the Y-axis, the eye position within the fixation window is plotted. Values 0.8, 0 and -0.8° (from top to bottom) represent the left/upper (A and B/C and D) boundary, the center and the right/lower (A and B/C and D) boundary of the average fixation window, respectively. Eye positions for shapes associated with a rightward or leftward saccade are plotted in grey and black, respectively. Eye positions for shapes close to the category boundary (i.e. with a parametric value of 33 or 66%) are displayed in dotted lines. Solid lines are used for shapes with extreme parametric values (i.e. 0 or 100%, and thus not close to the category boundary).

After about 150 ms, one of the monkeys made small, preparatory saccades towards the correct-response side, but still within the fixation window (Figure 6). These small saccades can, in principle, alter the visual input to the retina, which could in turn affect the neuronal responses in IT. To avoid any possible effect that this altered retinal input might have on the responses of the IT cells (which could occur after about 220 ms, given that the minimum latency of IT neurons is approximately 70 ms; see Vogels 1999b), we chose an analysis window up to 200 ms after stimulus onset.

The response of a neuron recorded in the pre-training phase was measured using the same procedure as in De Baene et al. (2007), excluding the first three stimuli as well as the last stimulus of a trial sequence. However, a response window of 70-200 ms poststimulus onset was used (instead of 50-200 ms in De Baene et al.). All analyses in the pre-training phase were performed on neurons showing shape selectivity. For every cell recorded in the pre-training phase, we tested the shape selectivity for each stimulus set using a permutation test to asses the statistical significance of the observed variance within a given shape set in the mean neuronal responses to stimuli. For each shape set, the distribution of the variances expected by chance was determined by calculating new variances of the data after permuting the order of the stimuli within each trial while maintaining the actual spike counts. We generated a distribution of 1,000 permuted variances, representing the distribution of variances that would have been expected to occur by a chance association between stimulus and neuronal firing. A neuron was considered to be shape selective within a shape set if the observed variance for responses within that shape set was larger than the 95^{th} percentile of the values in its own permuted variance distribution ($p < 0.05$, 1-tailed).

The responsiveness of cells in the post-training phase was assessed per set by a split-plot-design analysis of variance (ANOVA; Kirk 1995) comparing

baseline activity, measured in a -130 to 0 ms time window relative to stimulus onset, with stimulus-driven activity measured in a 70-200 ms time window, relative to stimulus onset. All analyses in the post-training phase were performed on the sets for which at least a main effect of this response variable ($p < 0.05$) was found. A significant interaction ($p < 0.05$) between this response variable and shape indicated that the cell was selective within this set. Comparisons between pre- and post-training phase were performed only for these shape selective neurons.

In both pre- and post-training recording phases, we calculated several indices for both the relevant and irrelevant dimension (thus for both the learned and unlearned categories, respectively) per tested set. Only trials with correct responses were included in these analyses. As a measure of the selectivity for the relevant versus the irrelevant dimension, we computed per set the depth of selectivity (DOS; Rainer and Miller 2000) for each dimension separately. This measure of the degree of selectivity of a neuron to a given stimulus set was defined as:

$$[n - (\sum_{i=1}^{n} R_i / R_{\max})]/(n-1),$$

where n = number of parametric values of the relevant/irrelevant dimension (i.c. 4: 0, 33, 66 and 100%); R_i = mean firing rate (averaged across the 4 values of the irrelevant/relevant dimension, respectively) to the i^{th} parametric value of the relevant/irrelevant dimension; and $R_{max} = \max\{R_i\}$. The DOS could vary between 0 (when the neuron responded equally for all parametric values) and 1 (when there was a response for only one parametric value). We employed the DOS index rather than a best-worst index (Sigala and Logothetis 2002) since the DOS index takes into account responses to all, rather than only 2, of the parametric values. As for the best-worst index used

by Sigala and Logothetis (2002), the DOS indices were computed on the marginal means of the parametric values of a dimension, i.e. by averaging across the mean responses for the 4 values of the other dimension (e.g. response for curvature 0% represents the average of the mean responses for the shapes having the 0, 33, 66 and 100% aspect ratio values of that curvature value).

To compare differences in responses to shapes belonging to the same versus different categories, we computed, for each neuron and set, the absolute differences in average response strength to all possible pairs of adjacent stimuli (separately along the relevant and irrelevant dimension of the shape configuration). These response differences were then divided by the square root of the mean of the variances in the response strength to these stimuli. These d' values take into account the difference in mean spike counts as well as the variance of the response over trials. The differences for pairs of stimuli that belonged to the same category were defined as the within-category differences (WCDs); between-category differences (BCDs) were calculated between adjacent stimuli belonging to two different categories. The average parametric distance between stimuli was identical for BCDs and WCDs. An index of the strength of category tuning was computed for each neuron by dividing the difference between the averages of the BCDs and WCDs by the sum of these averages, giving values ranging from -1 to 1, where positive values indicate larger response differences between categories compared with within a category, and negative values indicate the opposite. This category tuning index is identical to the one used by Freedman et al. (2003) in their analysis of category tuning, except that we computed the category tuning index using d' values instead of raw response differences.

REFERENCES

Afraz SR, Kiani R, Esteky H. Microstimulation of inferotemporal cortex influences face categorization. *Nature* 442: 692-695, 2006.

Ashby FG, Maddox WT. Human category learning. *Annu Rev Psychol* 56: 149-178, 2005.

Baker CI, Behrmann M, Olson CR. Impact of learning on representation of parts and wholes in monkey inferotemporal cortex. *Nat Neurosci* 5: 1210-1215, 2002.

Cheng K, Saleem KS, Tanaka K. Organization of corticostriatal and corticoamygdalar projections arising from the anterior inferotemporal area TE of the macaque monkey: a *Phaseolus vulgaris* leucoagglutinin study. *J Neurosci* 17: 7902-7925, 1997.

Dean P. Effects of inferotemporal lesions on the behavior of monkeys. *Psychol Bull* 83: 41-71, 1976.

De Baene W, Premereur E, Vogels R. Properties of shape tuning of macaque inferior temporal neurons examined using Rapid Serial Visual Presentation. *J Neurophysiol* 97: 2900-2916, 2007.

Denys K, Vanduffel W, Fize D, Nelissen K, Peuskens H, Van Essen D, Orban GA. The processing of visual shape in the cerebral cortex of human and nonhuman primates: A functional magnetic resonance imaging study. *J Neurosci* 24: 2551-2565, 2004.

Erickson CA, Jagadeesh B, Desimone R. Clustering of perirhinal neurons with similar properties following visual experience in adult monkeys. *Nat Neurosci* 3: 1143-1148, 2000.

Foster DH, Wagemans J. Viewpoint-invariant Weber fractions and standard contour-curvature discrimination. *Biol Cybern* 70: 29-36, 1993.

Freedman DJ, Assad JA. Experience-dependent representation of visual categories in parietal cortex. *Nature* 443: 85-88, 2006.

Freedman DJ, Riesenhuber M, Poggio T, Miller EK. A comparison of primate prefrontal and inferior temporal cortices during visual categorization. *J Neurosci* 23: 5235-5246, 2003.

Freedman DJ, Riesenhuber M, Poggio T, Miller EK. Experience-dependent sharpening of visual shape selectivity in inferior temporal cortex. *Cereb Cortex* 16: 1631-1644, 2006.

Garner WR. *The processing of information and structure*. Potomac, MD: Erlbaum, 1974.

Goldstone RL. Influences of categorization on perceptual discrimination. *J Exp Psychol Gen* 123: 178-200, 1994.

Goldstone RL, Lippa Y, Shiffrin RM. Altering object representations through category learning. *Cognition* 78: 27-43, 2001.

Gross CG, Bender DB, Rocha-Miranda, CE. Visual receptive fields of neurons in inferotemporal cortex of the monkey. *Science* 166: 1303-1306, 1969.

Janssen P, Vogels R, Orban GA. Selectivity for 3D shape that reveals distinct areas within macaque inferior temporal cortex. *Science* 288: 2054-2056, 2000.

Jiang X, Bradley E, Rini RA, Zeffiro T, VanMeter J, Riesenhuber M. Categorization training results in shape- and category-selective human neural plasticity. *Neuron* 53: 891-903, 2007.

Kayaert G, Biederman I, Vogels R. Shape tuning in macaque inferior temporal cortex. *J Neurosci* 23: 3016-3027, 2003.

Kayaert G, Biederman I, Op de Beeck H, Vogels R. Tuning for shape dimensions in macaque inferior temporal cortex. *Eur J Neurosci* 22: 212-224, 2005.

Keri S. The cognitive neuroscience of category learning. *Brain Res Rev* 43: 85-109, 2003.

Kiani R, Esteky H, Mirpour K, Tanaka K. Object category structure in response patterns of neuronal population in monkey inferior temporal cortex. *J Neurophysiol* 97: 4296-4309, 2007.

Kirk RE. *Experimental design procedures for the behavioral sciences*. Brooks/Cole, Pacific Grove, CA, 1995.

Kobatake E, Wang G, Tanaka K. Effects of shape-discrimination training on the selectivity of inferotemporal cells in adult monkeys. *J Neurophysiol* 80: 324-330, 1998.

Koida K, Komatsu H. Effects of task demands on the responses of color-selective neurons in the inferior temporal cortex. *Nat Neurosci* 10, 108-116, 2007.

Kruschke JK. ALCOVE: An exemplar-based connectionist model of category learning. *Psychol Rev* 99: 22-44, 1992.

Li S, Ostwald D, Giese M, Kourtzi Z. Flexible coding for categorical decisions in the human brain. *J Neurosci* 27, 12321-12330, 2007.

Livingston, KR, Andrews, JK, Harnad, S. Categorical perception effects induced by category learning. *J Exp Psychol Learn* 24: 732-753, 1998.

Logothetis NK, Sheinberg DL. Visual object recognition. *Annu Rev Neurosci* 19: 577-621, 1996.

Mirabella G, Bertini G, Samengo I, Kilavik BE, Frilli, D, Della Libera C, Chelazzi L. Neurons in area V4 of the macaque translate attended visual features into behaviorally relevant categories. *Neuron* 54: 303-318, 2007.

Miyashita Y, Date A, Okuno H. Configurational encoding of complex visual forms by single neurons of monkey temporal cortex. *Neuropsychologia* 31: 1119-1131, 1993.

Mogami T, Tanaka K. Reward association affects neuronal responses to visual stimuli in macaque TE and Perirhinal cortices. *J Neurosci* 26: 6761-6770, 2006.

Nosofsky RM. Attention, similarity, and the identification categorization relationship. *J Exp Psychol Gen* 115: 39-57, 1986.

Op de Beeck H, Wagemans J, Vogels R. Inferotemporal neurons represent low-dimensional configurations of parameterized shapes. *Nat Neurosci* 4: 1244-1252, 2001.

Op de Beeck H, Wagemans J, Vogels R. The effect of category learning on the representation of shape: dimensions can be biased but not differentiated. *J Exp Psychol Gen* 132: 491-511, 2003.

Rainer G, Asaad WF, Miller EK. Selective representation of relevant information by neurons in the primate prefrontal cortex. *Nature* 393: 577-579, 1998.

Rainer G, Miller EK. Effects of visual experience on the representation of objects in the prefrontal cortex. *Neuron* 27: 179-189, 2000.

Riesenhuber M, Poggio T. Models of object recognition. *Nat Neurosci [Suppl.]* 3: 1199-1204, 2000.

Seltzer B, Pandya DN. Afferent cortical connections and architectonics of the superior temporal sulcus and surrounding cortex in the rhesus monkey. *Brain Res* 149: 1-24, 1978.

Sigala N, Gabbiani F, Logothetis NK. Visual categorization and object representation in monkeys and humans. *J Cogn Neurosci* 14: 187-198, 2002.

Sigala N, Logothetis NK. Visual categorization shapes feature selectivity in the primate temporal cortex. *Nature* 415: 318-320, 2002.

Tanaka K. Inferotemporal cortex and object vision. *Annu Rev Neurosci* 19: 109-139, 1996.

Thomas E, Van Hulle MM, Vogels R. Encoding of categories by noncategory-specific neurons in the inferior temporal cortex. *J Cogn Neurosci* 13: 190-200, 2001.

Vogels R. Categorization of complex visual images by rhesus monkeys. Part 1: behavioural study. *Eur J Neurosci* 11: 1223-1238, 1999a.

Vogels R. Categorization of complex visual images by rhesus monkeys. Part 2: single-cell study. *Eur J Neurosci* 11: 1239-1255, 1999b.

Vogels R, Sary G, Dupont P, Orban GA. Human brain regions involved in visual categorization. *Neuroimage* 16: 401-414, 2002.

Vogels R. Representation of response categories in visual cortex. *Neuron* 54: 181-183, 2007.

Wagemans J, Ons B, Gillebert CR, Op de Beeck H. Effects of categorization learning on perceived shape similarity in humans. *Soc Neurosci Abstr* 438: 22, 2006.

CHAPTER 4
EFFECTS OF ADAPTATION ON STIMULUS SELECTIVITY OF MACAQUE INFERIOR TEMPORAL SPIKING ACTIVITY AND LOCAL FIELD POTENTIALS

In preparation

In many cortical areas, repeated presentation of a specific stimulus is commonly associated with a reduced neuronal response, i.e. adaptation. Recently, adaptation has been used in fMRI studies to infer the stimulus selectivity of neuronal populations based on the degree of cross-adaptation when the adapter and test stimulus differ. In the present study, we studied the effects of adaptation on the neuronal stimulus selectivity in IT cortex, both with single-cell spiking activity and local field potentials (LFPs). Sequences of 2 stimuli (stimulus durations 300ms, ISI 300ms) were presented to passively fixating monkeys. For one of the 4 parametric sets of 6 shapes (each created by morphing between 2 complex 3D shapes), for which the neuron was most selective, all 36 possible stimulus combinations were shown in a fully-crossed design. We observed that, both for the spiking activity and the LFP gamma power, stimulus repetition scaled down the neuronal responses without changing the tuning width. The degree of adaptation was not only response strength dependent but was affected by the relationship between adapter and test stimulus for both shape feature and position changes: a larger adaptation was found when adapter and test stimulus had identical shape features and were presented at the same position than when these stimuli differed in shape or position. Consequently, we found that the degree of adaptation decreased with decreasing similarity between the adapter and test stimulus. The present results suggest that adaptation occurs at or before the level of the synapses onto the neuron. The implications of these findings for models of adaptation and for the interpretation of fMRI studies using adaptation are discussed.

INTRODUCTION

Until recently, fMRI studies were limited to showing differences in activation of a brain region when different stimuli (e.g. moving versus static stimuli) were presented and were unable to reveal the neuronal selectivity for stimulus parameters in this activated region (e.g. direction selectivity). However, knowledge about the stimulus selectivity of neurons is essential to understand what these neurons code. This fMRI limitation has recently been overcome with the development of the functional magnetic resonance adaptation technique (fMR-A; Grill-Spector and Malach 2001; Nacache and Dehaene 2001). However, contrary to the single-cell recording technique used in macaques in which stimulus selectivity can be assessed directly, fMR-A studies may only provide an indirect measure of the average selectivity of neuronal populations (e.g. Toottel et al. 1998; Grill-Spector et al. 1999; Kourtzi and Kanwisher 2000; James et al. 2002; Piazza et al. 2004). The various fMR-A paradigms that have been used all need to infer this selectivity from the level of cross-adaptation.

The principle of cross-adaptation works as follows: Consider 3 stimuli (A, B and C) and that the same neurons respond to stimulus A and B, but not to stimulus C. When stimulus A is repeated, the neuronal activation will decrease, i.e. adaptation will occur (A-A sequence). Because the same neurons are responsive for stimulus A and B, one expects also that activation is decreased when B is followed by A, i.e. cross-adaptation (B-A sequence). However, since different neurons respond to stimulus A and C, one does not expect cross-adaptation for the C-A sequence.

A key assumption in inferring neuronal tunings from cross-adaptation is that the same tuning function underlies both the degree of adaptation and the responsiveness of the neurons. This match between the neuronal adaptation

and the neuronal tuning was examined by Sawamura et al. (2006) in a single-cell study in macaque inferior temporal (IT) cortex. This brain area at the endpoint of the ventral visual stream which is involved in object identification and categorization (Gross et al. 1969; Dean 1976; Tanaka 1996; Logothetis and Sheinberg 1996; Afraz et al. 2006) is known to show neuronal adaptation (Gross et al. 1967, 1969; Baylis and Rolls 1987; Miller et al. 1991a, b; Riches et al. 1991; Sobotka and Ringo 1993; Vogels et al. 1995) and also shows fMRI adaptation in macaques (Sawamura et al. 2005). Sawamura et al. (2006) measured the response for each sampled IT neuron to a shape stimulus A (i.e. the test stimulus), to which the neuron responded, as a function of a previous stimulus (i.e. the adapter). This previous stimulus was either the same shape (shape A) or a different one (shape B or C). Stimulus B was chosen to be equally effective for that particular neuron as shape A, while a shape to which the neuron responded much less or not was chosen as stimulus C. Sawamura et al. found little or no cross-adaptation for the C-A sequences, whereas lower average response reductions for the B-A sequences compared to the A-A sequences were observed. This lower then expected degree of cross-adaptation for the B-A sequences (based on the similarity of the responses to shape B and A) indicated a greater stimulus selectivity of the adaptation effect compared to the stimulus selectivity of the responses of the IT neurons. This, in turn, suggests a possible overestimation of the neuronal selectivity by the fMR-A method.

As Sawamura et al. (2006) only presented one test stimulus (shape A), they could not address issues related to the effects of adaptation on the stimulus selectivity of IT neurons. However, in order to interpret fMR-A results, it is crucial to know how adaptation affects the neuronal tuning and this as a function of the similarity between the adapter and the test stimulus. Additionally, changes in stimulus selectivity following adaptation could be used to distinguish two models of adaptation: the “fatigue” model (Grill-

Spector and Malach 2001) and the "sharpening" model (Desimone 1996; Wiggs and Martin 1998). The fatigue model predicts that stimulus repetition reduces the response in proportion to the original response, but predicts no change in selectivity with adaptation. The sharpening model, by contrast, predicts that adaptation causes a sharpening of the tuning curves, thus an increased selectivity after adaptation. This results in a sparser representation of the stimuli.

To study the effects of adaptation on the stimulus selectivity of IT neurons, we constructed sets of stimuli that varied systematically along a set of morphing dimensions. The use of such parameterized shape sets allows measuring the tunings of IT neurons to the parametric variation built into the stimulus sets (e.g. Op de Beeck et al. 2001; Sigala and Logothetis 2002; Brincat and Connor 2004; Kayaert et al. 2005; De Baene et al. 2007). By presenting all possible combinations of these stimuli in a fully crossed design in which all stimuli could serve as an adapter and as a test stimulus, we could assess the effect of adaptation on the tuning of IT neurons.

Recently, several studies showed a higher correlation between fMRI BOLD responses and Local Field Potentials (LFPs) compared to spiking activity (Logothetis et al. 2001; Viswanathan and Freeman 2007). Whereas single cells reflect the neuronal output, LFPs are thought to reflect the summation of synaptic activity from a radius of up to a few millimeters around the tip of the electrode (Mitzdorf 1985). Because LFPs, as does the fMRI BOLD response, embody a population response and reflect an energetically expensive activity (Logothetis et al. 2001; Rauch et al. 2008), they could possibly reconcile single-unit recordings in monkeys with neuroimaging results in humans. Kreiman et al. (2006) recorded both single cell activity and LFPs from the same electrode in macaque IT cortex. They reported that LFPs often showed stimulus selectivity, although the selectivity for the single units was stronger.

Additionally, they found only a weak correlation between the selectivity observed for the LFPs and that for the single units. Since LFPs can demonstrate stimulus selectivity in IT cortex, we compared the effects of adaptation on tuning of single units and LFPs in IT cortex by examining both responses of single cells and LFPs recorded from the same electrode in this present study.

In order for our findings to add to the understanding of the fMR-A results, we used stimulus timing parameters which were very similar to those used in rapid, event-related fMR-A paradigms (e.g. Kourtzi and Kanwisher 2000). Parts of the results of the present study have been published in abstract form (De Baene and Vogels 2007).

METHODS

SUBJECTS AND RECORDING

The data were collected from two rhesus monkeys (*Macaca mulatta*; Monkey G and M). All animal care and experimental and surgical protocols complied with national and European guidelines and were approved by the K.U. Leuven Ethical Committee for animal experiments.

Prior to the experiments, we attached a plastic head-fixation post to the skull and stereotactically implanted a recording chamber under aseptic conditions and isoflurane anesthesia. The positioning of the recording chamber was guided by structural magnetic resonance (MRI) images taken before surgery. A reliable estimation of the recording positions was obtained by visualization of a copper sulphate filled tube, inserted into the grid (Crist, Hagerstown, MD) at one of the recording positions, using MRI scans obtained in the beginning and the midst of the recording sessions. The depths of the

recording positions were estimated using microdrive depth readings corresponding to white/grey matter transitions and to contacts with the skull base during electrode penetrations.

Across animals, the recording locations were estimated to range from 13 to 22 anterior to the external auditory meatus and included the lower bank of the superior temporal sulcus (STS), the cortical convexity lateral to the anterior middle temporal sulcus (aMTS) and the lip of the STS (area TEm; Seltzer and Pandya 1978) of the left hemisphere.

Standard extracellular recordings were performed with Tungsten microelectrodes that were placed in a guiding tube position in a grid and lowered with a Narishige hydraulic microdrive which was firmly mounted onto the recording chamber. The LFPs were recorded simultaneously from the same Tungsten microelectrodes as the spikes using a Plexon data acquisition system (Plexon, Dallas, TX). The input impedance of the head-stage was > 1GOhm.

The guiding tube was grounded and served as a reference. The recorded signal was amplified and split into spiking activity (band-passed signal between 250Hz and 8kHz) and LFPs (band-passed signal between 0.7Hz and 170Hz, sampled at 1kHz). Single spikes were isolated online using Plexon-software. Timings of the discriminated single units were stored (with a 1-ms resolution), together with stimulus and behavioral events, on a personal computer for later off-line analysis.

STIMULI

We generated 4 sets of greyscale, 3D stimuli using *3ds Max 7* (Autodesk, Inc., San Rafael, CA). First, we designed 2 largely dissimilar, complex 3D shapes with the same number of vertices per set, which served as the base and

target object in the subsequent morphing procedure. Next, we applied the morphing algorithm implemented in the *3ds Max 7* software, resulting in a set of 6 different shapes (labeled A to F in Figure 1) that smoothly changed their appearance from one of the two original shapes (the base) to the other (the target) by translating the position of the vertices from their arrangement in the base shape to the arrangement in the target shape in 5 equal steps.

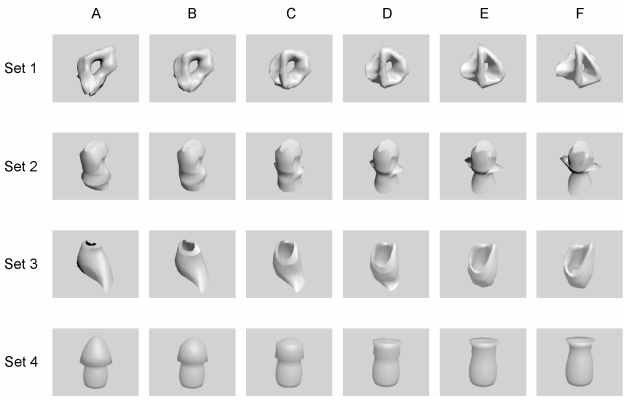

Figure 1. Stimuli. The parametric configurations consisted of 4 sets of 6 shapes each. The shapes B to E of each set were obtained by morphing between shapes A and F of that set.

The height of the shapes ranged from 5.4° to 7.2° visual angle and the area of the different shapes within one set was largely equated (max difference within a set = 0.8% of the total area). The greylevels of the images were adjusted resulting in equal mean luminance for all stimuli within a set after gamma-correction. The stimuli were presented on a uniform grey background (ca 17 cd/m²) on a monitor positioned 60cm from the eye of the monkeys.

Additionally, we generated different scrambled versions of each image by dividing the original image into rectangular blocks of equal size (16x16 pixels) and repositioning them in a random way. We repeated this 5 times per stimulus per set, resulting in a total of 120 scrambled images.

FIXATION TASK

Eye position was measured online through the pupil position using an infrared eye tracking system (ISCAN, EC-240A) at a sampling rate of 120Hz. Monkeys were trained to keep their gaze within 0.8° (monkey G) or 1.0° (monkey M) of a red fixation target square (size: 0.18°) that was presented in the center of the display during the trials. When the animals maintained fixation throughout a trial, they were rewarded with a drop of apple juice.

The stimulus selectivity of an isolated single unit was first tested using all 6 stimuli of every shape set (N = 6 x 4 = 24 conditions) in a search test. For this initial search test, a stimulus was presented for 300ms after a stable fixation period of 500ms. A trial ended after another 300ms of stable fixation. After 1000ms, the next trial started. The shapes of the different sets were pseudo-randomly intermixed with the constraint that 2 subsequent shapes were from a different shape set. The stimuli were presented foveally with their center of mass at the center of the screen.

Central adaptation test

Based on the visual inspection of the single unit responses in the initial search test described above, which were on line visualized per stimulus in a peristimulus time histogram (PSTH), averaged across trials, we selected a stimulus set for which the neuron was judged to be selectively responsive for the subsequent test. In this test, we presented each of the 36 possible stimulus combinations (sequences A-A, A-B, A-C, …, F-E, F-F) of the selected shape set. Thus, in this fully crossed design, each of the 6 shapes could serve as an adapter and a test stimulus. We used maximally one repetition of a stimulus per sequence, since Sawamura et al. (2006) found that one stimulus presentation sufficed to produce strong adaptation. Within each sequence, after a stable fixation of 500ms, the stimuli were presented foveally for

300ms with an ISI of 300ms. After another period of 300ms of stable fixation, a trial ended. After a 500ms period in which a blank screen was presented, the fixation point was presented again, marking the start of a new trial. The different stimulus sequences were shown in pseudo-random order so that a stimulus presented in trial *n* (as an adapter or test stimulus) could not occur in trial *n*+1. In order to dis-adapt the neuron, we presented 2 dis-adaptation sequences in between two of these so-called adaptation sequences. In a dis-adaptation sequence, 2 randomly chosen scrambled versions of the images were presented. To assure that minimally 4 scrambled images were presented in between two adaptation trials, a dis-adaptation sequence was repeated (with different scrambled images) whenever this sequence was aborted. The actual central adaptation test (following the initial search test) always started with a dis-adaptation trial (Figure 2A).

Peripheral adaptation test

For about one third of the recorded cells, a peripheral adaptation test was used instead of the aforementioned central adaptation test. Based on the visual inspection of the PSTHs of the single unit responses in the initial search test, we selected two stimuli from within a stimulus set for which the neuron was judged to be selective for the subsequent test. The stimulus eliciting the best response was always selected. The second selected stimulus was chosen to be as different from the first one as possible, but still eliciting a clear response.

In the subsequent test, the monkeys also needed to passively fixate the fixation point as in the central adaptation test. However, the shapes were not presented foveally, but at an eccentricity of 4° above or below the fixation point. In this fully crossed design, both selected stimuli could serve as an adapter and as a test stimulus, and they could be presented at both positions as

adapter or test stimulus, resulting in 16 (2 stimuli x adapter vs test stimulus x 2 adapter positions x 2 test stimulus positions) different conditions.

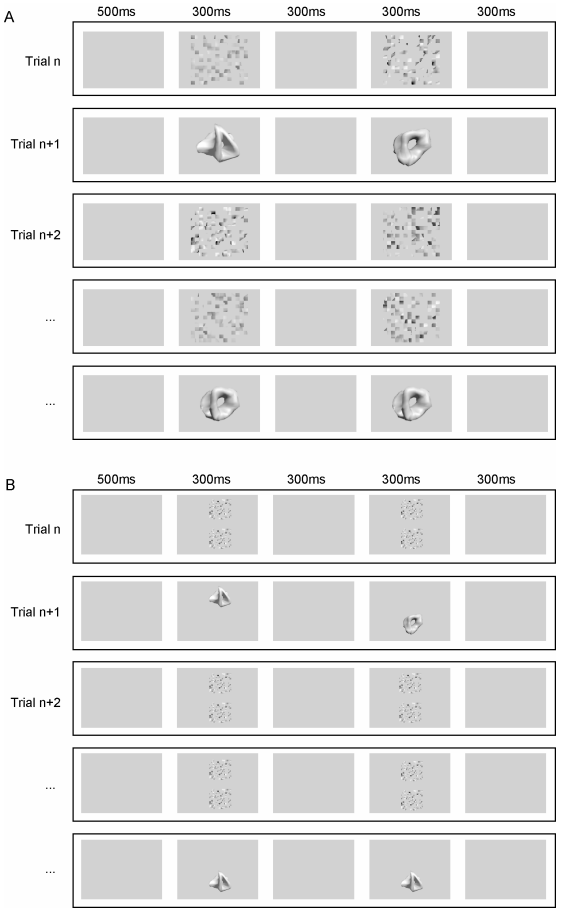

Figure 2. Procedure. A. Design of the central adaptation test. The monkey initiated each trial by fixating a red fixation target at the screen center. After 500 ms, a first stimulus appeared at the center of the screen for 300 ms. After an interstimulus interval of 300 ms, a second stimulus appeared for 300 ms. After another 300 ms of stable fixation, the monkey was rewarded with a drop of apple juice. After an intertrial interval of 500 ms in which a blank screen was presented, a new fixation target appeared. The test always started with a dis-adaptation trial, in which two scrambled images were presented. In between two adaptation trials (in which two regular shapes were presented), two non-aborted dis-adaptation trials were presented. B. Peripheral adaptation test. The succession of sequences was identical to that in the central adaptation test. However, stimuli were no longer presented at the center of the screen but at 4° above or below the fixation target. In the dis-adaptation trials, each centered scrambled image of the central adaptation test was replaced by two scrambled images presented above and below the fixation target.

The timing of the sequence was identical to the one used in the central adaptation test. Again, we presented 2 non-aborted dis-adaptation sequences in between two adaptation sequences. Instead of showing 2 randomly chosen scrambled image versions at the screen center, 4 randomly chosen scrambled images were presented in each dis-adaptation sequence: Two randomly chosen scrambled images were presented in parallel above and below the fixation point as adapters. Two other randomly chosen scrambled images,

presented in parallel above and below the fixation point, served as test stimuli (Figure 2B).

Eye movement analysis

Central adaptation test. Eye positions during the presentations of the test stimuli were compared between different sequences based on the parametric distance between the adapter and test stimulus. The within-trial standard deviation of the eye position was measured in a 300ms interval starting at the onset of the test stimulus presentation and averaged across trials having the same parametric distance between adapter and test stimulus. The mean standard deviation averaged across all trials of all parametric distances equaled 0.07° and 0.08° for the x direction in monkeys 1 and 2, respectively, and 0.08° for both monkeys in the y direction. There was no significant difference in standard deviation between the "same" conditions (i.e. parametric distance = 0: "same" trials) and the conditions with a maximal parametric difference between adapter and test stimulus (i.e. distance = 5: sequences A-F and F-A) in either direction (mean standard deviations of these conditions differed by less than 0.002° and 0.001° in the x and y direction, respectively), as tested with a general linear model (GLM) repeated-measures ANOVA with parametric distance (distance 0 or 5) as a within-neuron factor and monkey (monkey 1 or 2) as a between-neurons factor ($F(1,78)=2.44$, $p > .12$ and $F(1,78)=1.00$, $p > .32$ for the main effect of x and y direction, respectively). This suggests that the monkeys fixated equally well during the presentation of the test stimuli in the different sequences.

Peripheral adaptation test. Eye positions during the presentations of the test stimuli were compared between different sequences based on the relation between the positions of the adapter and the test stimulus. Only trials in which the most effective stimulus (see below) served both as an adapter and

test stimulus were included in these analyses. The within-trial standard deviation of the eye position was measured in a 300ms interval starting at the onset of the test stimulus presentation and averaged across trials of the same condition (adapter and test stimulus at the same or different position). The mean standard deviation averaged across all trials of both conditions equaled 0.10° and 0.08° for the x direction and 0.09° and 0.08° for the y direction in monkeys 1 and 2, respectively. There was no significant difference in standard deviation between the "same position" condition (i.e. adapter and test stimulus at same position) and the "different position" condition (i.e. adapter and test stimulus at different positions) in either direction (mean standard deviations of these conditions differed by less than 0.002° and 0.001° in the x and y direction, respectively), as tested with a general linear model (GLM) repeated-measures ANOVA with condition (same or different position) as a within-neuron factor and monkey (monkey 1 or 2) as a between-neurons factor ($F(1,38)=1.64$, $p > .20$ and $F < 1$ for the main effect of x and y direction, respectively). This suggests that the monkeys fixated equally well during the presentation of the test stimuli in the different sequences.

DATA ANALYSES

SPIKING ACTIVITY

Unless otherwise stated, net neuronal responses were used in all analyses, i.e. the mean firing rate in the response window 50 to 350 ms relative to stimulus onset after subtraction of the mean firing rate in the baseline window 300 to 0 ms before onset of the adapter. For each cell, the responsiveness to each stimulus, presented as an adapter, was tested with a Wilcoxon test ($p < .05$).

For the analyses in the central adaptation test, only those cells responsive to at least one stimulus and showing shape-selectivity (one-way ANOVA, $p < .05$) within the selected shape set were included, unless otherwise stated.

For the analyses in the peripheral adaptation test, we defined the response to a particular adapter at a particular position as the average net response across all conditions in which that particular shape, presented at that particular position, served as an adapter. The analyses were restricted to the most effective stimulus, i.e. the shape eliciting the largest response when presented as an adapter at one of both positions.

LOCAL FIELD POTENTIALS

For the LFPs, we applied a digital 50Hz notch filter off-line (fourth-order Butterworth FIR filter; Fieldtrip Toolbox[1]). Trials in which the signal exceeded the 5 to 95% window of the total input range were excluded from the analyses. The LFP data were analyzed in two ways. First, we computed the visually evoked potentials (VEPs) by stimulus-locked averaging of the LFP waveforms (Figure 3A and 3B). Second, we used a time-frequency wavelet decomposition of the signal between 15 and 100Hz for a spectral analysis of the LFPs. By convolving single-trial data using complex Morlet's wavelets (Tallon-Baudry et al. 1997) and taking the square of the convolution between wavelet and signal, we obtained the time-varying power of the signal for every frequency (Figure 3C and 3D). Per frequency, we took the median power across trials. The complex Gaussian Morlet's wavelets had a constant center frequency – spectral bandwidth ratio (f_0/σ_f) of 7, with f_0 ranging from 15 to 100Hz in steps of 1Hz. At 15Hz, this led to a wavelet duration ($2\sigma_t$) of 148.5ms and a spectral bandwidth ($2\sigma_f$) of 4.29Hz. At 100Hz, the wavelet duration and spectral bandwidth were 22.3ms and 28.6Hz, respectively. Thus,

[1] Fieldtrip toolbox: http://www.ru.nl/fcdonders/fieldtrip

for a higher frequency, the time resolution increased, but the frequency resolution decreased. At frequencies below 15Hz, for which the wavelet duration exceeds 150ms, there could be an overlap between a wavelet containing information about the adapter and a wavelet containing information about the test stimulus, as the inter stimulus interval between these two stimuli was 300 ms. As a consequence, the estimated power to the test stimulus would be contaminated by that to the adapter and vice versa. To avoid this, we excluded frequencies below 15Hz from our analyses.

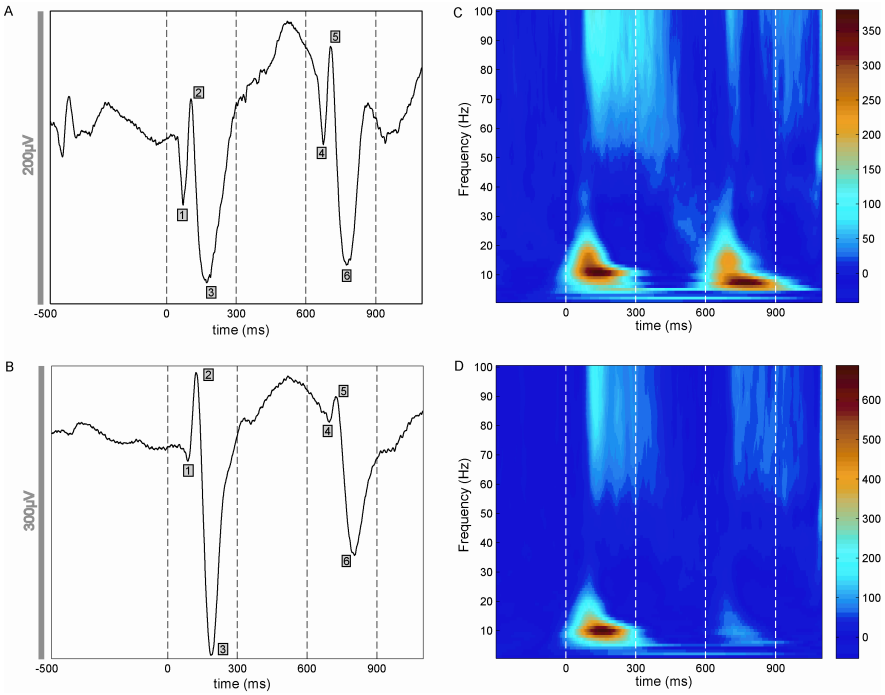

Figure 3. LFP results averaged across all "same" trials and across all sites per monkey (monkey G: N = 40, panels A and C; monkey M: N = 37, panels B and D). A and B: Visual evoked potentials. The vertical black dotted lines depict the on- and offsets of the adapter and test stimulus. The black numbers in grey squares depict the peaks used to compute the adaptation index for the different components. C and D: LFP power spectra. For illustration purposes, the baseline power was subtracted from the energy at each frequency, before dividing these values by the baseline power and multiplying it by 100. As a consequence, the values and their corresponding colors as indicated by the color bars, reflect the percent signal increase relative to baseline. The vertical white dotted lines depict the on- and offsets of the adapter and test stimulus.

The LFP power response was computed by taking the average energy at each frequency in a 50 to 350ms response window relative to stimulus onset, dividing by the baseline power (ranging from 300 to 0ms before adapter onset) and averaging across the frequencies of the frequency band of interest. The frequency bands were defined based on a visual inspection of the power spectra (Figure 3C and 3D) as follows: the low frequency band ranged from 15 to 30Hz; the gamma band ranged from 61 to 100Hz (see Results). The intermediate frequencies (31 to 60Hz) were not included in the analyses, as only weak differences compared to the baseline power were observed for these frequencies during the whole time period of the sequences.

Contrary to the spiking activity analyses, power analyses were not restricted to sites showing shape-selectivity within the selected shape set, but included all sites (except 3, see Results) we recorded from.

ANALYSES FOR BOTH SPIKING ACTIVITY AND LFPS

For each cell (spiking activity) and each recording site (LFP), we calculated an adaptation index. The adaptation index measured the mean percent response difference between adapter and test stimulus across all "same" trials i.e. trials in which the adapter and test stimulus were identical. The adaptation index (AI) was defined as:

$$\frac{\sum Ra_i - \sum Rt_i}{\sum Ra_i} \times 100 ,$$

where Ra_i = mean response to ith adapter; Rt_i = mean response to ith test stimulus, with i ranging from 1 (stimulus A) to 6 (stimulus F) for the central adaptation test. For the peripheral adaptation test, however, Ra_i = mean response to adapter on ith position; Rt_i = mean response to test stimulus on ith

position, with *i* having a value of 1 (position above fixation point) or 2 (position below fixation point).

The degree of adaptation for the VEPs was computed slightly differently: First, we averaged the VEPS across all "same" trials across all sites per monkey. Then, we measured the peak-to-peak amplitudes for two components by computing the amplitude difference between peak 1 and peak 2 (component 1) and between peak 2 and peak 3 (component 2) for the adapter and between peak 4 and peak 5 (component 1) and between peak 5 and peak 6 (component 2) for the test stimulus (peaks shown in Figure 3A and 3B). The adaptation indices for the VEP components were computed as follows:

$$\text{AI component i} = (\text{Adapter PPAcomp}_i - \text{test stimulus PPAcomp}_i)/\text{Adapter PPAcomp}_i \text{x} 100,$$

where PPAcomp_i = peak-to-peak amplitude component i (with value 1 or 2).

To compare the degree of selectivity for stimuli presented as adapters with the degree of selectivity for these same stimuli when repeated, we computed per cell/site the depth of selectivity (DOS; Rainer and Miller 2000) for both the adapters and the test stimuli. This selectivity metric was defined as:

$$\frac{n - \sum R_i / R_{\max}}{n-1},$$

where n = number of shapes (i.c. 6); R_i = mean response to the ith shape; and $R_{max} = \max\{R_i\}$. The DOS could vary between 0 (when the response was equal to all shapes) and 1 (when there was a response to only one shape). The DOS for the test stimuli was calculated on the responses in all "same" trials. The DOS for the adapters, however, was not computed on these "same"

conditions, to prevent that correlations between the DOS-indices for the test stimuli and the DOS-indices for the adapters were induced by common artifacts. Instead, as each stimulus was presented as an adapter in 6 different conditions (each time combined with another test stimulus), we randomly selected per stimulus one of the 5 other (non-same) conditions and used the responses in these trials to compute the DOS index for the adapters. For the computation of the DOS for a cell, absolute responses instead of net responses (i.e. without subtracting the mean firing rate in the baseline window) were used.

To compare the tuning curves for the adapters and for the test stimuli in the "same" trials, we subdivided the cells/sites in three groups based on the responses to the different adapters. A first group of cells/sites showed monotonic tuning: these cells/sites showed maximum responses to one of the extremes of the shape set when presented as an adapter (shape A or F, Figure 1). For the cells/sites with shape A as the most effective adapter, both adapter and test stimuli were ranked in ascending order (i.e., ABCDEF). If shape F was the most effective adapter, a descending ranking was used (i.e., FEDCBA), both for the adapter and test stimuli. A second group of cells/sites showed a maximum adapter response to shape B or E, whereas a third group of cells/sites had a maximum adapter response for shape C or D. For the cells/sites with shape B or C as most effective adapter, both adapters and test stimuli were ranked in ascending order (i.e., ABCDEF). If the maximum adapter response was found for shape E or D, a descending ranking was used (i.e., FEDCBA).

RESULTS

CENTRAL ADAPTATION TEST

Database

We recorded single unit activity and local field potentials simultaneously from the same electrode from 80 sites (40 in each monkey). For each cell/site, each stimulus combination was, on average, presented 8.15 times (minimum = 3, maximum = 14). All 80 neurons were responsive to at least one stimulus of the selected shape set presented as an adapter. Of these 80 neurons, 71 cells showed shape selectivity within the selected shape set. After filtering out the outlier trials (see Methods), 3 sites were excluded from further analyses because of a lack of data on one or more conditions. Because no systematic differences were found between recordings in the lower bank of the STS and recordings in the lateral convexity, we pooled the results of the different recording positions.

Example cell and site

The single unit responses to all 36 possible stimulus combinations of a shape set are shown for one IT neuron in Figure 4A. This neuron responded to all 6 shapes presented as an adapter, and had a preference for shape A (first row). This neuron also showed a clear response suppression with repetition of the same stimulus ("same" trials depicted by red boxes). Figure 4B shows the visually evoked potentials (VEPs) for all 36 possible stimulus combinations of a shape set for one site. These responses were simultaneously recorded with the same electrode as the single unit responses presented in Figure 4A. Inspection of the VEPs in the "same" conditions (depicted by the red boxes) showed a clear decrease in peak-to-peak amplitude, both for component 1 and 2 (as denoted in Figure 3A and B) for this site.

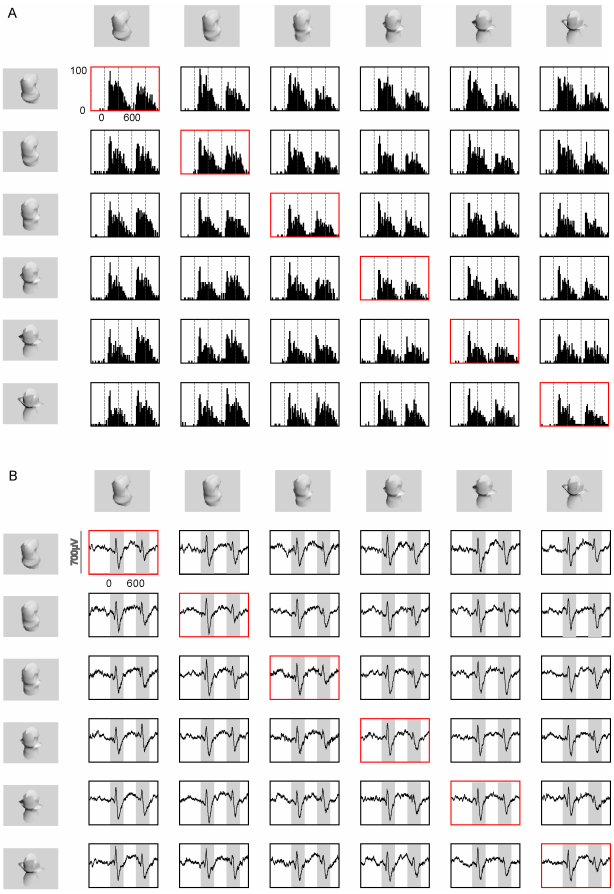

Figure 4. Peri-stimulus time histograms (bin width 20ms; panel A) and visually evoked potentials (panel B) recorded simultaneously from the same electrode for a single cell and site in IT cortex for all 36 possible stimulus combinations. The stimulus shown at the left of each row was presented as an adapter in all 6 conditions of this row. The stimulus shown on top of each column was presented as a test stimulus in all 6 conditions of this column. Each combination of a specific row and a specific column represents one of the 36 possible stimulus combinations. The dotted grey lines in panel A and the grey rectangles in panel B depict the on- and offset of both adapter and test stimulus. The red boxes depict the "same" conditions, in which the adapter and test stimulus are identical.

Degree of adaptation

The median neuronal response at population level (80 cells were included, irrespective of their shape selectivity) dropped substantially when the same stimulus was repeated: The median adaptation index for the spiking activity was 36.97% and was very similar across monkeys (monkey G: 39.81%; monkey M: 33.96%; Figure 5a). The median response to the adapter was significantly larger than the median response to the test stimulus in these

"same" trials (Wilcoxon test across data of both monkeys, $p < .001$ and in each of the two monkeys: $p < .001$).

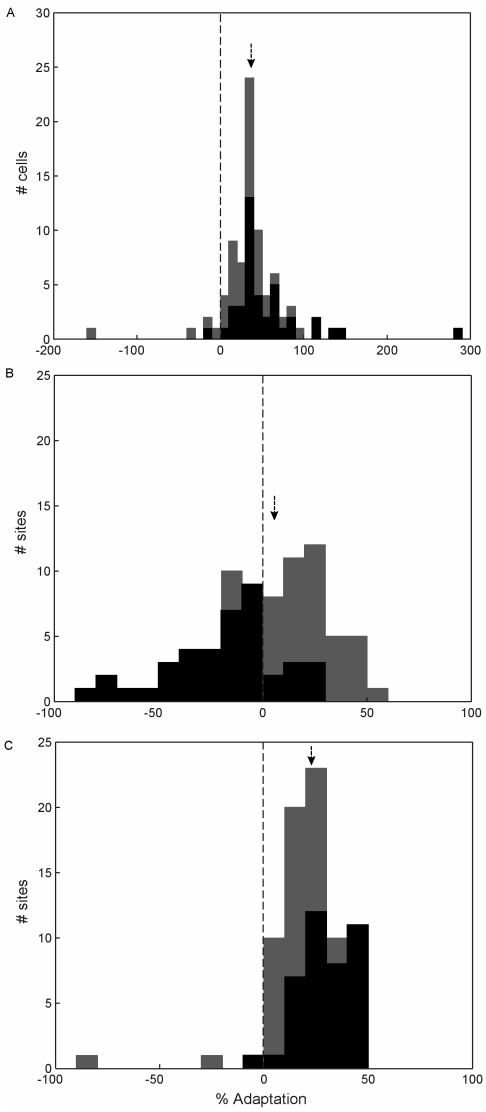

Figure 5. Population distribution of percent adaptation across "same" trials. In panel A, the distribution of the percent adaptation for the spiking activity (N = 80), calculated on net responses, is presented. Panels B and C (N = 77) show the respective distributions of the percent adaptation for the power in the lower frequency bands (15-30Hz) and for the power in the gamma band (61-100Hz). Black bars represent cells/sites recorded in monkey G. Grey bars represent cells/sites recorded in monkey M. The black arrow indicates the median percent adaptation. Note that the scale of the X-axis differs in the A-panel compared to panels B and C.

The peak-to-peak amplitude of both components of the VEPs measured at a population level decreased substantially with the repetition of a same stimulus

for monkey M (AI component 1 = 70.84%; AI component 2 = 43.77%). However, monkey G showed very different results: the peak-to-peak amplitude for the first component decreased only slightly (AI = 7.48%) when the same stimulus was repeated and, additionally, the peak-to-peak amplitude for the second component increased with stimulus repetition (AI = -18.90%).

For the median power averaged across the lower frequencies (15 to 30Hz), the decrease with stimulus repetition at population level (N = 77) was very small across monkeys: The median adaptation index for the power in the lower frequency band was 5.19% (Figure 5b). Across monkeys, the median response to the adapter was not significantly different from the median response to the test stimulus in these "same" trials (Wilcoxon test, $p > .50$). However, both monkeys showed very different results: in monkey G, power at these low frequencies significantly increased with stimulus repetition (median AI = -15.47%; Wilcoxon test, $p < .001$), whereas the power significantly decreased with repetition in monkey M (median AI = 20.91%; Wilcoxon test, $p < .001$).

In contrast to the power at lower frequencies, the median energy at population level averaged across the gamma band frequencies (61 to 100Hz) decreased substantially with the repetition of a stimulus (Figure 5c): The median adaptation index was 22.83% and, as was the case for the spiking activity, this result pattern was present in both monkeys (median AI = 29.69% and 15.49% for monkey G and M, respectively). The median response to the adapter was significantly larger than the median response to the test stimulus in these "same" trials (Wilcoxon test across monkeys, $p < .001$ and in each of the two monkeys: $p < .001$). Note that the adaptation index for the spiking activity was computed on net responses, whereas the adaptation index for the power (lower frequencies and gamma) was computed on absolute responses (no baseline activity was subtracted). Using absolute responses to calculate

the adaptation index for the spiking activity resulted in a median adaptation index of 21.67% (median AI monkey G and M, respectively: 28.96% and 18.39%), which was very similar to the one obtained for the gamma power.

As no significant adaptation was found with stimulus repetition for the power at lower frequencies (15 to 30Hz) and as the results were inconsistent across monkeys for both the VEPs and the power at the lower frequencies, we focused on the effects of adaptation on the selectivity of the single units and of the power across the frequencies in the gamma band (61 to 100Hz) for the remainder of the paper. This is a reasonable thing to do, given the fact that the fMRI BOLD signal appears to be most closely tied to the LFP gamma band activity (Niessing et al. 2005; Mukamel et al. 2005; Viswanathan and Freeman 2007) and that stimulus selectivity in the visual cortex is mainly observed for the gamma band, in contrast to activity at lower frequencies (Gray and Singer 1989; Frien and Eckhorn 2000; Frien et al. 2000; Fries et al. 2002; Siegel and Konig 2003; Kayser and Konig 2004; Henrie and Shapley 2005; Liu and Newsome 2006).

Effect of response strength to the adapter on adaptation

According to a model linking fMR-A to neuronal tuning (Piazza et al. 2004), the reduction in a neurons firing rate is proportional to the strength of its initial response to a stimulus: the more a neuron fires, the greater the reduction of the subsequent response. To examine this, we quantified the relationship between the response strength to the adapter and the corresponding degree of adaptation in that same condition on a population level by performing a linear regression analysis. The analyses were restricted to the "same" trials. The response to a particular adapter was defined as the average response across all 6 conditions in which this stimulus served as an adapter. For the analyses of the spiking activity, we used absolute responses

instead of net responses and only "same" conditions in which the (shape-selective) cell was responsive to the adapter (as tested with a Wilcoxon test, $p < .05$) were included. For the analyses of the gamma power, we included only those "same" conditions in which the adapter response was larger compared to the baseline activity, thus exceeding a ratio adapter response/baseline response of 1. A single neuron/site could contribute potentially 6 data points to the regression analysis, because in 6 conditions, the adapter and test stimulus were identical.

For both the spiking activity and the gamma power (Figure 6A and 6B, respectively), the linear regression analysis revealed a weak but significant positive correlation ($r = .18$ and $r = .13$; $p < .001$ and $p < .01$, respectively) between the response strength to the adapter and the adaptation level (with regression equations $y = .18x + 20.73$ and $y = 6.03x + 9.44$ for spiking activity and gamma power, respectively). Very similar results were found when extreme values were rejected from these analyses, by excluding the percentiles 1 and 99 for both dependent and independent variable (with respective regression equations for spiking activity and gamma power: $y = .14x + 22.51$ [$r = .14$; $p < .01$] and $y = 6.05x + 10.36$ [$r = .14$; $p < .01$]), indicating that the results were not caused by a few outliers. These findings suggest that, at a population level, adaptation was indeed response strength dependent but only weakly: the adaptation level increased slightly with increasing response strength to the adapter. This is in line with the Piazza et al. (2004) model linking fMR-A to neuronal tuning and fits a view of adaptation as a passive process of neuronal fatigue which is based on a firing-rate adaptation mechanism. This mechanism is similar to a gain mechanism in which the reduction of the neuronal response is proportional to its initial response.

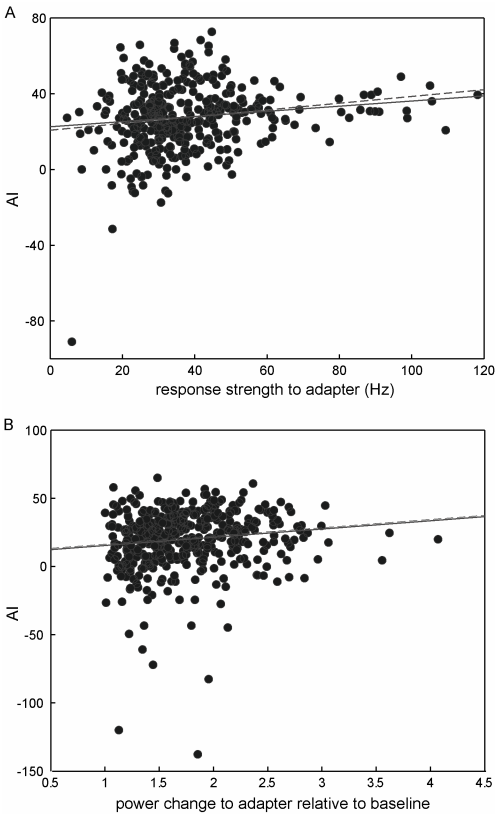

Figure 6. Effect of response strength to adapter on adaptation level. For every cell/site, the percent adaptation in a "same" condition is plotted against the response strength to the adapter in that condition. A single neuron/site could contribute 6 data points to the plot. For the spiking activity (panel A), only "same" conditions in which the cells were responsive to the adapter are included. For the gamma power (panel B), only "same" conditions in which the adapter response was larger compared to the baseline activity are included. The regression lines computed on the whole data are depicted by the solid lines (with respective regression equations for spiking activity and gamma power: $y = .18x + 20.73$ and $y = 6.03x + 9.44$). The regression lines computed on the 1 to 99% range of the data are depicted by the dotted lines (with respective regression equations for spiking activity and gamma power: $y = .14x + 22.51$ and $y = 6.05x + 10.36$).

Effect of repetition on neuronal selectivity

One key prediction in which the fatigue model and the sharpening model of adaptation clearly differ is related to changes in stimulus selectivity with stimulus repetition: whereas the fatigue model predicts no change in selectivity with adaptation, the sharpening model predicts that adaptation causes a sharpening of the tuning curves, thus an increased selectivity after adaptation, as it assumes a proportionally greater adaptation for stimuli that elicit a weak neuronal response than for more effective stimuli.

To possibly distinguish these two adaptation models, we examined the effect of stimulus repetition on the selectivity of the spiking activity and of the power in the gamma band by comparing the tuning curves for the adapter and for the test stimuli in the "same" trials. The response to a particular adapter was defined as the average response across all non-same conditions, i.e. all conditions, except for the "same" condition, in which that particular shape served as an adapter. For the test stimuli, tuning curves were based on the average responses in the "same" conditions. Because the tuning curves for the adapters and for the test stimuli were based on different conditions, a possible similarity between these tuning curves could not be induced by common artifacts – which is important for LFPs.

We subdivided the cells/sites in three groups based on the responses to the different adapters (see Methods). Inspection of Figure 7A showed a very clear correspondence for the spiking activity between the tuning curves for the adapters and the tuning curves for the test stimuli: For all three groups of cells, the most effective shape was the same whether it was presented as an adapter or as a test stimulus. Additionally, the modulation for the test stimuli was significant, as tested with a general linear model (GLM) repeated-measures ANOVA with stimulus rank as a within-neuron factor ($F(5,155)=14.22$, $p < .001$; $F(5,80)=13.91$, $p < .001$; $F(5,105)=7.02$, $p < .001$, for group 1 to 3 respectively). Additional post-hoc analyses on the responses to these test stimuli (Fisher LSD) showed a significant preference for the most effective shape when presented as an adapter compared to the stimulus which differed the most from the former shape (i.e. stimulus with rank 6), as was (of course) also the case for the adapter stimuli ($p < .001$ for adapters and test stimuli in all three panels).

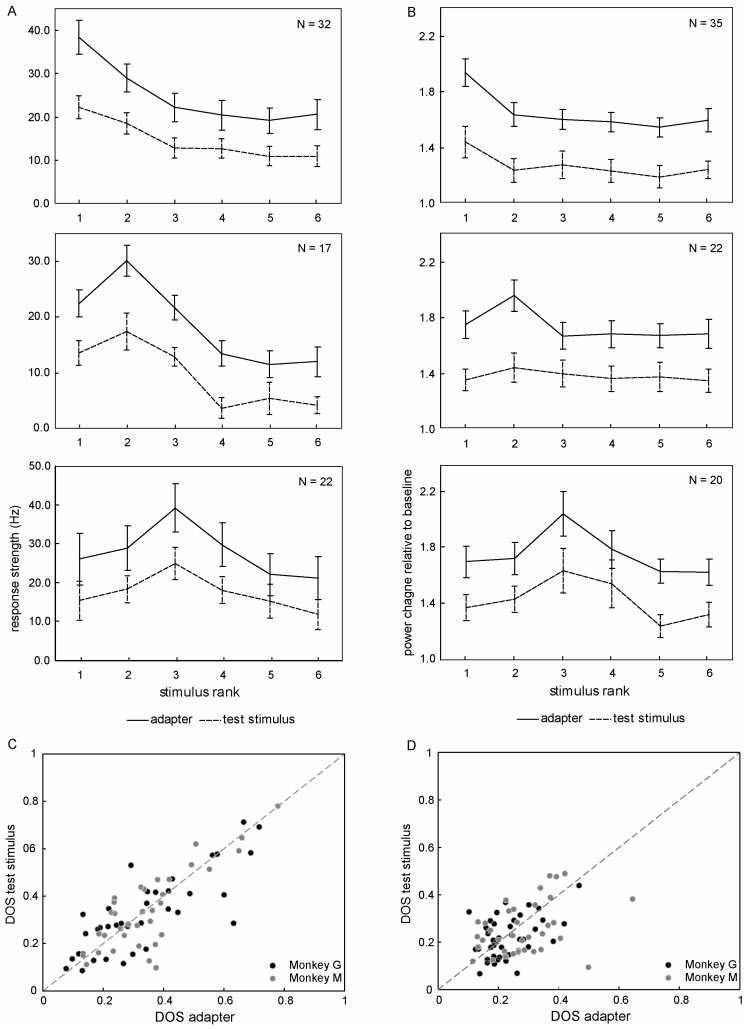

Figure 7. Effect of repetition on neuronal selectivity. The left column (A and C) shows the results for the spiking activity. The right column (B and D) shows the results for the gamma power. Panels A and B show the tuning curves for the adapter (solid line) and the test stimuli (dotted line) averaged across the "same" trials (with SEs), subdivided in three rows. In the top row, the results of cells/sites showing monotonic tuning are presented. Shapes were ranked in ascending (A to F, as labeled in Fig. 1) or descending order (F to A), depending on which shape was the most effective stimulus (A or F, respectively) when presented as an adapter. In the second and third row, the results of cells/sites showing a maximum adapter response for shapes B or E or for shapes C or D, respectively, are presented. Shapes were ranked in ascending order (A to F) when the most effective adapter was shape B or C. When shape E or D where the most effective adapters, shapes were ranked in a descending order (F to A). In panels C and D, the DOS indices for the test stimuli are plotted against the DOS indices for the adapters, both for the data obtained in Monkey G (black dots) and in Monkey M (grey dots). Each dot represents the values of one single neuron/site.

The correspondence between the tuning curves for the adapters and the tuning curves for the test stimuli was also clear for the gamma band, especially in the groups 1 and 3 of Figure 7B. For these panels, the most effective shape was the same whether it was presented as an adapter or as a test stimulus and the modulation for the test stimuli was significant, as tested with a general linear model (GLM) repeated-measures ANOVA with stimulus rank as a within-site factor ($F(5,170)=3;23$, $p < .01$; $F(5,95)=3.14$, $p < .05$, for group 1 and 3 respectively). Additional post-hoc analyses on the responses to these test stimuli (Fisher LSD) showed a significant preference for the most effective shape when presented as an adapter compared to the stimulus which differed the most from the former shape (i.e. stimulus with rank 6) in both groups 1 and 3, as was the case for the adapter stimuli ($p < .001$ for adapters; $p < .01$ for test stimuli). This correspondence for the gamma band between the tuning curves for the adapters and the tuning curves for the test stimuli was less evident in the second group of neurons. Although the most effective shape was the same whether it was presented as an adapter or as a test stimulus, the modulation for the ranked test stimuli was not significant ($F < 1$). Additional post-hoc analyses on the responses to the test stimuli (Fisher LSD) did also not reveal a significant preference for the most effective shape when presented as an adapter compared to the stimulus which differed the most from the former shape (i.e. stimulus with rank 6), although this was (of course) the case for the adapters ($p < .001$ for adapters; $p = .23$ for test stimuli). Thus, although the results for the LFPs are somewhat less straightforward compared to the spiking activity results, we can conclude that, in general, the single cell and LFP results show a similar tuning for the test stimulus and for the adapter.

To directly compare the degree of selectivity for the adapters and for the test stimuli, we computed per cell/site the Depth of Selectivity (DOS, see Methods) for both the adapters and the test stimuli. The DOS index for the

test stimuli was calculated on the responses in all "same" trials. The DOS index for the adapters was computed for a non-same condition which was randomly selected per stimulus (see Methods). We found a significant positive correlation between the depth of selectivity for the adapter and test stimuli, both for the spiking activity ($r = .80$, $p < .001$; Figure 7C) and for the gamma power ($r = .43$, $p < .001$; Figure 7D). The average differences between the DOS for the adapters and the test stimuli were very small and not significant, both for the single unit activity (median difference = -.007, $p = .94$, as tested with a Wilcoxon test) and for the gamma band activity (median difference = .014, $p = .24$, as tested with a Wilcoxon test). These results indicate that the degree of selectivity and, more generally, the tuning for the first and second stimulus was similar when these two stimuli had the same shape. This suggests that the key assumptions of the sharpening model do not hold for the present paradigm in IT cortex. However, these results are in line with the predictions of the fatigue model: the tuning width did not change with stimulus repetition.

Effect of adapter value on response reduction to the test stimulus

The results for the "same" trials presented above, that adaptation was dependent on the strength of the response to the adapter and that stimulus repetition did not change the tuning width but scaled down the responses, fit the view that adaptation is merely a passive process of neural fatigue caused by some kind of gain mechanism. In this view, the test stimulus is considered to be a neutral probe, so most adaptation is expected to be observed in sequences where the test stimuli followed the most effective adapter, compared to less effective adapters, irrespective of the relationship between the adapter and test stimulus value. This prediction was examined in the next analysis. For this analysis, we defined the response to a particular adapter as the average response across all conditions (including the "same"-condition) in

which that particular shape served as an adapter. These analyses were restricted to those cells and sites which demonstrated an adaptation level of at least 10%. Only shape selective cells were included.

Per cell/site, the responses to only two stimuli were used: the most effective shape when presented as an adapter (further denoted as stimulus 1) and the shape which parametrically differed from that shape the most (i.e. shape F when the most effective shape was stimulus A, B or C; shape A when the most effective shape was stimulus D, E or F). This latter shape (further denoted as stimulus 2) was not necessarily the least effective shape when presented as an adapter. A prerequisite for each cell to be included was to respond significantly to both stimulus 1 and 2 when presented as an adapter (as tested with a Wilcoxon test). We compared the responses to these two shapes presented as test stimuli under two conditions (following stimulus 1 or following stimulus 2) using a general linear model (GLM) repeated-measures ANOVA with stimulus (effective vs less effective stimulus; i.e. stimulus 1 vs stimulus 2) and presentation number (adapter vs test stimulus) as within-neuron factors. If adaptation was only dependent on the strength of the response to the adapter, we would not expect the interaction between stimulus and presentation number to be significant and most adaptation should be found for test stimulus 1 and 2 following the most effective adapter, stimulus 1. However, for both the spiking activity and the gamma power, the interaction between stimulus and presentation number was significant ($F(1,62)=30.71$, $p < .001$ and $F(1,63)=14.94$, $p < .001$, respectively). Zooming in on this interaction for the spiking activity (Figure 8A) showed indeed significantly more adaptation when test stimulus 1 was repeated compared to when this test stimulus followed the less effective adapter, stimulus 2 ($p < .001$ as tested with a Fisher LSD test), as was expected from a response strength driven mechanism. For test stimulus 2, however, the opposite was true: most adaptation was not found when this test stimulus

followed the most effective adapter, stimulus 1. Instead, significantly more adaptation was found when this test stimulus followed the identical, but less effective adapter, stimulus 2 ($p < .05$ as tested with a Fisher LSD test). For the gamma power (Figure 8B), also significantly more adaptation was found when the less effective shape, stimulus 2, was repeated compared to when this shape followed the most effective adapter, stimulus 1 ($p < .001$ as tested with a Fisher LSD test). Inspection of Figure 8B shows that also most adaptation was found when the most effective stimulus was repeated compared to when this stimulus 1 followed the less effective adapter, stimulus 2. However, this difference in adaptation failed to reach significance ($p = .48$ as tested with a Fisher LSD test).

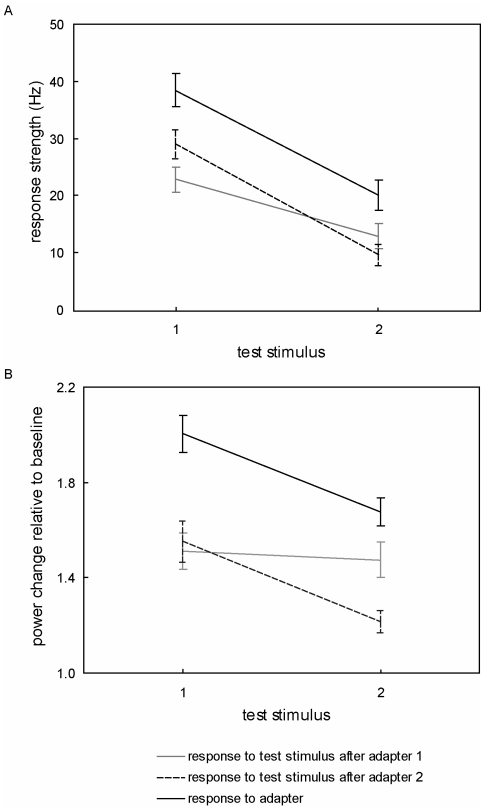

Figure 8. Effect of adapter value on response reduction to the test stimulus. The response strength to two shapes presented as test stimuli when following one or the other shape presented as an adapter is plotted. Shape 1 was defined as the most effective shape when presented as an adapter, whereas shape 2 was defined as the shape which (parametrically) differed from shape 1 the most. Only cells (N = 63, panel A) and sites (N = 64, panel B) showing an adaptation level of at least 10% were included. The solid black line depicts the responses to shapes 1 and 2 when presented as an adapter. The responses to the test stimuli following shape 1 or shape 2 presented as an adapter are depicted by the grey and black dotted line, respectively (with SEs).

These results suggest that the degree of adaptation was not only response strength dependent, but was also depending on the relationship between adapter and test stimulus: the adaptation was larger for identical than for different subsequent stimuli. The finding that more adaptation occurred when a suboptimal stimulus was repeated compared to when this stimulus followed the preferred stimulus contradicts the assumptions of a fatigue model based on a firing-rate adaptation mechanism which only assumes a change in gain, thus a maximal adaptation when a stimulus followed the most effective adapter.

Effect of shape similarity between adapter and test stimulus on adaptation level

If the degree of adaptation indeed depends on the relation between the values of the adapter and the test stimulus and most adaptation is observed when the same stimulus is repeated, one could expect that adaptation is reduced with decreasing shape similarity between adapter and test stimulus (Jiang et al. 2006). To examine the effect of adaptation on the tuning of IT neurons as a function of the similarity between the adapter and the test shape, we computed for each of the 36 conditions the difference between the response to the test stimulus in that condition and the response to this particular stimulus when presented as an adapter. The latter response to a stimulus was obtained by averaging across all 6 conditions in which that particular stimulus served as an adapter. Next, we averaged across all conditions with a same parametric distance between the adapter and the test stimulus, resulting in six values per cell/site (i.e. a value for parametric distance 0 to 5). These analyses were restricted to those cells and sites which demonstrated an adaptation level of at least 10%. Only shape selective cells were included.

We examined the effect of similarity by performing a general linear model (GLM) repeated-measures ANOVA on the differences in response strength to the adapter and to the test stimulus with parametric distance (distance 0 to 5) between the test stimulus and the preceding adapter stimulus as a within-neuron factor. For both the spiking activity and the gamma power, there was a significant effect of parametric distance on the response strength difference for the adapter and test stimulus ($F(5,310)=15.69$, $p < .001$; $F(5,315) = 13.00$, $p < .001$, respectively): the more dissimilar the adapter and test shape became, the less response strength difference was found, thus the less adaptation was observed (Figure 9A and 9B).

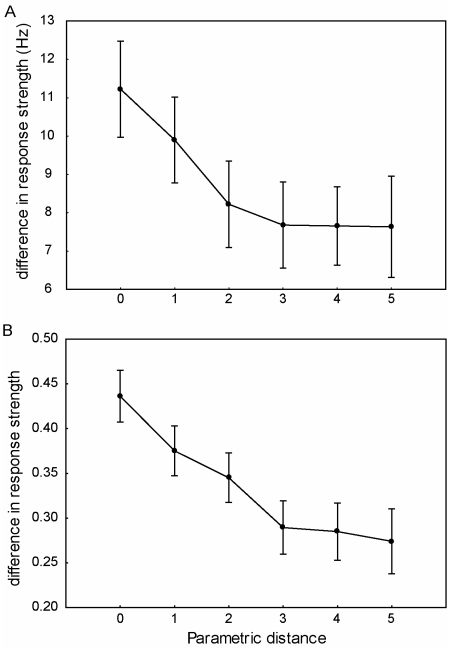

Figure 9. Effect of adapter-test stimulus similarity on adaptation level. Panels A and B show the mean difference in response strength to the adapter and the test stimulus (larger differences indicate more adaptation) as a function of the parametric distance between the adapter and the test stimulus for the spiking activity and the gamma power, respectively (with SEs). Only cells (N = 63) and sites (N = 64) showing an adaptation level of at least 10% were included.

Spike contamination in gamma power

The results described above showed very similar findings across spiking activity and gamma power. A possible trivial explanation for these highly similar results for spikes and gamma power is that spiking residuals were dominantly present in the gamma power, despite the low-pass filtering of the LFP signal. To examine this possibility, we compared the degree of adaptation and the DOS index for the spiking activity and for the LFP gamma power recorded at the same time with the same electrode. The correlation between the adaptation indices for the spiking activity and the gamma power was low and marginally significant ($r = .21$, $p > .06$). When these adaptation indices for the spiking activity were computed on the absolute response strength (thus without subtraction of the baseline), the correlation was higher and reached significance ($r = .28$, $p < .05$). Also the DOS-indices for the spiking activity and the gamma power, computed on the "same" trials, correlated significantly ($r = .32$, $p < .01$).

We also compared the stimulus preferences for the spiking activity and the gamma power. To this end, for each cell showing significant shape selectivity, we ranked the 6 stimuli according to their response strength for the spiking activity. The same ranking was then used to order the stimuli for the corresponding gamma power obtained from the same electrode. A general linear model (GLM) repeated measures ANOVA with rank as a within-site factor showed that the mean responses for the gamma power decreased with stimulus rank ($F(5,340)=17.04$, $p < .001$), indicating that the overall ranking was preserved for the gamma power. A similar overall preservation of shape rank was obtained for the spiking activity if the shapes were ranked based on the gamma power responses using a GLM repeated measures ANOVA with rank as a within-neuron factor ($F(5,340)=15.80$, $p < .001$).

Additionally, we computed the noise correlations between the spiking activity and the gamma power obtained simultaneously with the same electrode in the following way. First, we computed per cell/site the average and the standard deviation of the response strength for each stimulus across conditions in which this stimulus served as an adapter. Then, for each trial, a z-score was computed by standardizing the response strength to the stimulus in that trial (by subtracting the average response strength for that stimulus and dividing it by the respective standard deviation). The correlation between the z-values of all trials of all cells and the corresponding z-values obtained for the gamma power was 0.00 (p = .98) across monkeys (monkey G: r = 0.00, p = .92; monkey M: r = 0.00, p = .87). This suggests that there is no direct relation between the gamma power and the activity of the single unit obtained simultaneously with the same electrode.

PERIPHERAL ADAPTATION TEST

The adaptation effects observed in IT cortex, as presented above, did not necessarily originate in this area. Possibly, adaptation was generated in earlier visual areas and simply passed on to IT. Tracing the origin of the adaptation effects is important for the interpretation of fMR-A results, as in these studies, the observation of stimulus-selective adaptation effects in a particular area is seen as evidence for stimulus selective processing in that area.

To determine whether the adaptation effects observed in IT originate in earlier visual areas with small receptive field sizes, we presented the adapter and test stimuli at different, non-overlapping locations within the receptive field of an IT neuron. Under these circumstances, no adaptation is expected to be found if adaptation was indeed inherited from earlier cortical areas because the adapter and test stimulus do no longer fall inside the same receptive field at these earlier levels.

Database

For the peripheral adaptation test, we recorded single unit activity and local field potentials from 40 sites (20 in each monkey). For each cell/site, there was an average of 9.61 presentations per condition (minimum = 4, maximum = 13). All cells were responsive to at least one stimulus presented at one of the two positions.

Degree of adaptation for peripheral stimulus presentations

The median neuronal response at population level (N = 40 cells) dropped substantially when the same stimulus was repeated at the same position: The median adaptation index for the spiking activity was 37.20% and was very similar across monkeys (monkey G: 35.69%; monkey M: 38.08%) and to the one obtained in the central adaptation test (see above). The median response to the adapter was significantly larger than the median response to the test stimulus in these "same" trials (Wilcoxon test across monkeys, $p < .001$).

The median power at population level (N = 40 sites) averaged across the gamma band frequencies (61 to 100Hz) decreased substantially with the repetition of a stimulus at the same position: The median adaptation index was 20.26% and, as was the case for the spiking activity, this result pattern appeared for both monkeys (median AD: 12.42% and 25.84% for monkey G and M, respectively) and again was similar to the median value obtained in the central adaptation test. The median response to the adapter was significantly larger than the median response to the test stimulus in these "same" trials (Wilcoxon test across monkeys, $p < .001$). Thus adaptation occurred when stimuli are presented peripherally for both spiking activity and gamma power.

Effect of adapter and test stimulus position on response reduction to the test stimulus

To examine the effect of adapter and test stimulus position on adaptation, we restricted our analyses to those conditions in which the most effective stimulus served both as the adapter and test stimulus. The best position was defined as the position at which the most effective shape elicited the best response when presented as the adapter. The other position was labeled worst position. Note that all cells were also responsive to the most effective shape when presented at this worst position.

We computed the degree of adaptation to the most effective shape, averaged across best and worst positions, in conditions where the adapter and test stimulus were presented at different positions. In these conditions, no adaptation was expected to be found if the adaptation observed in IT was merely a reflection of the adaptation originating in other areas with smaller receptive fields. However, the median adaptation index was 21.24% for the spiking activity (monkey G: 20.20%; monkey M: 23.27%) and 18.17% for the gamma power (monkey G: 11.48%; monkey M: 21.73%). This response reduction with stimulus repetition was significant (Wilcoxon test across monkeys, $p < .001$ for both spiking activity and gamma power), but smaller (about 42.9% for the spiking activity and about 10.3% for the gamma power) compared to the conditions in which adapter and test stimulus were presented at the same position (see Degree of adaptation). The robustness of the response reduction with stimulus repetition across position variations between adapter and test stimulus suggests that this adaptation was, at least partially, generated in a high level visual area in the visual processing stream rather than merely being inherited from earlier stages with smaller receptive fields.

As adaptation was also present when adapter and test stimulus were shown at different positions, we could compare the responses to the most effective shape at the two positions presented as test stimuli as a function of the position of the adapter (best or worst position). To this end, we used a general linear model (GLM) repeated-measures ANOVA with position of adapter (best or worst position) and position of test stimulus (best or worst position) as within-neuron factors. For this analysis, only those cells and sites which demonstrated an adaptation level (computed on the "same" trials only) of at least 10% were included. If adaptation was not dependent on the relation between the positions of the adapter and the test stimulus, but did depend on the strength of the response to the adapter, most adaptation was expected to be found when the test stimulus followed the adapter presented at the best position, irrespective of the position of the test stimulus. This is the same logic as employed above when considering the effect of the relationship between adapter and test shape on the adaptation. For both the spiking activity and the gamma power, the interaction between adapter position and test stimulus position was significant ($F(1,31)=27.61$, $p < .001$ and $F(1,31)=7.21$, $p < .05$, respectively). Zooming in on this interaction for the spiking activity (Figure 10A) showed indeed significantly more adaptation when the test stimulus was repeated on the best position compared to when this test stimulus on the best position followed the adapter on the worst position ($p < .001$ as tested with a Fisher LSD test), as was expected. For the test stimulus presented at the worst position, however, the opposite was true: most adaptation was not found when this test stimulus followed the adapter on the best position. In fact, significantly more adaptation was found when this test stimulus followed the adapter on the worst position ($p < .01$ as tested with a Fisher LSD test).

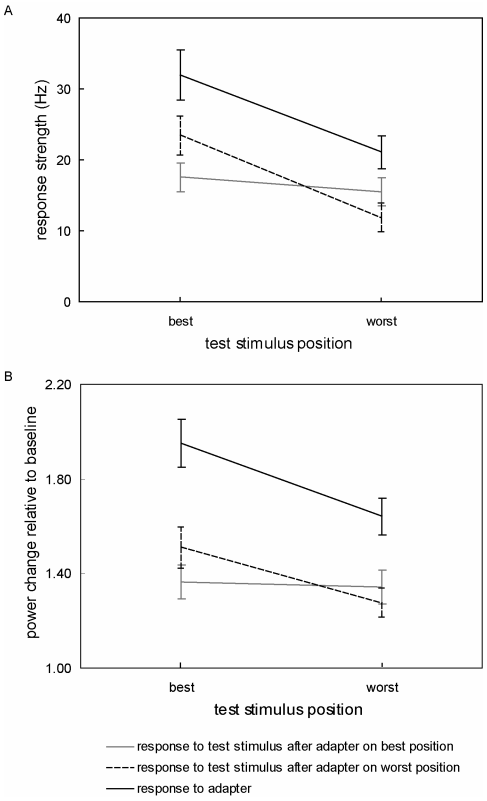

Figure 10. Effect of adapter and test stimulus position on response reduction to the test stimulus. The response strength to the most effective shape presented at two different positions when following this shape presented as an adapter at the same or at a different position is plotted. The best position was defined as the position on which this shape elicited the best response when presented as the adapter. The other position was labeled worst position. Only cells (N = 32, panel A) and sites (N = 32, panel B) showing an adaptation level of at least 10% were included. The solid black line depicts the responses to the most effective shape when presented as an adapter at the two different positions. The responses to the test stimulus following this shape presented at the best or at the worst position are depicted by the grey and black dotted line, respectively (with SEs).

For the gamma power (Figure 10B), also significantly more adaptation was found when the test stimulus on the best position followed the adapter on the best position compared to when this test stimulus followed the adapter on the worst position ($p < .05$ as tested with a Fisher LSD test). Inspection of Figure 10B shows that also most adaptation was found when the test stimulus on the worst position followed the adapter on this same, worst position, compared to when this test stimulus followed the adapter on the best position. However, this difference in adaptation level failed to reach significance ($p = .24$ as tested with a Fisher LSD test).

These results suggest that adaptation depended on the relation between the positions of the adapter and test stimulus. This is very similar to the way adaptation depended on the relation between the shape features of the first and second stimulus in the central adaptation test, as presented above.

For some specific combinations of selected stimuli, there could be a retinal overlap between the adapter presented at one position and the test stimulus presented at the other position, as in these cases, both the extreme lower part of the shape presented above the fixation point and the extreme upper part of the shape presented below the fixation point overlapped with the fixation window. To examine if the observed adaptation was merely a result of this potential overlap, we excluded all trials in which the monkeys' eye movements entered this overlapping part of the fixation window and the stimuli presented in that trial. The analyses performed on the remaining trials showed very similar results as those reported above, suggesting that the observed adaptation was not merely caused by this possible retinal overlap between the adapter and test stimulus.

TIMING OF ADAPTATION EFFECTS

To examine the temporal window in which adaptation occurred in the central adaptation test, we compared the response course for the adapter stimuli and the test stimuli averaged across the "same" trials, for both the spiking activity and the power in the gamma band. For the peripheral adaptation test, we compared the responses to the adapter stimuli and the responses to the test stimuli, both for the conditions in which adapter and test stimuli were presented at the same position and for conditions in which the position of these two stimuli differed. For the spiking activity as well as for the power in the gamma band, we averaged the responses across the best and worst position for these analyses.

For each cell, we divided the spiking responses in bins of 10ms, starting 5ms before stimulus onset (thus ranging from -5 to 5ms relative to stimulus onset) up to 480ms after stimulus onset (thus ranging from 475 to 485ms relative to stimulus onset). For the central adaptation test, we then compared the population response to the adapter to the population response to the test stimulus per 10 ms bin, using a Wilcoxon matched pairs test ($p < .05$). For the peripheral adaptation test, we compared the population responses to the adapter with the responses to the test stimulus presented at the same or at the other position per bin, again using a Wilcoxon matched pairs test ($p < .05$). Only when three out of four successive bins reached this significance level, these bins were assumed to reflect significant differences.

For the gamma power, we compared the adapter and test stimulus responses per millisecond, starting at stimulus onset and lasting 480ms, also using a Wilcoxon matched pairs test ($p < .05$). Only when this significance level was reached for 20 out of 25 successive milliseconds, the response differences in these millisecond bins were assumed to reflect significant differences.

For the spiking activity in the central adaptation test, the response strength to the test stimulus started to differ significantly from the response strength to the adapter at 70ms after stimulus onset (i.e. the bin ranging from 65 to 75ms)(Figure 11A). This difference remained significant up till 340ms (i.e. the 335-345ms bin). For the gamma power, the test stimulus showed a significant reduced response compared to the adapter stimulus from 67ms to 388ms relative to stimulus onset (Figure 11B). Thus, the onset of adaptation was fast and similar for spiking and gamma activity.

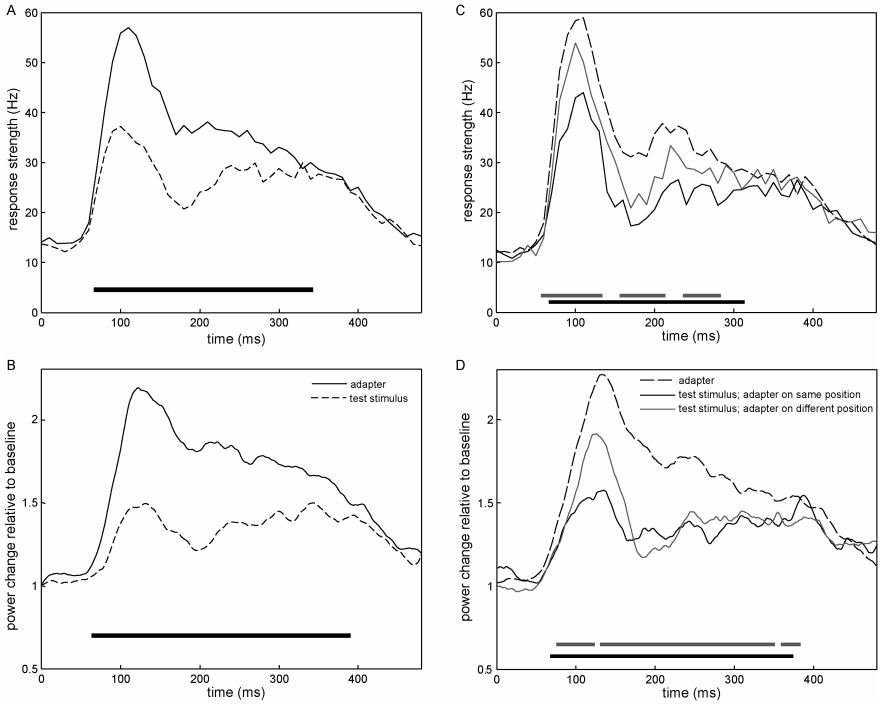

Figure 11. Timing of adaptation at a population level for the spiking activity (A and C) and the gamma power (B and D). A and B: Central adaptation test. Adapter and test stimulus responses, averaged across all "same" trials, are depicted by the solid and dotted line, respectively. C and D: Peripheral adaptation test. Adapter responses, averaged across the best and worst position, are depicted by the black dotted line. The mean response strength to the test stimulus, averaged across best and worst position, is depicted by the black solid line for conditions where adapter and test stimulus were presented at the same position and by the grey solid line when both stimuli were presented at a different position. In all panels, response strength is plotted relative to the onset of the first and second stimulus (against the center of the 10ms bins or per ms, for the spiking activity and gamma power, respectively). The black dots on the bottom in panel A and B indicate the bins/ms for which the response strength to the adapter and to the test stimulus differed significantly ($p < .05$). The dots on the bottom in panel C and D indicate the bins/ms for which the response strength to the adapter and the response strength to the test stimulus presented at the same (in black) or at the other position (in grey) as the adapter differed significantly ($p < .05$).

For the spiking activity in the peripheral adaptation test, the response strength to the test stimulus started to differ significantly from the response strength to the adapter at 70ms relative to stimulus onset (i.e. the bin ranging from 65 to 75ms) when adapter and test stimulus were presented at the same position (Figure 11C). When these stimuli were presented at a different position, their response strengths started to differ significantly at 60ms relative to stimulus

onset. This difference remained significant up till 310ms in the "same position" condition (i.e. the 305-315ms bin) and up till 280ms (i.e. the 275-285ms bin) in the "different position" condition, although for some bins, the difference did not reach significance, probably due to a lack of statistical power. For the gamma power, the test stimulus showed a significant reduced response compared to the adapter stimulus from 69ms to 373ms relative to stimulus onset when adapter and test stimulus were presented at the same position (Figure 11D). When the position was different for the adapter and test stimulus, their response strengths started to differ from 77ms relative to stimulus onset up till 350ms (with some rare exceptions where the difference did not reach significant) to continue to be significant from 362 to 382ms.

These results for both the central and peripheral adaptation test suggest that, although adaptation seems to last longer for the gamma power compared to the single unit activity, the repetition suppression starts at about the same time relative to stimulus onset for the single units and the gamma power. This can be appreciated by comparing Figure 11A and 11B for the central adaptation test and Figure 11C and 11D for the peripheral adaptation test. Additionally, despite some small differences, the timing of the adaptation in the condition in which the adapter and test stimulus were presented at the same position was very similar compared to that in the condition in which these stimuli were presented at a different position in the peripheral adaptation test. This was observed both for the spiking activity and the gamma power results. This can be appreciated by comparing Figure 11C and 11D.

Important to note is that one should be careful in comparing the adaptation latencies for the spiking activity and gamma power. Not only were the analyses performed with a different bin width (i.e. 10ms bins for the spiking activity vs 1ms for the gamma power), also the time-frequency wavelet decomposition for the spectral analysis of the LFPs resulted in a smoothing of

the signal (temporal resolution of 36.5ms for 61Hz to 22.3ms for 100Hz), by which the temporal resolution was reduced.

DISCUSSION

The present study was set up to examine the effects of adaptation on the neuronal stimulus selectivity in IT cortex. We observed, both for the spiking activity and the LFP gamma power, that stimulus repetition did not change the tuning width, but scaled down the neuronal responses. The degree of adaptation, however, was not only response strength dependent, but depended also on the relationship between adapter and test stimulus: the adaptation was larger for identical than for different subsequent stimuli. Consequently, we found that the degree of adaptation decreased with increasing dissimilarity between the adapter and test stimulus. The effect of relationship between adapter and test stimulus held for both shape feature and position changes: a larger adaptation was found when adapter and test stimulus had identical shape features and were presented at a different position than when these stimuli differed in shape or position.

ROBUSTNESS OF DEGREE OF ADAPTATION

In the present study, we found an approximate response decrease for the spiking activity of 37% when stimuli were repeated foveally. This is strikingly similar to the 40% adaptation reported by Sawamura et al. (2006) for the same 300ms inter stimulus interval, although they used very different stimuli and another paradigm. Besides this seemingly large robustness of degree of adaptation across stimuli and paradigm, also very similar results (~37% adaptation) were found in the present study when stimuli were presented peripherally 4° above or below the fixation target.

A somewhat lower degree of adaptation (~ 23%) was found for the power in the gamma band when the stimuli were repeated foveally. However, the degree of adaptation for the spiking activity was computed on net responses, thus by subtracting the baseline activity from the response to the stimulus, whereas no such baseline subtraction was done for the LFP power. When the degree of adaptation for the spiking activity was computed on absolute responses (thus without baseline subtraction), a median adaptation index of about 22% was found which was very similar to the adaptation obtained for the gamma power. Additionally, a very similar degree of adaptation (~ 20%) was found for the gamma band when stimuli were repeatedly presented at a position above or below the fixation target. For these conditions, a somewhat higher, but quite similar degree of adaptation (~ 26%) was found for the spiking activity when this activity was computed on absolute responses (thus without baseline subtraction).

These results suggest not only a large robustness of the degree of adaptation for the gamma power across different positions when adapter and test stimulus are presented at the same position. These findings also suggest a large robustness across different measures of neuronal activity (i.e. single unit or LFP gamma power).

Robust adaptation, however, was not found for the power in the lower frequencies (15 to 30Hz). The results for both monkeys were very different: whereas the power significantly decreased with repetition (i.e. adaptation) in one monkey, the opposite pattern was observed in the other monkey: the power at these lower frequencies significantly increased with stimulus repetition. As yet, the cause of this discrepancy across monkeys remains unclear.

ADAPTATION FOR SINGLE UNITS VS GAMMA POWER

As described above, the degree of adaptation was very similar for the single units and the power in the gamma band when the indices were computed in the same way (i.e. without baseline subtraction). The similarity between the spiking activity and the gamma power was striking: all effects of adaptation that we observed for the spiking activity (e.g. dependence on adapter-test stimulus relation, preservation of tuning width, effect of similarity, …) were also found for the gamma power. Although, at present, it cannot be excluded that these similar results could be partly due to spike contamination in the gamma power, this similarity could be induced by the fact that gamma power and spikes might be generated within the same local network. This was recently proposed by Belitski et al. (2008), who showed a strong positive signal correlation between the LFPs in the 60 to 100Hz gamma band and the spikes in anesthetized monkeys. Based on their findings, Belitski et al. (2008) suggested that local stimulus-related input possibly affects both the spiking activity and the engagement of a recurrent loop between local cortical populations in the region around the tip of the electrode. This latter is reflected in the LFP power in the 60 – 100Hz gamma band.

If we zoom in on the differences between the spiking activity and the gamma power, a higher stimulus selectivity of adaptation for the spiking activity compared to the gamma power can be deduced from the effect of similarity on the adaptation level. Indeed, inspection of Figure 9 shows a gradual decrease in adaptation with larger differences between adapter and test stimulus for the gamma power. For the spiking activity, however, the decrease in adaptation is particularly evident for the first two steps (i.e. from same stimuli to stimuli with a parametric distance of 1 and 2), whereas the adaptation remains stable when the adapter and test stimulus differ by 3 or more parametric steps. This higher stimulus selectivity for spikes compared to

LFPs agrees with other findings that show that the LFP power reflects population activity from within a broad area around the electrode tip where different cells do not necessarily show the same preferences and selectivities (Mitzdorf 1987; Juergens et al. 1999; Kreiman et al. 2006; Goense and Logothetis 2008).

ORIGIN OF ADAPTATION EFFECTS

Although the observed adaptation effects in IT cortex could very well have been generated in this area itself, other possible origins need to be considered. A first alternative is that adaptation in IT cortex is merely a reflection from adaptation in early visual areas with small receptive fields (e.g. V1, V2), which was transferred to IT. If this were the case, no adaptation is expected to occur when the adapter and the test stimulus are presented at different positions, because both stimuli would fall within different receptive fields at these early areas (Hubel and Wiesel 1968). The results in our peripheral adaptation test, however, showed significant adaptation when the adapter and test stimulus were presented at different positions, which supports the thought of adaptation in IT cortex being highly invariant over the relative locations of the adapter and test stimulus, as reported by Lueschow et al. (1994). These findings clearly suggest that the observed adaptation did not originate in early visual areas with small receptive fields.

A second possibility is that the adaptation is caused by feedback from other visual areas high in the visual processing hierarchy. This seems unlikely in the present study, as adaptation was already present close to response onset (~ 70 ms). Although feedback could occur very fast, this early adaptation onset makes feedback a very unlikely origin of the observed adaptation in IT cortex (Xiang and Brown 1998). This is also supported by the results in the peripheral adaptation test, as the timing of the adaptation for stimuli presented

at the same or at different positions did not markedly differ and also started close to response onset.

A third possibility is that the adaptation in the anterior region of IT cortex where we recorded, is merely a reflection of adaptation originated in more posterior areas (e.g. posterior IT) with large enough receptive fields to show adaptation when adapter and test stimuli are presented at the different positions tested in the present study. Some indications for this can be found by comparing spiking activity and LFPs: one can assume that spiking activity will show adaptation before LFPs in the brain region where the adaptation occurs. Adaptation in LFPs will be seen prior to or simultaneously with adaptation in the spiking activity in a brain area which receives this processing information from other regions (Nielsen et al. 2006; Monosov et al. 2008). In the present study, no clear difference in adaptation latency was found for the spiking activity and the LFPs, suggesting that adaptation is present at the input of the recorded neurons. This input can be from units in the same region – explaining the similar timing of LFP and single unit adaptation responses and possibly also the high similarity between adaptation effects found for spiking activity and for gamma power – or from another more posterior region. However, as noted before, one should be very careful in comparing latencies from single units and LFP power because of their difference in temporal resolution.

NEED FOR AN ALTERNATIVE MODEL OF ADAPTATION

As this present study was set up to study the changes in stimulus selectivity following adaptation, the hypotheses of two adaptation models could be examined: the sharpening model and the fatigue model. Our findings clearly suggested that the sharpening model does not hold in the present paradigm in IT cortex, as one of the key assumptions of this model was falsified:

adaptation did not cause a sharpening of the tuning curves, but scaled down the neuronal responses. A similar lack of evidence for the validity of this sharpening model in IT cortex was recently reported by McMahon and Olson (2007) for a priming paradigm.

In contrast, some of the key assumptions of the fatigue model based on a firing-rate adaptation mechanism were corroborated: adaptation scaled down the neuronal responses without changing the tuning width and the adaptation level increased slightly with increasing response strength to the adapter. However, this model could not account for the interaction of test and adapter stimulus in determining the degree of adaptation: as the test stimulus is considered to be a neutral probe, this model can not account for the fact that adaptation depended on the relationship between the adapter and the test stimulus value. A trivial explanation for the effect of the relationship between adapter and test stimulus value is that it is caused by a sustained firing to the most effective adapter which might be larger compared to the sustained firing to the less effective adapter. This explanation however, does not hold since the response to the test stimulus at stimulus onset is very similar across conditions, which can be seen in Figure 9.

Because neither the sharpening model nor the fatigue model based on a firing-rate adaptation mechanism could account for all of our findings, an alternative model needed to be put forward. Based on their finding that the stimulus selectivity of the neuronal adaptation was greater compared to that of the neuronal response, Sawamura et al. (2006) suggested that adaptation is occurring *at* or *before* the level of the synapses onto the neuron. The case in which adaptation occurs *at* the synapse level corresponds to the synaptic depression mechanism put forward as an alternative to the firing-rate adaptation mechanism by Grill-Spector et al. (2006). Sawamura et al. (2006) suggested that, in this case, the degree of cross-adaptation for two different

stimuli would be a function of the number of synapses common to the processing of the two stimuli onto the tested neuron. The case in which adaptation occurs *before* the level of the synapses onto the neuron corresponds to what Kohn (2007) suggested as an alternative for the synaptic mechanism, as Kohn (2007) questioned the necessity of a synaptic mechanism to explain several adaptation effects, given the fact that neurons are embedded in recurrent networks. Sawamura et al. (2006) suggested that, in this case, the degree of cross-adaptation for two different stimuli would correlate with the number of neurons providing input to the tested neuron that can be adapted and respond to common features for these two stimuli. Both modes, synaptic adaptation and input adaptation, agree with the similar timing of the adaptation found for the LFPs and spiking activity.

An alternative model, based on either assumption put forward by Sawamura et al. (2006), i.e. that adaptation is occurring *at* or *before* the level of the synapses onto the neuron, will essentially be a fatigue model. As a consequence, this model will be able to account for the same effects as the fatigue model based on a firing-rate adaptation mechanism: tuning width does not change with repetition and slightly more adaptation will be found with increasing response strength to the adapter. However, this alternative model will also be able to account for the effect of the relationship between the adapter and the test stimulus value, in contrast with a firing-rate adaptation mechanism.

Although this alternative model could account for the observed adaptation effects in IT cortex in the current paradigm at this particular time scale, additional research is necessary for a possible validation of this model in other areas and at other time scales. The observation that the adapter and the test stimulus interact in recordings in V1 and MT (e.g. Dragoi et al. 2000;

Kohn and Movshon 2004; Krekelberg et al. 2005), suggests that this model might be legitimate in other areas.

EFFECT OF ATTENTION ON ADAPTATION

Because in the present study, as in the Sawamura et al. (2006) study, the monkeys were passively fixating during the recording sessions, no direct evidence is available that a difference in attention towards the test stimulus under different conditions ("same" vs "non-same") did not contribute to the adaptation effects observed in this present study. However, the analysis of the monkeys' eye movements could provide some indirect evidence. One could assume that more attention will be drawn to the test stimulus in sequences where this test stimulus differs from the adapter compared to when the adapter is repeated. However, the fixations of the monkeys were very similar across "same" and "non-same" trials, suggesting a similar degree of attention towards the test stimulus in these different conditions. Additional indirect evidence against the causal relationship between attentional differences and adaptation effects comes from fMR-A studies: Sawamura et al. (2005) found equal fMRI activation differences in monkey IT cortex and human LOC between "same" sequences and "non-same" sequences under passive fixation conditions and under attention-equated conditions. Similar findings under passive fixation conditions and in conditions in which the stimulus had to be attended were also reported in human LOC by Kourtzi and Kanwisher (2001).

Although this indirect evidence suggests that attentional differences did not cause or contribute to the adaptation effects reported in this study, directly controlling the level of attention towards both the adapter and test stimulus could add to our understanding of the observed adaptation effects. Not only could the level of attention paid to the first and second stimulus within a sequence be different, possibly in function of the degree of similarity between

the two stimuli, controlling the attentional level towards both stimuli by drawing attention towards both stimuli possibly changes the level of processing of these stimuli, which, in turn, could have an impact on the effects of adaptation.

IMPLICATIONS FOR FMR-A STUDIES

Because of the stimulus timing parameters used in the present study, the results are most relevant for rapid, event-related fMR-A paradigms in which two stimuli are successively presented with only a short lag in between (e.g. Kourtzi and Kanwisher 2000; Piazza et al. 2004). Using this paradigm, adaptation effects were found both for the spiking activity and the LFP power in the gamma band (61 – 100Hz) in IT cortex. As the LFP signal in the gamma band is assumed to reflect neural activity that originated locally (Gray and Singer 1989; Frien and Eckhorn 2000; Frien et al. 2000; Fries et al. 2002; Siegel and Konig 2003; Kayser and Konig 2004; Henrie and Shapley 2005; Liu and Newsome 2006), the assumption in fMR-A studies that stimulus-selective adaptation effects in a particular area indicate stimulus selective processing in that area seems reasonable. However, one cannot forcefully exclude that this adaptation is merely a reflection of adaptation generated in other areas which was transferred there. Our findings support another common assumption in fMR-A studies: when the similarity between the adapter and test stimulus was reduced, less adaptation was found.

However, the reported interactions between the adapter and the test stimulus suggest that adaptation occurs *at* or *before* the level of the synapses onto the neuron, instead of being caused by postsynaptic mechanisms. Both input and synaptic adaptation prevent a straightforward deduction of the neuronal selectivity based solely on fMR-A data. Further single-cell studies, preferably

in combination with LFPs and fMR-A, are needed to verify the interpretation of fMR-A results in different brain regions in humans and macaques.

REFERENCES

Afraz SR, Kiani R, Esteky H. Microstimulation of inferotemporal cortex influences face categorization. *Nature* 442: 692-695, 2006.

Baylis GC, Rolls ET. Responses of neurons in the inferior temporal cortex in short term and serial recognition memory tasks. *Exp Brain Res* 65: 614-622, 1987.

Belitski A, Gretton A, Magri C, Murayama Y, Montemurro MA Logothetis NK, Panzeri S. Low-frequency local field potentials and spikes in primary visual cortex convey independent visual information. *J Neurosci* 28: 5696-5709, 2008.

Brincat SL, Connor CE. Underlying principles of visual shape selectivity in posterior inferotemporal cortex. *Nat Neurosci* 7: 880-886, 2004.

Dean P. Effects of inferotemporal lesions on the behavior of monkeys. *Psychol Bull* 83: 41-71, 1976.

De Baene W, Premereur E, Vogels R. Properties of shape tuning of macaque inferior temporal neurons examined using Rapid Serial Visual Presentation. *J Neurophysiol* 97: 2900-2916, 2007.

De Baene W, Vogels R. Effects of adaptation on stimulus selectivity of macaque inferior temporal spiking activity and local field potentials. *Soc Neurosci Abstr* 554: 6, 2007.

Desimone R. Neural mechanisms for visual memory and their role in attention. *Proc Natl Acad Sci USA* 93: 13494-13499, 1996.

Dragoi V, Sharma J, Sur M. Adaptation-induced plasticity of orientation tuning in adult visual cortex. *Neuron* 28: 287-298, 2000.

Frien A, Eckhorn R, Bauer R, Woelbern T, Gabriel A. Fast oscillations display sharper orientation tuning than slower components of the same recordings in striate cortex of the awake monkey. *Eur J Neurosci* 12: 1453-1465, 2000.

Frien A, Eckhorn R. Functional coupling shows stronger stimulus dependency for fast oscillations than for low-frequency components in striate cortex of awake monkey. *Eur J Neurosci* 12: 1466-1478, 2000.

Fries P, Schroder JH, Roelfsema PR, Singer W, Engel AK. Oscillatory neuronal synchronization in primary visual cortex as a correlate of stimulus selection. *J Neurosci* 22: 3739-3754, 2002.

Goense JB, Logothetis NK. Neurophysiology of the BOLD fMRI Signal in Awake Monkeys. *Curr Biol* 18: 631-640, 2008.

Gray CM, Singer W. Stimulus-specific neuronal oscillations in orientation columns of cat visual cortex. *Proc Natl Acad Sci USA* 86: 1698-1702, 1989.

Grill-Spector K, Kushnir T, Edelman S, Avidan G, Itzchak Y, Malach R. Differential processing of objects under various viewing conditions in the human lateral occipital complex. *Neuron* 24: 187-203, 1999.

Grill-Spector K, Malach R. fMR-adaptation: a tool for studying the functional properties of human cortical neurons. *Acta Psychologica* 107: 293-321, 2001.

Grill-Spector K, Henson R, Martin A. Repetition and the brain: neural models of stimulus-specific effects. *Trends Cogn Sci* 10: 15-23, 2006.

Gross CG, Schiller PH, Wells C, Gerstein GL. Single-unit activity in temporal association cortex of the monkey. *J Neurophysiol* 30: 833–843, 1967.

Gross CG, Bender DB, Rocha-Miranda CE. Visual receptive fields of neurons in inferotemporal cortex of the monkey. *Science* 166: 1303-1306, 1969.

Henrie JA, Shapley R. LFP power spectra in V1 cortex: the graded effect of stimulus contrast. *J Neurophysiol* 94: 479-490, 2005.

Hubel DH, Wiesel TN. Receptive fields and functional architecture of monkey striate cortex. *J Physiol* 195: 215-243, 1968.

James TW, Humphrey GK, Gati JS, Menson RS, Goodale MA. Differential effects of viewpoint on object-driven activation in dorsal and ventral streams. *Neuron* 35: 793-801, 2002.

Jiang X, Rosen E, Zeffiro T, VanMeter J, Blanz V, Riesenhuber M. Evaluation of a shape-based model of human face discrimination using FMRI and behavioral techniques. *Neuron* 50: 159-172, 2006.

Juergens E, Guettler A, Eckhorn R. Visual stimulation elicits locked and induced gamma oscillations in monkey intracortical and EEG-potentials, but not in human EEG. *Exp Brain Res* 129: 247-259, 1999.

Kayaert G, Biederman I, Op de Beeck H, Vogels R. Tuning for shape dimensions in macaque inferior temporal cortex. *Eur J Neurosci* 22: 212-224, 2005.

Kayser C, Konig P. Stimulus locking and feature selectivity prevail in complementary frequency ranges of V1 local field potentials. *Eur J Neurosci* 19: 485-489, 2004.

Kohn A, Movshon JA. Adaptation changes the direction tuning of macaque MT neurons. *Nat Neurosci* 7: 764-772, 2004.

Kohn A. Visual adaptation: Physiology, mechanisms, and functional benefits. *J Neurophysiol* 97: 3155-3164, 2007.

Kourtzi Z, Kanwisher N. Cortical regions involved in perceiving object shape. *J Neurosci* 20: 3310-3318, 2000.

Kourtzi Z, Kanwisher N. Representation of perceived object shape by the human lateral occipital complex. *Science* 293: 1506-1509, 2001.

Kreiman G, Hung CP, Kraskov A, Quirogq RQ, Poggio T, DiCarlo JJ. Object selectivity of local field potentials and spikes in the macaque inferior temporal cortex. *Neuron* 49: 433-445, 2006.

Krekelberg B, Vatakis A, Kourtzi Z. Implied motion from form in the human visual cortex. *J Neurophysiol* 94: 4373-4386, 2005.

Liu J, Newsome WT. Local field potential in cortical area MT: stimulus tuning and behavioral correlations. *J Neurosci* 26: 7779-7790, 2006.

Logothetis NK, Sheinberg DL. Visual object recognition. *Annu Rev Neurosci* 19: 577-621, 1996.

Logothetis NK, Pauls J, Augath M, Trinath T, Oeltermann A. Neurophysiological investigation of the basis of the fMRI signal. *Nature* 412: 150-157, 2001.

Lueschow A, Miller EK, Desimone R. Inferior temporal mechanisms for invariant object recognition. *Cereb Cortex* 5: 523-531, 1994.

McMahon DBT, Olson CR. Repetition suppression in monkey inferotemporal cortex: relation to behavioural priming. *J Neurophysiol* 97: 3532-3543, 2007.

Miller EK, Gochin PM, Gross CG. Habituation-like decrease in the responses of neurons in inferior temporal cortex of the macaque. *Vis Neurosci* 7: 357-362, 1991a.

Miller EK, Li L, Desimone R. A neural mechanism for working and recognition memory in inferior temporal cortex. *Science* 254: 1377-1379, 1991b.

Mitzdorf U. Current source-density method and application in cat cerebral cortex: investigation of evoked potentials and EEG phenomena. *Physiol Rev* 65: 37-100, 1985.

Mitzdorf U. Properties of the evoked potential generators: current source-density analysis of visually evoked potentials in the cat visual cortex. *Int J Neurosci* 33: 33-59, 1987.

Monosov IE, Trageser JC, Thompson KG. Measurements of simultaneously recorded spiking activity and local field potentials suggest

that spatial selection emerges in the frontal eye field. *Neuron* 57: 614-625, 2008.

Mukamel R, Gelbard H, Arieli A, Hasson U, Fried I, Malach R. Coupling between neuronal firing, field potentials, and fMR1 in human auditory cortex. *Science* 309: 951-954, 2005.

Naccache L, Dehaene S. The priming method: imaging unconscious repetition priming reveals an abstract representation of number in the parietal lobes. *Cereb Cortex* 11: 966-974, 2001.

Nielsen KJ, Logothetis NK, Rainer G. Dissociation between local field potentials and spiking activity in macaque inferior temporal cortex reveals diagnosticity-based encoding of complex objects. *J Neurosci* 26: 9639-9645, 2006.

Niessing J, Ebisch B, Schmidt KE, Niessing M, Singer W, Galuske RAW. Hemodynamic signals correlate tightly with synchronized gamma oscillations. *Science* 309: 948-951, 2005.

Op de Beeck H, Wagemans J, Vogels R. Inferotemporal neurons represent low-dimensional configurations of parameterized shapes. *Nat Neurosci* 4: 1244-1252, 2001.

Piazza M, Izard V, Pinel P, Le Bihan D, Dehaene S. Tuning curves for approximate numerosity in the human intraparietal sulcus. *Neuron* 44: 547-555, 2004.

Rainer G, Miller EK. Effects of visual experience on the representation of objects in the prefrontal cortex. *Neuron* 27: 179-189, 2000.

Rauch A, Rainer G, Logothetis NK. The effect of a serotonin-induced dissociation between spiking and perisynaptic activity on BOLD functional MRI. *Proc Natl Acad Sci USA* 105: 6759-6764, 2008.

Riches IP, Wilson FAW, Brown MW. The effects of visual stimulation and memory on neurons of the hippocampal formation and neighboring parahippocampal gyrus and inferior temporal cortex of the primate. *J Neurosci* 11: 1763-1779, 1991.

Sawamura H, Georgieva S, Vogels R, Van Duffel W, Orban GA. Using functional magnetic resonance imaging to assess adaptation and size invariance of shape processing by humans and monkeys. *J Neurosci* 25: 4294-4306, 2005.

Sawamura H, Orban GA, Vogels R. Selectivity of neuronal adaptation does not match response selectivity: a single cell study of the fMRI adaptation paradigm. *Neuron* 49: 307-318, 2006.

Seltzer B, Pandya DN. Afferent cortical connections and architectonics of the superior temporal sulcus and surrounding cortex in the rhesus monkey. *Brain Res* 149: 1-24, 1978.

Siegel M, Konig P. A functional gamma-band defined by stimulusdependent synchronization in area 18 of awake behaving cats. *J Neurosci* 23: 4251-4260, 2003.

Sigala N, Logothetis NK. Visual categorization shapes feature selectivity in the primate temporal cortex. *Nature* 415: 318-320, 2002.

Sobotka SS, Ringo JL. Investigation of long term recognition and association memory in unit responses from inferotemporal cortex. *Exp Brain Res* 96: 28-38, 1993.

Tallon-Baudry C, Bertrand O, Delpuech C, Pernier J. Oscillatory gamma-band (30–70 Hz) activity induced by a visual search task in human. *J Neurosci* 17: 722–734, 1997.

Tanaka K. Inferotemporal cortex and object vision. *Annu Rev Neurosci* 19: 109-139, 1996.

Tootell RBH, Hadjikhani NK, Van Duffel W, Liu AK, Mendola JD, Sereno MJ, Dale AM. Functional analysis of primary visual cortex (V1) in humans. *Proc Natl Acad Sci USA* 95: 811-817, 1998.

Viswanathan A, Freeman RD. Neurometabolic coupling in cerebral cortex reflects synaptic more than spiking activity. *Nat Neurosci* 10: 1308-1312, 2007.

Vogels R, Sary G, Orban GA. How task-related are the responses of inferior temporal neurons. *Vis Neurosci* 12: 207-214, 1995.

Wiggs CL, Martin A. Properties and mechanisms of perceptual priming. *Curr Opin Neurobiol* 8: 227-233, 1998.

Xiang JZ, Brown MW. Differential neuronal encoding of novelty, familiarity and recency in regions of the anterior temporal lobe. *Neuropharmacol* 37: 657-676, 1998.

CHAPTER 5
GENERAL CONCLUSIONS AND PERSPECTIVES

The aim of the experimental research presented in this doctoral dissertation was threefold. First, it was investigated, using a Rapid Serial Visual Presentation paradigm, whether IT neurons adapt their tuning to the properties of the stimulus distribution. Secondly, we tried to gain further knowledge with respect to the effects of categorization learning on the stimulus selectivity of IT neurons. Thirdly, we examined the effects of adaptation on the neuronal tuning in IT cortex. In this final chapter, the main empirical findings of this dissertation are summarized. The chapter is concluded with some directions for future experimental investigations of experience-related effects.

RESEARCH OVERVIEW

In the first part of this dissertation (Chapter 2), we examined the effects of changes in the stimulus distribution statistics on the stimulus selectivity of IT neurons. To this end, we used the Rapid Serial Visual Presentation (RSVP) paradigm. This paradigm, however, has rarely been used in single-cell studies in higher visual cortex, particularly with parametric shape sets in which the stimulus differences are much smaller compared to previous RSVP studies in IT cortex (Keysers et al. 2001; Földiák et al. 2004; Kiani et al. 2005). As a consequence, its validity to study shape selectivity of IT neurons under these conditions needed to be ascertained. A comparison of the RSVP technique using 100-ms presentations with that using a longer duration showed that shape selectivity can be determined using RSVP. Our results obtained with the RSVP paradigm also supported and extended findings of previous studies

using a standard testing paradigm (e.g. Op de Beeck et al. 2001; Kayaert et al. 2005): we found that the large majority of neurons preferred extremes of the shape configuration and we could show that, at a population level, IT neurons were able to represent the shape similarities at an ordinal level without faithfully representing the physical shape similarities.

Once the validity of the RSVP technique to study shape selectivity of IT neurons within parametric shape sets was ascertained, we used this technique to study how IT neurons adapt their selectivity to changes in the stimulus distribution statistics. When a shape set with a narrower stimulus range (which was inextricably bound up with less variance, less (pixel-based) dissimilarity and higher density) was presented, the neural shape discrimination improved, suggesting that the tuning of IT neurons adapts to the stimulus distribution statistics.

Given the positive results of the RSVP paradigm validity to study shape selectivity of IT neurons (Chapter 2), we used this technique to collect neuronal stimulus selectivities which could serve as a baseline in a study on the effects of categorization learning on the neural representation of complex shapes in IT cortex (Chapter 3). By comparing the IT responses in two monkeys before and after categorization learning, while counterbalancing the relevant categorization dimension across animals, we could resolve the inadequacies in the design of previous studies (Sigala and Logothetis 2002; Freedman et al. 2003) and disentangle the learned category-related effects from the pre-learned stimulus selectivity effects. Only when disentangling these two effects, we found that categorization learning resulted in an expansion of the representation of the trained dimension (i.e. a dimension-specific increase in selectivity) and that the responses of the neurons were somewhat more similar for exemplars that belong to the same, compared to different, categories. These results thus suggest that learning to categorize

shapes can only induce minor category-related changes in the shape selectivity of IT neurons in these adult monkeys. This led us to propose a two-stage model of categorization in adults in which: a) IT neurons are tuned to exemplars in a category-biased way; and b) learned categories become explicitly represented in extra-visual cortical regions that read-out IT.

In a last part (Chapter 4), we examined the effects of adaptation on the stimulus selectivity of IT neurons, both with single-cell spiking activity and local field potentials. Using a passive fixation task and a fully-crossed design, we found robust adaptation for the spiking activity and the LFP power in the gamma band (61-100Hz). For lower frequencies, this kind of robust adaptation was not found, as clear discrepancies were observed between monkeys. Our results, both for the spiking activity and the LFP gamma power, also showed that the repetition of a stimulus did not change the tuning width but scaled down the neuronal responses. At a population level, the degree of adaptation increased slightly with increasing response strength to the adapter. But the degree of adaptation was not only response strength dependent: the degree of adaptation was also affected by the relationship between the adapter and test stimulus value, since more adaptation was found when the adapter and test stimulus were identical compared to when these stimuli differed. A similar result pattern was found when stimuli were no longer presented centrally but above or below the fixation target: more adaptation was found when the adapter and test stimulus were presented at the same position, compared to a different position. Finally, we found a decreasing level of adaptation with increasing dissimilarity between the adapter and test stimulus. Because neither the sharpening model (Desimone 1996; Wiggs and Martin 1998) nor the fatigue model (Grill-Spector and Malach 2001) based on a firing-rate adaptation mechanism could account for all of our findings, we needed to fall back on an alternative model, suggested

by Sawamura et al. (2006), in which adaptation is assumed to occur at or before the level of the synapses onto the neuron.

PERSPECTIVES

As reported in Chapter 2, IT neurons can dynamically adjust their selectivity based on the input statistics. Although this was a small effect, it would be interesting to examine if a similar effect could also be observed at a behavioral level. One procedure that might serve to test whether changes in stimulus distribution statistics alter the behavioral responses of monkeys or humans is based on the attentional blink phenomenon. An attentional blink is the impaired ability to identify a second target, T2, in an RSVP stream following the successful identification of a first target, T1 (Raymond et al. 1992). Hommel and Akyürek (2005) suggested that the discriminability between T1 and T2 played an important role in this phenomenon. As we observed a change in shape discriminability when the stimulus distribution statistics were altered in Chapter 2, this change could possibly be revealed behaviorally using the attentional blink paradigm.

As discussed in Chapter 2, we could not exclude that similarity-based adaptation on a longer time scale caused the observed differences between the two ranges because the shapes in the narrow-range condition were packed at a higher density and were more similar than in the wide-range condition. Additional studies in which the variance is altered without changing the density and similarity within a shape set (by presenting a different amount of stimuli in the two sets) or in which other stimulus statistics are manipulated could add to our understanding of the origin of this dynamical adjustment of the neuronal selectivity in IT cortex.

Following our proposal of a two-stage model of categorization in which learned categories become only explicitly represented in extra-visual cortical regions that read-out IT, it would surely be interesting to determine the neuronal shape tuning in these areas after categorization learning. Two areas seem likely to be involved, based on several functional imaging studies in humans (Li et al. 2007; Vogels et al. 2002; for review see Keri (2003) and Ashby and Maddox (2005)): the prefrontal cortex (PFC) and the striatum. Freedman et al. (2001) found that the responses of prefrontal neurons were more similar for exemplars that belong to the same, compared to different, categories, as was the case for IT neurons. However, this effect was much stronger in PFC. Because Freedman et al. (2001) used a working memory task and PFC is known to be involved in working memory (Miller et al. 1996), it remains unclear whether this effect in PFC is limited to this task or will also be present when the monkey is engaged in different tasks. As the striatum can integrate the outputs of multiple IT neurons (Cheng et al. 1997), also striatal neurons could represent learned categories. Single cell recordings in both the prefrontal cortex and the striatum, using different behavioral tasks, could add to our understanding of the categorization process in adults.

As discussed in Chapter 4, indirect evidence suggested that the reported adaptation effects were not merely caused by attentional differences towards the adapter and test stimulus. However, it would certainly be useful to examine the effect of attention on adaptation in a direct way. Controlling the attentional load for both stimuli could be achieved by equally drawing attention towards both stimuli. One possibility to obtain this is by extending the adaptation test as described in Chapter 4 by randomly introducing sequences in which the luminance of the adapter or the test stimulus changes. To receive a reward in these “dimming” sequences, the monkey has to make a saccade as soon as he detects the luminance change. Because the dimming occurs randomly but counterbalanced across adapter and test stimulus and

these dimming sequences are randomly intermixed with regular fixation sequences, one can assume that the attention the monkey pays to both adapter and test stimulus will be largely equal, regardless of the sequence condition (dimming or fixation). In this way, the effect of attention on adaptation can be directly assessed. Recordings using this dimming task have already been initiated.

Because of the stimulus timing parameters used in our study, the adaptation results presented in Chapter 4 are most relevant for rapid, event-related fMR-A paradigms in which two stimuli are successively presented with only a short lag in between. Several fMR-A studies in different areas (e.g. V1 or MT), however, used long-duration adaptation (e.g. Van Wezel and Britten 2002; Kohn and Movshon 2004; Fang et al. 2005; Larsson et al. 2006) in which the adapters were presented for a much longer time. Recently, Fang et al. (2007) compared short-duration adaptation, in which the adapter was presented for 300ms, with long-duration adaptation, in which the adapter was shown for 25s. Based on the discrepant results between the two conditions in this human fMR-A study, Fang et al. (2007) suggested that the short-duration and long-duration adaptation mechanisms might be qualitatively different. Recordings in IT cortex using longer presentations durations would thus be very interesting to reveal whether and to what extent the observed adaptation effects using short-term presentations of the adapter can be generalized to long-duration adaptation.

REFERENCES

Ashby FG, Maddox WT. Human category learning. *Annu Rev Psychol* 56: 149-178, 2005.

Cheng K, Saleem KS, Tanaka K. Organization of corticostriatal and corticoamygdalar projections arising from the anterior inferotemporal area TE of the macaque monkey: a *Phaseolus vulgaris* leucoagglutinin study. *J Neurosci* 17: 7902-7925, 1997.

Desimone R. Neural mechanisms for visual memory and their role in attention. *Proc Natl Acad Sci USA* 93: 13494-13499, 1996.

Fang F, He S. Viewer-centered object representation in the human visual system revealed by viewpoint aftereffects. *Neuron* 45: 793-800, 2005.

Fang F, Murray SO, He S. Duration-dependent fMRI adaptation and distributed viewer-centered face representation in human visual cortex. *Cereb Cortex* 17: 1402-1411, 2007.

Földiák P, Xiao DK, Keysers C, Edwards R, Perrett DI. Rapid serial visual presentation for the determination of neural selectivity in area STSa. *Prog Brain Res* 144: 107-116, 2004.

Freedman DJ, Riesenhuber M, Poggio T, Miller EK. Categorical representation of visual stimuli in the primate prefrontal cortex. *Science* 291: 312-316, 2001.

Freedman DJ, Riesenhuber M, Poggio T, Miller EK. A comparison of primate prefrontal and inferior temporal cortices during visual categorization. *J Neurosci* 23: 5235-5246, 2003.

Grill-Spector K, Malach R. fMR-adaptation: a tool for studying the functional properties of human cortical neurons. *Acta Psychologica* 107: 293-321, 2001.

Hommel R, Akyürek EG. Lag-1 sparing in the attentional blink: benefits and cost of integrating two events into a single episode. *Q J Exp Psychol Sect A Hum Exp Psychol* 58A: 1415-1433, 2005.

Kayaert G, Biederman I, Op de Beeck H, Vogels R. Tuning for shape dimensions in macaque inferior temporal cortex. *Eur J Neurosci* 22: 212-224, 2005.

Keri S. The cognitive neuroscience of category learning. *Brain Res Rev* 43: 85-109, 2003.

Keysers C, Xiao DK, Földiák P, Perrett DI. The speed of sight. *J Cogn Neurosci* 13: 90-101, 2001.

Kiani R, Esteky H, Tanaka K. Differences in onset latency of macaque inferotemporal neural responses to primate and non-primate faces. *J Neurophysiol* 94: 1587-1596, 2005.

Kohn A, Movshon JA. Adaptation changes the direction of tuning of macaque MT neurons. *Nat Neurosci* 7: 764-772, 2004.

Larsson J, Landy MS, Heeger DJ. Orientation-selective adaptation to first- and second-order patterns in human visual cortex. *J Neurophysiol* 95: 862-881, 2006.

Li S, Ostwald D, Giese M, Kourtzi Z. Flexible coding for categorical decisions in the human brain. *J Neurosci* 27: 12321-12330, 2007.

Miller EK, Erickson CA, Desimone R. Neural mechanisms of visual working memory in prefrontal cortex of the macaque. *J Neurosci* 16: 5154-5167, 1996.

Op de Beeck H, Wagemans J, Vogels R. Inferotemporal neurons represent low-dimensional configurations of parameterized shapes. *Nat Neurosci* 4: 1244-1252, 2001.

Raymond JE, Shapiro KL, Arnell KM. Temporary suppression of visual processing in an RSVP task: an attentional blink. *J Exp Psychol* 18: 849-860, 1992.

Sawamura H, Vogels R, Orban GA. Selectivity of neuronal adaptation does not match response selectivity: a single-cell study of the FMRI adaptation paradigm. *Neuron* 49: 307-318, 2006.

Sigala N, Logothetis NK. Visual categorization shapes feature selectivity in the primate temporal cortex. *Nature* 415: 318-320, 2002.

Van Wezel RJ, Britten KH. Motion adaptation in area MT. *J Neurophysiol* 88: 3469-3476, 2002.

Vogels R, Sary G, Dupont P, Orban GA. Human brain regions involved in visual categorization. *Neuroimage* 16: 401-414, 2002.

Wiggs CL, Martin A. Properties and mechanisms of perceptual priming. *Curr Opin Neurobiol* 8: 227-233, 1998.